



VILNIAUS GEDIMINO TECHNIKOS UNIVERSITETAS

APLINKOS INŽINERIJOS FAKULTETAS

GEODEZIJOS IR KADASTRO KATEDRA

Aušra Pranskevičiūtė

**SKAITMENINIŲ NUOTRAUKŲ APDOROJIMAS FOTOGRAMETRINĖMIS
SISTEMOMIS**

**PROCESSING OF THE DIGITAL IMAGES USING PHOTOGRAMMETRY
SYSTEMS**

Baigiamasis magistro darbas

Geodezijos ir kartografijos studijų programa, valstybinis kodas 62410T102

Kadastro informacinių sistemų specializacija

Matavimų inžinerijos studijų kryptis

Vadovas: doc. dr. Jūratė Sužiedelytė-Visockienė

Vilnius, 2011

VILNIAUS GEDIMINO TECHNIKOS UNIVERSITETAS
APLINKOS INŽINERIJOS FAKULTETAS
GEODEZIJOS IR KADASTRO KATEDRA

TVIRTINU
Katedros vedėjas

(Parašas)
Vladislovas Česlovas Aksamitauskas
(Vardas, pavardė)

(Data)

Aušra Pranskevičiūtė

**SKAITMENINIŲ NUOTRAUKŲ APDOROJIMAS FOTOGRAMETRINĖMIS
SISTEMOMIS**

**PROCESSING OF THE DIGITAL IMAGES USING PHOTOGRAMMETRY
SYSTEMS**

Baigiamasis magistro darbas

Geodezijos ir kartografijos studijų programa, valstybinis kodas 62410T102

Kadastro informacinių sistemų specializacija

Matavimų inžinerijos studijų kryptis

Vadovas doc. dr. Jūratė Sužiedėlytė-Visockienė

(Moksl. laipsnis, vardas, pavardė)

(Parašas)

(Data)

Konsultantas

(Moksl. laipsnis, vardas, pavardė)

(Parašas)

(Data)

Vilnius, 2011

VILNIAUS GEDIMINO TECHNIKOS UNIVERSITETAS
APLINKOS INŽINERIJOS FAKULTETAS
GEODEZIJOS IR KADASTRO KATEDRA

Technologijos mokslų sritis
Matavimų inžinerijos mokslo kryptis
Matavimų inžinerijos studijų kryptis

Geodezijos ir kartografijos studijų programa, valstybinis
kodas 62410T102

Kadastro informacinių sistemų specializacija

TVIRTINU
Katedros vedėjas

(Parašas)
Vladislovas Česlovas Aksamitauskas
(Vardas, pavardė)

(Data)

BAIGIAMOJO MAGISTRO DARBO

UŽDUOTIS

2009-12-09Nr.

Vilnius

Studentui (ei)
Aušrai Pranskevičiūtei
(Vardas, pavardė)

Baigiamojo darbo tema: ..Skaitmeninių nuotraukų apdorojimas fotogrametrinėmis sistemomis.....

patvirtinta 2009 m. gruodžio 01 d. dekanų potvarkiu Nr. 374ap

Baigiamojo darbo užbaigimo terminas 2011 m. birželio 01 d.

BAIGIAMOJO DARBO UŽDUOTIS:

Apdoroti skaitmenines artimų nuotolių fotonuotraukas fotogrametrinėmis sistemomis *PhotoMod* ir *Inpho*; Atlikti trianguliacijos skaičiavimus sistema *BLUH*; Atlikti skaitmeninės fotokameros *Canon EOS 1D Mark III* kalibravimą. Išanalizuoti gautus rezultatus ir pateikti apibendrinančias išvadas.

BAIGIAMOJO DARBO RENGIMO KONSULTANTAI:

.....
(Moksl. laipsnis, vardas, pavardė)

Vadovas
(Parašas)

.....
doc. dr. Jūratė Sužiedelytė-Visockienė

.....
(Moksl. laipsnis, vardas, pavardė)

Užduotį gavau

.....
(Parašas)

.....
Aušra Pranskevičiūtė

.....
(Vardas, pavardė)

.....
2009-12-09

.....
(Data)

Vilniaus Gedimino technikos universiteto egzaminų
sesijų ir baigiamųjų darbų rengimo bei gynimo
organizavimo tvarkos aprašo 2010–2011 m. m.
6 priedas

(Baigiamojo darbo sąžiningumo deklaracijos forma)

VILNIAUS GEDIMINO TECHNIKOS UNIVERSITETAS

Aušra Pranskevičiūtė, 20053319

(Studento vardas ir pavardė, studento pažymėjimo Nr.)

Aplinkos inžinerijos

(Fakultetas)

Geodezijos ir kartografijos, KISmf-09

(Studijų programa, akademinė grupė)

**BAIGIAMOJO DARBO (PROJEKTO)
SĄŽININGUMO DEKLARACIJA**

2011 m. _____ birželio 01 _____ d.

(Data)

Patvirtinu, kad mano baigiamasis darbas (projektas) tema _____
Skaitmeninių nuotraukų
apdorojimas fotogrametrinėmis sistemomis

patvirtintas 20 09 m. _____ gruodžio 01 _____ d. dekanų potvarkiu Nr. _____ 374ap _____, yra
savarankiškai parašytas. Šiame darbe (projekte) pateikta medžiaga nėra plagijuota. Tiesiogiai ar
netiesiogiai panaudotos kitų šaltinių citatos pažymėtos literatūros nuorodose.

Prenkant ir įvertinant medžiagą bei rengiant baigiamąjį darbą (projektą), mane konsultavo
mokslininkai ir specialistai: _____

Mano darbo (projekto) vadovas _____ doc. dr. Jūratė Sužiedelytė-Visockienė

Kitų asmenų indėlio į parengtą baigiamąjį darbą (projektą) nėra. Jokių įstatymų nenumatytų
piniginių sumų už šį darbą niekam nesu mokėjęs(-usi).

Aušra Pranskevičiūtė

(Parašas)

(Vardas ir pavardė)

ANOTACIJA

Vilniaus Gedimino technikos universitetas
Aplinkos inžinerijos fakultetas
Geodezijos ir kadastro katedra

ISBN ISSN
Egz. sk.
Data-.....-.....

Antrosios pakopos studijų **Geodezijos ir kartografijos** programos baigiamasis darbas
Pavadinimas **Skaitmeninių nuotraukų apdorojimas fotogrametrinėmis sistemomis**
Autorius **Aušra Pranskevičiūtė**
Vadovas **doc. dr. Jūratė Sužiedelytė-Visockienė**

Kalba: anglų

Anotacija

Baigiamojo magistro darbo tikslas - nustatyti, ar aerofotogrametrinėms reikmėms skirtos programinės įrangos PhotoMod ir Inpho yra tinkamos antžeminiams fotogrametriniams darbams atlikti. Taip pat, remiantis tyrimais, atliktais skirtingomis fotogrametrinėmis sistemomis, nustatyti fotonuotraukų apdorojimo darbų etapų tikslumo reikalavimus. Šiuo tikslu magistro baigiamajame darbe atliktas artimų nuotolių skaitmeninių fotonuotraukų apdorojimas PhotoMod ir Inpho fotogrametrinėmis sistemomis, kurios yra skirtos aerofotonuotraukoms, taip pat palydovinėms nuotraukoms apdoroti ir sistema BLUH, kuri naudojama artimų nuotolių fotonuotraukų trianguliacijai atlikti. Baigiamojo magistro darbo metu, naudojantis analitine fotogrametrine sistema AICON 3D Studio, atliktas skaitmeninės fotokameros Canon EOS 1D Mark III kalibravimas, o naujai gauti kameros kalibravimo parametrai įtraukti apdorojant skaitmenines fotonuotraukas. Darbo pabaigoje pateiktos išvados, atspindinčios darbo tikslus bei uždavinius. Darbą sudaro 10 dalių: įvadas, 7 skyriai, išvados, literatūros sąrašas. Darbo apimtis – 83 p. teksto be priedų, 13 iliustr., 25 lent., 42 bibliografiniai šaltiniai. Atskirai pridedami 8 darbo priedai.

Prasminiai žodžiai

Artimų nuotolių skaitmeninės fotonuotraukos; artimų nuotolių skaitmeninių fotonuotraukų apdorojimas; skaitmeninė fotogrametrinė sistema; trianguliacija; trianguliacijos tikslumas; skaitmeninės fotokameros kalibravimas.

ANNOTATION

Vilnius Gediminas Technical University
Faculty of Environmental Engineering
Department of Geodesy and Cadastre

ISBN ISSN
Egz. sk.
Data-.....-.....

Master Degree Studies **Geodesy and Cartography** study programme Final Thesis
Title **Processing of the Digital Images Using Photogrammetry Systems**
Author **Aušra Pranskevičiūtė**
Academic supervisor **Assoc Prof Dr Jūratė Sužiedelytė-Visockienė**

Thesis language:
English

Annotation

The purpose of the Master thesis is to test if the digital photogrammetric systems PhotoMod and Inpho, which are designed for aerial photogrammetry, are suitable for close range photogrammetric applications. Also, according to performed analysis, to estimate the accuracy requirements of the images processing by using different photogrammetric softwares. For this purpose the digital close-range images were processed by using above mentioned photogrammetric softwares and that same images were processed by using for close-range images designed bundle triangulation system BLUH. The digital camera Canon EOS 1D Mark III calibration procedure using analyzing photogrammetric software AICON 3D Studio was performed. The new camera's calibration parameters were involved to the images processing procedure. Finally, the conclusions, which reflects the purpose of the Master thesis has been listed. The Master thesis consists of 10 parts: introduction, 7 chapters, conclusions and list of literature. Work volume – 83 pages of text without appendixes, 13 illustrations, 25 charts, 42 bibliographical sources. The 8 appendixes have been added separate.

Keywords

Close-range digital images; close-range digital images processing; digital photogrammetric workstation; bundle triangulation; bundle triangulation accuracy control; the calibration procedure of a digital camera.

PROCESSING OF THE DIGITAL IMAGES USING PHOTOGRAMMETRY SYSTEMS

CONTENT

LIST OF FIGURES	9
LIST OF TABLES	10
INTRODUCTION	12
1. DIGITAL PHOTOGRAMMETRIC WORKSTATIONS	14
1.1. Development of digital photogrammetric workstations	14
1.2. Images processing work stages	16
1.3. Digital images processing accuracy control	18
2. DIGITAL PHOTOGRAMMETRIC SYSTEM <i>PHOTOMOD</i>	21
2.1. The modules of digital photogrammetric system <i>PhotoMod</i>	21
2.2. Images processing by using photogrammetric software	29
2.3. Accuracy control of photogrammetric work stages	37
2.4. Processing of the images by using digital photogrammetric software <i>PhotoMod</i>	40
3. DIGITAL PHOTOGRAMMETRIC SYSTEM <i>INPHO</i>	47
3.1. The components of digital photogrammetric system <i>Inpho</i>	47
3.2. Accuracy control of photogrammetric work stages	49
3.3. Processing of the images by using digital photogrammetric software <i>Inpho</i>	51
4. BUNDLE BLOCK ADJUSTMENT <i>BLUH</i>	56
4.1. Purpose of bundle block adjustment	56
4.2. The modules of <i>BLUH</i>	58
4.3. Results of the <i>BLUH</i> processing	59
5. ANALYZING PHOTOGRAMMETRIC SOFTWARE <i>AICON 3D STUDIO</i>	63
5.1. Purpose of <i>AICON 3D Studio</i>	63
5.2. The modules of the analyzing photogrammetric software <i>AICON 3D STUDIO</i>	63
6. CAMERA CALIBRATION	65
6.1. The goal of a camera calibration.....	65
6.2. Measurements for the digital camera calibration.....	66
6.3. Computation of the digital camera calibration parameters.....	68
6.4. Results of the digital camera calibration	69

7. THE RESULTS ANALYSIS OF PROCESSED IMAGES AND THE DIGITAL CAMERA CALIBRATION PARAMETERS	71
7.1. Aerial triangulation results analysis before camera calibration.....	71
7.2. Aerial triangulation results analysis after camera calibration.....	72
7.3. Comparison of aerial triangulation results before camera calibration and after camera calibration.....	73
7.4. Comparison of camera calibration parameters	75
CONCLUSIONS	78
REFERENCES	80
APPENDIXES.....	83
Appendix 1. <i>PhotoMod</i> aerial triangulation report	
Appendix 2. <i>Inpho</i> aerial triangulation statistics file of the images which are corrected from the digital camera <i>Canon EOS 1D Mark III</i> objective distortions	
Appendix 3. <i>Inpho</i> aerial triangulation report of the images which are corrected from the digital camera <i>Canon EOS 1D Mark III</i> objective distortions	
Appendix 4. <i>Inpho</i> aerial triangulation statistics file of the original images	
Appendix 5. <i>Inpho</i> aerial triangulation report of the original images	
Appendix 6. <i>BLUH</i> bundle triangulation report of the images which are corrected from the digital camera <i>Canon EOS 1D Mark III</i> objective distortions	
Appendix 7. <i>BLUH</i> bundle triangulation report of the original images	
Appendix 8. The programme of Republican scientific conference “ <i>Civil Engineering and Geodesy</i> ”	

LIST OF FIGURES

Fig. 1.1. Images processing.....	17
Fig. 1.2. Accuracy potential of imaging and analysis systems	19
Fig. 2.1. Structure of the digital photogrammetric system <i>PhotoMod</i>	22
Fig. 2.2. Grouping of tie points in the images overlap	31
Fig. 2.3. Grouping of inter-strip tie points in the images side lap areas	31
Fig. 2.4. Three overlapping images (P915-P912-P918)	40
Fig. 2.5. Break lines of the object.....	45
Fig. 2.6. Orthophoto of the object	46
Fig. 3.1. <i>Inpho</i> 's modules.....	47
Fig. 4.1. The modules of <i>BLUH</i>	58
Fig. 6.1. Test-field for the camera calibration.....	67
Fig. 6.2. Photo camera position.....	67
Fig. 6.3. Numbered targets.....	68

LIST OF TABLES

Table 2.1. The basic capabilities of <i>PhotoMod Core</i>	22
Table 2.1. continuation	23
Table 2.2. The main features of <i>PhotoMod StereoDraw</i>	24
Table 2.2. continuation:	25
Table 2.3. The main features of <i>PhotoMod Vector</i>	26
Table 2.4. Calculated maximum error and root mean squared error to the digital camera <i>Canon EOS 1D Mark III</i>	38
Table 2.5. Quality of measurements of GCP and tie points	38
Table 2.6. Characteristics of digital camera <i>Canon EOS 1D Mark III</i>	40
Table 2.7. Result of camera <i>Canon EOS 1D Mark III</i> calibration (2008).....	41
Table 2.8. Relative orientation result	42
Table 2.9. Quality of triplets.....	42
Table 2.10. Residuals between adjusted coordinates and between measured coordinates in the images	43
Table 2.10. continuation:	44
Table 2.11. Residuals of measured the image points of the ground control point.....	45
Table 3.1. Residuals between adjusted coordinates and between measured coordinates in the images	52
Table 3.1. continuation:	53
Table 3.1. continuation (1):	54
Table 3.2. Residuals of measured the image points of the ground control point.....	55
Table 4.1. Residuals between adjusted coordinates and between measured coordinates in the images	59
Table 4.1. continuation:	60
Table 4.1. continuation (1):	61
Table 4.2. Residuals of measured the image points of the ground control point.....	62
Table. 6.1. Results of bundle block adjustment	69
Table. 6.2. The new calibration results of the digital camera <i>Canon EOS 1D Mark III</i>	69
Table. 6.2. continuation:	70
Table. 7.1. Comparison of standard deviation between adjusted and between measured points in image space	71
Table. 7.2. Bundle triangulation results.....	72

Table. 7.3. Comparison of standard deviation between adjusted and between measured points in the image space after camera calibration procedure.....	73
Table. 7.4. Bundle triangulation results after the camera calibration procedure	73
Table. 7.5. Comparison of standard deviation between adjusted and between measured points in image space before and after camera calibration.....	74
Table. 7.6. Comparison of bundle triangulation results before and after camera calibration procedure.....	74
Table. 7.7. Comparison of camera calibration parameters	75
Table. 7.7. continuation:	76
Table. 7.8. Camera calibration parameters in <i>PhotoMod</i> , <i>Inpho</i> and <i>BLUH</i>	77

INTRODUCTION

The main product of photogrammetry is a digital image of the object in a three-dimensional (3D) space. There are a lot of digital photogrammetric workstations (DPW) (also called *softcopy workstation* (WS)) designed for this result to be achieved (Schenk 1999). All kinds of images, like a taken from the air (from airplanes or satellites) or taken from the surface of the earth (close-range photogrammetry) can be processed by using digital photogrammetric workstations. The requirements of different photogrammetric systems can differ depending on algorithms, used for photogrammetric processing (Atkinson 2001). Therefore it is important to test capabilities and accuracy of data using more than one digital photogrammetric system.

In this Master thesis the images of the research object were taken using the digital camera *Canon EOS 1D Mark III* from the surface of the earth. These close-range digital images were processed – the triangulation procedure was done by using digital photogrammetric systems (*PhotoMod* and *Inpho*) which are suitable for above-mentioned images processing. Triangulation procedure was also performed by using the bundle triangulation program *BLUH*. The accuracy of triangulation influences the accuracy of 3D data (Sužiedelytė-Visockienė, Bručas 2009). **Thus, the aims of Master thesis are:**

- To test if the above mentioned digital photogrammetric systems for aerial photogrammetry are suitable for close-range photogrammetric applications;
- Based on the performed analysis to estimate the accuracy requirements of images processing by using different photogrammetric systems;
- To evaluate the results of 50 mm objective-lens of the digital camera *Canon EOS 1D Mark III* calibration related to the type of images of the object.

To reach the aims of the Master thesis, the followed tasks should be performed:

- The digital close-range images should be processed by using digital photogrammetric softwares *PhotoMod* and *Inpho*;
- The bundle block adjustment of the digital close-range images by using for this purpose developed system *BLUH* should be performed;
- The camera calibration procedure should be performed.

Novelty of the science:

- According to performed processing of the digital close-range images and the analysis of the results, the suitability of explored digital photogrammetric systems for aerial photogrammetry was stated;

- The optical calibration parameters of the digital camera *Canon EOS 1D Mark III* were specified.

Practical importance:

- After the close-range digital images processing by using digital photogrammetric systems, which are designed for satellite images and aerial photographs processing and after processing of those same images with *BLUH* system, which are designed for close-range images triangulation, it was found that *PhotoMod* and *Inpho* softwares can be used for processing of close-range digital images. Thus, the analysis that was carried out allows the user to choose one software to perform tasks with aerial photographs, satellite images and close-range photogrammetry;

- The digital camera *Canon EOS 1D Mark III* is used for photogrammetrical fixation of heritage objects in scientific and manufacturing enterprise company *Cad and F Projektsevisas*. Therefore, the qualified optical parameters of the digital camera and the analysis which was performed during research work will be useful in the further close-range photogrammetry works.

Acknowledgements

The Master thesis was performed in Lithuania and in Germany at Neubrandenburg University of Applied Sciences. Initial data for analysis (the digital images of the object) was provided by scientific-industrial company *Cad and F Projektsevisas*. The images were taken with this company's digital photo camera *Canon EOS 1D Mark III* and were processed with this company's digital photogrammetric software *PhotoMod*. Thus, I would like to thank to the head of company *Cad and F Projektsevisas* Dalius Čekanavičius for supplied data, technical equipment and software. Also I would like to thank to the supervisor of my Master thesis doc. Jūratė Sužiedelytė Visockienė for the help during images processing procedure by using *PhotoMod* photogrammetric software. In addition I would like to thank to Neubrandenburg's University Prof. Dr.-Ing. Wolfgang Kresse for the help and given possibility to make further researches by using digital photogrammetric software *Inpho*, analyzing photogrammetric software *AICON 3D Studio* and system *Bluh* in photogrammetry laboratory at the Neubrandenburg University of Applied Sciences.

1. DIGITAL PHOTOGRAMMETRIC WORKSTATIONS

At the heart of digital images processing side is a DPWs. Thus, DPWs are the single most significant product of digital photogrammetry.

This chapter consist of a brief history of the development of DPW, discussion of digital images processing work stages and accuracy of the images processing.

1.1. Development of digital photogrammetric workstations

According to the International Society for Photogrammetry and Remote Sensing (ISPRS), a digital photogrammetric system is defined as: hardware and software designed to derive photogrammetric products from digital imagery using manual and automated techniques (Available from internet: <http://www.gim-international.com>)

The photogrammetrist Gülch splits the development of the digital photogrammetric workstations into three phases. The first phase began in 1955 and ended in 1981 (Schenk 1999). Perhaps the most important development in this period was the invention of the analytical stereo plotter by Helava in 1957. The analytical stereo plotter is essentially an instrument with a built-in digital computer as its main component, which handles the physical and mathematical relationship between object (ground) space and image space (Madani 2001). Shortly after the invention of the analytical plotter, its inventor, Helava, mentioned the possibility of replacing the human operator by an automatic correlator – a typical consideration of digital photogrammetry (Schenk 1999).

The first reasonably detailed concept of a DPW was described by photogrammetrist Sarjakoski in 1981. Referred to as a fully digital stereoplotter, the functionality strongly resembles that of an analytical plotter, the major difference being the fact that the photographs are replaced by digital images. Sarjakoski proposed building the digital stereoplotter using image processing systems and analytical plotter software as a basis. The other photogrammetrist Case in 1982 provided another fundamental concept of a digital image exploitation system. Again, the proposed system had the functionality of an analytical plotter with the potential of automating photogrammetric task such as DEM generation (Schenk 1999).

These two design concepts paved the way for the development of DPWs from 1982 – 1988, which photogrammetrist Gülch considers the second phase in the rather short history of DPWs. Additional concepts were presented and experiments began with prototypes in different research institutions. Finally, two digital photogrammetric workstations were introduced during the XVIth ISPRS Congress in Kyoto, 1988 (Madani 2001). Major efforts were directed towards implementing hardware components and developing low-level system software. The application

software was “borrowed” from analytical plotters. The systems of that period were very much characterized by minimal functionality and performance; it is not surprising that the photogrammetric community met these first softcopy workstations with a healthy dose of skepticism. No first generation system survived (Schenk 1999).

Finally, in 1990 the third phase of DPW development began with increased activities by researchers, developers and photogrammetric societies. For example, an ISPRS working group was charged with the task of defining the functionality and performance of digital photogrammetric systems, including a critical evaluation of existing systems. The working group provided the following broad definition: “A digital photogrammetric system is defined as hardware and software to derive photogrammetric products from digital imagery using manual and automated techniques” (Schenk 1999).

From the past two decades till nowadays great strides the powerful image processing workstations has appeared. This development of DPWs is related to (Madani 2001):

- Availability of ever increasing quantities of digital images from satellite sensors, charge-coupled device (CCD) cameras and scanners;
- Availability of fast and powerful workstations/computers with many innovative and reliable hightech peripherals, such as storage devices, true color monitors, fast data transfer, and compression/decompression techniques;
- Integration of all types of data in a unified and comprehensive information system such as geographic information systems (GIS);
- Real-time applications such a quality control and robotics;
- Computer aided design (CAD) and industrial applications;
- Lack of trained and experienced photogrammetric operators and high cost of photogrammetric instruments.

Because of these key technological advances - cost, labor, and new areas of applications GIS and CAD - digital photogrammetric systems have been and are still developed. The main idea is the use of digital images for the data capture within the model area with a 3D “floating mark” with sub-pixel accuracy. Then use a digital workstation to compile the required features to form an intelligent description for an information system such as GIS and CAD systems (Madani 2001).

Close range photogrammetry has significant links with aspects of graphics and photographic science, for example computer graphics and computer vision, digital image processing, CAD, GIS and cartography (Luhmann et al. 2006).

The DPW looks much like an ordinary graphics workstation with some additional features, such as stereo display, 3D cursor, and, most likely, increased storage capacity to hold all the digital images of the entire project (Schenk 1999).

The important advantage of digital photogrammetry is the possibility of automation of photogrammetric task that human operators perform with great ease, thereby making use of our most impressive sense, namely “seeing” (Jacobsen 2001; Schenk 1999).

The difference between the first digital processing systems and today’s digital processing systems is noticeable in orientation procedures: typically, the parameters of the exterior orientation are determined by two steps orientation in the previous DPW and the third phase - the parameters of the exterior orientation are determined in the two separate steps of the relative orientation and the absolute orientation. In nowadays digital photogrammetric software the exterior orientation parameters are determined during the fully automatic aerial triangulation procedure. The aerial triangulation is the basic procedure, on which the final result of image processing (orthophoto) depends. Nowadays nearly all block triangulation is done using the bundle method (Luhmann et al. 2006).

A more comprehensive description about today’s digital photogrammetric systems *PhotoMod* and *Inpho* will be written in the further chapters. Also, in the further chapters will be written about the bundle block adjustment system *BLUH* and photogrammetric analyzing software *AICON 3D Studio*.

1.2. Images processing work stages

Digital image processing is concerned with acquiring, transmitting, processing and representing images (Schenk 1999). The principal procedures in close range photogrammetry is shown in figure 1.1 (Luhmann et al. 2006):

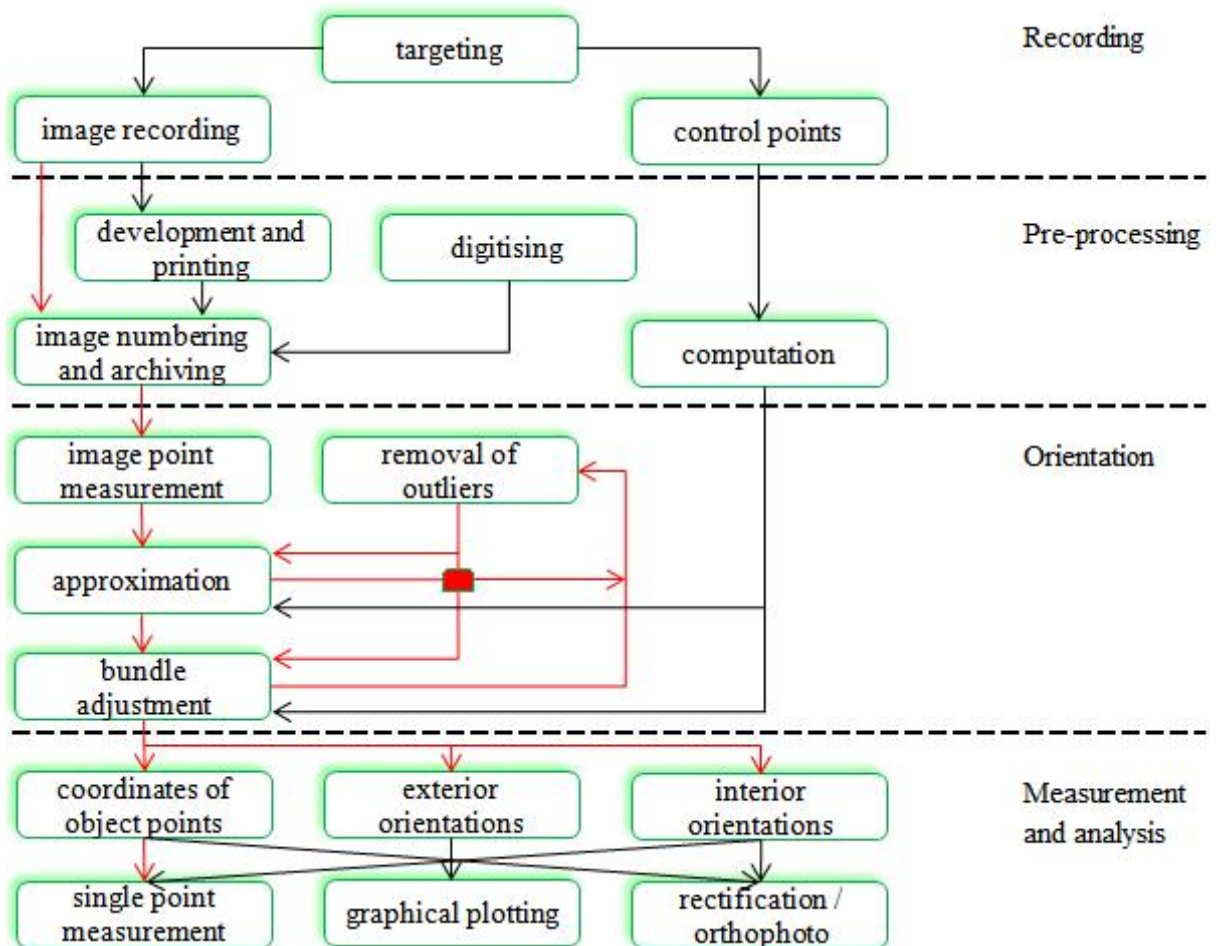


Fig. 1.1. Images processing

1. Recording

a) Targeting: target selection and attachment to object features to improve automation and increase the accuracy of target measurement in the image.

b) Determination of control points or scaling lengths: creation of a global object coordinate system by definition of reference (control) points and/or reference lengths (scales).

c) Image recording: analogue or digital image recording of the object with a photogrammetric system.

2. Pre-processing

a) Computation: calculation of reference point coordinates and/or distance from survey observations (e.g. using network adjustment).

b) Development and printing: photographic laboratory work (developing film, making photographic prints).

c) Digitising: conversion of analogue photographs into digital images (scanning).

d) Numbering and archiving: assigning photo numbers to identify individual images and archiving or storing the images.

3. Orientation

a) Measurement of image points: identification and measurement of reference and scale points; identification and measurement of tie points (points observed into two or more images simply to strengthen the network).

b) Approximation: calculation of approximate (starting) values for unknown quantities to be calculated by the bundle adjustment).

c) Bundle adjustment: adjustment program which simultaneously calculates parameters of the both interior and exterior orientation as well as the object point coordinates which are required for subsequent analysis.

d) Removal of outliers: detection and removal of gross errors which mainly arise during (manual) measurements of image points.

4. Measurement and analysis

a) Single point measurement: creation of three dimensional object point coordinates for further numerical processing.

b) Graphic plotting: production of scales maps or plans in analogue or digital form (e.g. hard copies for maps and electronics files for CAD model or GIS).

c) Rectification / Orthophoto: generation of transformed images or image mosaics which remove the effects of tilt relative to a reference plane (rectification) and/or remove the effects of perspective (orthophoto).

This sequence can, to a large extent, be automated (connections in red in Fig. 1.1). Provided that the object features are suitably marked and identified using coded targets, initial values can be calculated and measurement outliers (gross errors) removed by robust estimation methods (Luhmann et al. 2006).

1.3. Digital images processing accuracy control

Triangulation is the basic procedure, on which the final result (orthophoto) of image processing depends. Thus, the quality of triangulation is highly important (Sužiedelytė-Visockienė, Bručas 2009). In order to analyse the quality of the bundle adjustment, it is possible to calculate image coordinate residuals (corrections), standard deviations of object points and orientations data, correlations between parameters and reliability numbers for the detection of gross errors (Luhmann et al. 2006).

Image measurement accuracy depends on various factors: the performance of the camera (stability and calibration), the accuracy of the image processing system (image quality,

measurement algorithm, instrumental precision) and the positioning capability (identification of features) (Luhmann et al. 2006).

Figure 1.2 illustrates schematically the accuracy potential of typical imaging and processing systems as well as common and optimal system combinations (Luhmann et al. 2006).

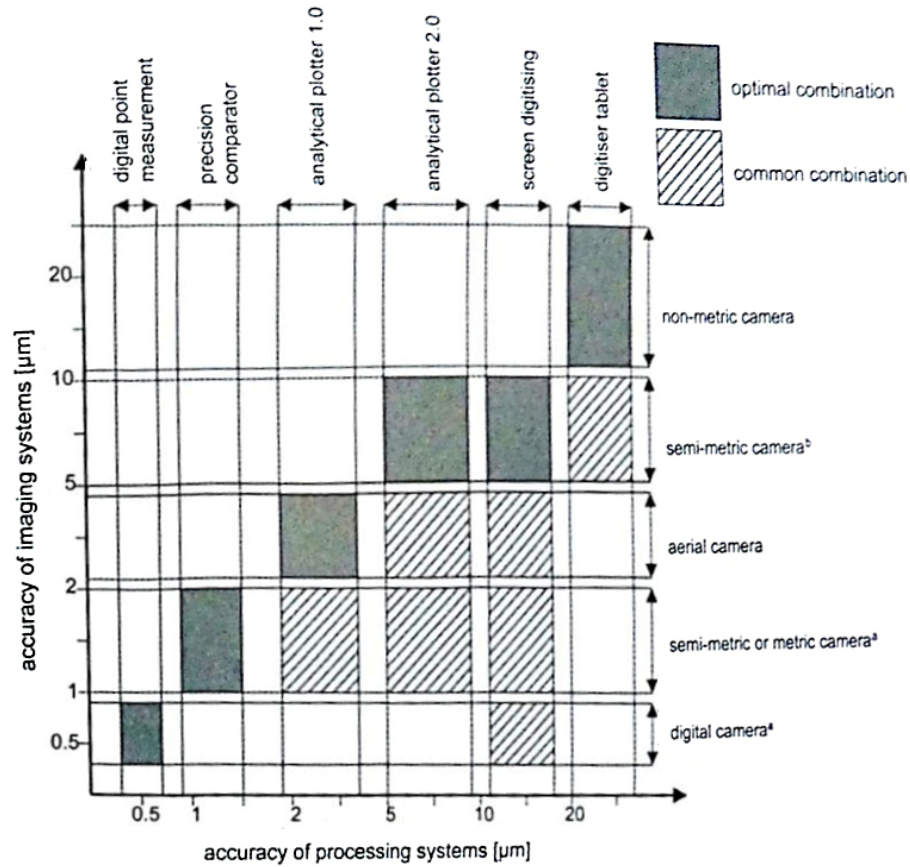


Fig. 1.2. Accuracy potential of imaging and analysis systems

a) with self-calibration and b) without self-calibration

If all above mentioned factors have a minimal influence, the digital imaging systems can reach image measurement accuracies of 0,2 – 1 μm (see fig. 1.2).

The accuracy result of triangulation is defined by standard deviation of unit weight (σ_0) (Luhmann et al. 2006):

$$\sigma_0 = \sqrt{\frac{[v^T P_v]}{n-u}}, \quad (1.1)$$

where: $v^T P_v$ – vectors residuals of observations; n – number of observations; u - number of unknowns.

However, in many cases adjustment results are reported as root mean square errors (RMS) of the control points instead of the above defined standard deviation of unit weight. The RMS value is the square root of the mean squared difference between n given nominal values X_{nom} and corresponding adjusted observations X_{obs} (Luhmann et al. 2006; Kersten 1999):

$$\text{RMS} = \sqrt{\frac{\sum(X_{nom} - X_{obs})^2}{n}}, \quad (1.2)$$

According analysed treatises during literature review, the value of standard deviation of unit weight (σ_0) can be achieved, for example from 1/3 pixel size to 1/5 pixel size.

More about accuracy control at various stages of photogrammetric processing and triangulation results by using different photogrammetric systems will be written in followed sections during images processing procedure.

2. DIGITAL PHOTOGRAMMETRIC SYSTEM *PHOTOMOD*

PhotoMod is a digital modular system providing full photogrammetric production line from the aerial triangulation to the output of digital terrain models, digital maps and orthomosaics. *PhotoMod* system contains tools for processing aerial photos and scanner satellite images from different sensors. Due to the system modular structure the user can choose the necessary configuration when purchasing the software. Network system version opens wide opportunities of working with a project simultaneously from several workplaces.

PhotoMod system is produced by Racurs Co. (Moscow, Russia) and has been dynamically developed since the version 1.1 in 1994. *PhotoMod's* growing user base includes organizations throughout more than 45 countries worldwide. The main fields of application include: photogrammetric production, cadastral mapping, cartography and remote sensing, academic photogrammetry, mining, architecture and construction (Available from internet: <http://www2.racurs.ru>).

The shutter / anaglyph glasses for stereo visualisation and hardware key is included in the *PhotoMod* system (Available from internet: <http://www.infomap-rs.net>).

Further in this chapter will be written about the modules of photogrammetric system *PhotoMod*, basic theory of images processing, accuracy control of photogrammetric measurements data and processing of the digital images.

2.1. The modules of digital photogrammetric system *PhotoMod*

PhotoMod is a modular system and each module of this system performs specific operations during a certain stage of processing. Consequently, there is no need to have all *PhotoMod* modules if they are not necessary for particular workflow.

Each module has a unique place in the overall workflow, making it possible to construct consistent project processing sequences. The fundamental concept of *PhotoMod* is to enable project work through a series of well-defined steps (data preparation, block adjustment, processing) and provide the support of a flexible set of tools at every stage.

The newest version of *PhotoMod* includes its main operating shell whose name is *PhotoMod Core* (in the old system - *Montage Desktop*) and 11 other modules (Fig. 2.1) (Available from internet: <http://www.racurs.ru>).

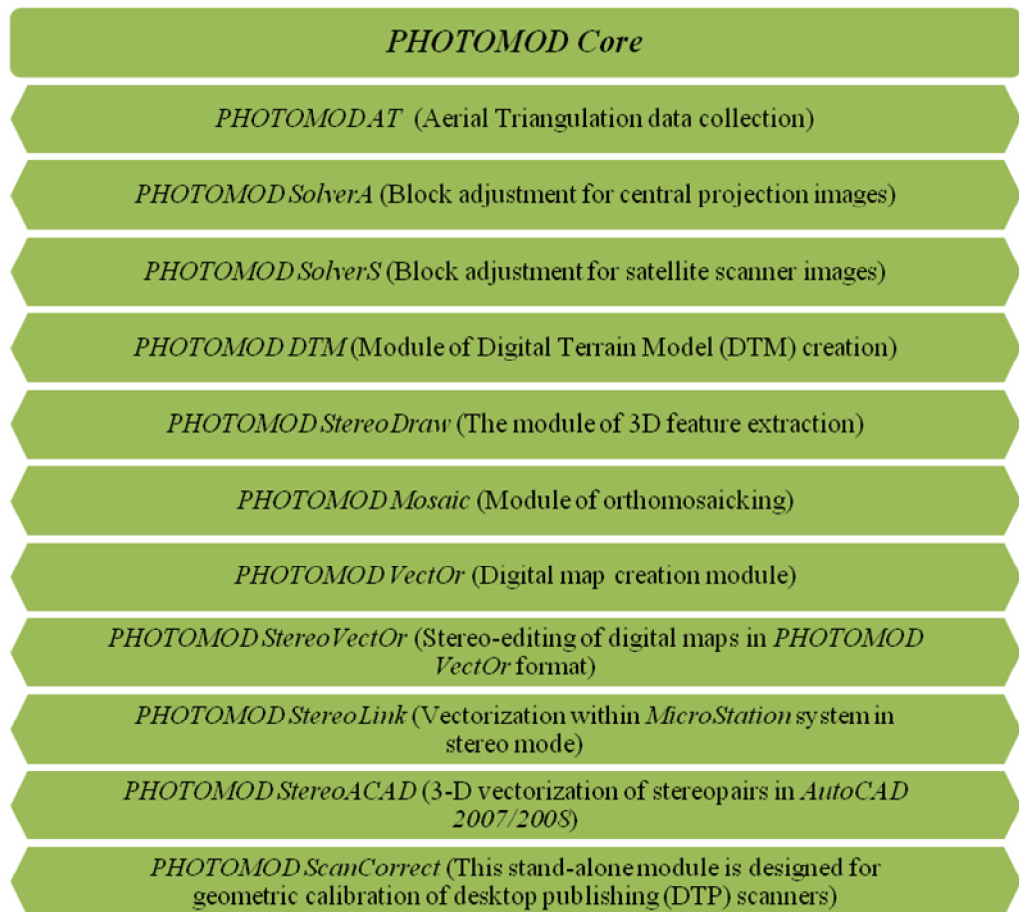


Fig. 2.1. Structure of the digital photogrammetric system *PhotoMod*

PhotoMod Core (Montage Desktop) functionality. *PhotoMod Core*, the main shell of the *PhotoMod* system, initiates and manages an array of modules that guide the processing of photogrammetric project through every step. Also, *PhotoMod Core* is equipped with a wide range of auxiliary functions which are designed to simplify and optimize the project processing. The basic capabilities of *PhotoMod Core* is given in table 2.1 (Available from internet: <http://www.racurs.ru>):

Table 2.1. The basic capabilities of *PhotoMod Core*

Capabilities	Description
Project creation	<i>Type selection of the new project:</i> central projection, satellite scanner imagery or Airborne Digital Sensor (ADS 40). <i>Selection of coordinate system:</i> database supplied coordinate system, edition of existing coordinate systems or creation new coordinate systems.
Project management	Edition of the project properties; Projects duplication/deletion; backup/restore function; project location by using new “virtual folder” technology; importation of the projects from older <i>PhotoMod</i> versions (<i>PhotoMod 4.x</i>)

Table 2.1. continuation

Capabilities	Description
Block formation	<p><i>Images preparation for the project:</i> transformation of non-photogrammetric scanner images (<i>PhotoMod ScanCorrect</i>); radiometric image correction (most commonly used for 16-bit rasters); rasters convert to internal format; optional image compression; batch conversion processing.</p> <p><i>Images loading and block formation:</i> load images to strips; rotate and replace images; the same images (without copying those) could be usable for multiple projects; block could be automatically spitted into strips; image could be corrected with <i>Image Wizard</i>.</p>
Input of camera parameter for “Central projection” projects	<p><i>Camera passport data introduction:</i> type of the camera (digital or film) introduction; coordinates of principal point introduction; focal length introduction; coordinates of fiducial mark introduction (for film cameras); distortion coefficients introduction.</p> <p>Cameras duplication, renaming, or deleting; assignation to project images; importation/exportation.</p>
Basic project operations	<p>Interior orientation; importation/exportation of triangulation points; importation of exterior orientation parameters from different formats (can be used for direct georeferencing or precise block layout); importation of interior and exterior orientation parameters from Ultra Cam metadata; block layout creation from different data sources; reports generation of interior and relative orientation; importation/exportation and mono-edition of vector objects; importation/exportation of DEM, TIN and contour lines; window for viewing 3D objects from different angles; distributed processing.</p>
Auxiliary utilities:	Explorer; Control Panel; Raster Converter; Image Wizard; GeoCalculator.

PhotoMod AT functionality. This module is used to recognize and measure ground control points and tie points on the images. Ground control points (GCP) coordinates can be imported from a text file or entered directly by using keyboard. After coordinates are entered, the points are measured on the images in semi-automatic or stereo mode. In addition, to fully automatic aerial triangulation, *PhotoMod AT* includes tools for interior orientation, as well as GCP search and measurement. Collected data is passed to *PhotoMod SolverA* or *PhotoMod SolverS* for block adjustment and computing exterior orientation parameters (Available from internet: <http://www.racurs.ru>).

PhotoMod SolverA and SolverS functionality. The modules *PhotoMod SolverA* and *SolverS* was named *PhotoMod Solver* before. The main difference between older module (*Solver*) and the newest modules (*SolverA* and *SolverS*) is that the newest modules are used for block adjustment of central projection (*SolverA*) and scanner satellite images (*SolverS*) individually. Sophisticated adjustment and error detection algorithms ensure successful aerial triangulation and highly accurate of Digital Terrain Model (DTM), orthomosaic and vector map output. *PhotoMod SolverA* and *SolverS* is capable to import/export aerial triangulation results which is get by using the software for block adjustment *PATB* (Available from internet: <http://www.racurs.ru> ; <http://www.k2-photogrammetry.de/products/patb.html>).

PhotoMod DTM functionality. The *PhotoMod DTM* module creates and edits the digital terrain model (DTM). The module supports any type of digital terrain model: pickets, breaklines, Triangulated Irregular Network (TIN), DEM, contour lines, ect. DTMs may be edited in either mono or stereo mode. A special 3D window is used to view and analyze DTMs from different angles (Available from internet: <http://www.racurs.ru>).

PhotoMod DTM has a powerful set of tools for creating, editing, filtering and checking vector objects. External vector data can also be imported for use.

PhotoMod StereoDraw functionality. *PhotoMod StereoDraw* is a module for 3D vector objects drawing and editing in stereo mode. 3D vectors can be used for digital map creation and for digital elevation model generation in *PhotoMod DTM* as relief model elements. Besides 3D vectors creation in *PhotoMod StereoDraw*, vector objects can be imported from popular formats. *PhotoMod StereoDraw* has a full tool set for editing 3D vectors, topological reconciliation, dividing into thematic layers, attaching to classifier records. Like other modules - *StereoDraw* supports page-flipping and anaglyph stereomodels.

StereoDraw includes a *3D-Mode* program for 3D modelling and exporting specially prepared 3D objects to *DXF* format.

Main features of the module of *StereoDraw* is given in table 2.2 (Available from internet: <http://www.racurs.ru>):

Table 2.2. The main features of *PhotoMod StereoDraw*

Capabilities	Description
Marker control	3D marker could be: moved by mouse or keyboard; switched to “Marker - mouse” mode; Automated to “Snap to ground” mode. Adjust form, color and size of marker; 2D and 3D snapping mode during vectorization.

Table 2.2. continuation:

Capabilities	Description
Vector objects drawing	Supports point, line, and polygon object types; Create objects by code using classifier; Classifier editing; Create table of attributes linked to a classifier record, or unique for some objects; Supports thematic layers; Supports of topological links during vector object creating; 90-degree turns during polyline or polygon drawing; Measures of lengths, area and angle.
Editing of vector objects	Select objects, groups of objects, objects by layer, objects by code; Insert, delete or move of vertices and reversing point numeration; Edit topology links; Change object types; Check and correct topology; Create 2D and 3D buffer zones; Group operations with vertices — deletion, plane movement, move to chosen Z-position or step along Z-axis; Group operations with objects — deletion, move to chosen Z-position or step along Z-axis; Draws
Tuning and additional interface capabilities	Parallax tuning for better stereo effect; Undo with predefined history length; Correlator parameter tuning; Tune visualization parameters, etc.
Import/export of vector objects	Supported formats (ASCII, ASCII-A, MIF/MID, DXF, DGN and etc.); Export Classifier and attributes to DBF file, linked to the vector objects file.

PhotoMod Mosaic functionality. *PhotoMod Mosaic* module performs orthotransformation and mosaic creation in a single inseparable process. All geometric and photometric distortions are corrected during the orthomosaic creation process. The result of mosaic can be represented in a given cartographic projection both as a single image and as a set of sheets of specified size.

Any image which is available for *PhotoMod* software can be input for mosaic creation.

Created mosaics can be stored in the following files formats: *TIFF*, *Windows BMP*, *Vector RSW*, *GeoTIFF*, *ERDAS Imagine*, *NITF*, *JPEG* and *PNG*.

Formats for saving georeferencing data could be saved into these separate files: *PhotoMod Geo*, *ArcWorld TFW*, *ArcWorld BPW*, *MapInfo TAB*.

If a mosaic is cut into a number of sheets, raster and georeferencing files are created separately for each sheet (Available from internet: <http://www.racurs.ru>).

PhotoMod Vector functionality. *PhotoMod Vector* module is designed to create and edit digital vector maps.

Main features of *PhotoMod Vector* is given in table 2.3 (Available from internet: <http://www.racurs.ru>):

Table 2.3. The main features of *PhotoMod Vector*

Capabilities	Description
Digital map creation	Full support of topographic, geographic and navigation maps nomenclature; Maps creation with specified parameters; Map generalization; Special map symbology editor; Merge or split maps sheets; Maps transformation to/from different coordinate systems and cartographic projections; Maps printing with full marginalia and coordinate grid; Map updating.
Vector editor	Powerful tools for digitizing and editing; Topological operations (buffer zones, spatial joining and intersection of objects, variety of snapping functions, object creation using existing objects, and more); Map object measurements; Objects selection through queries; Group operations performing with objects; Smoothing of vector objects; Place inscriptions along curves; Inscription placement by selected attributes; Vector objects creation by coordinates from file or user input; Semiautomatic vectorization of linear objects.
Working with raster files	Georeferencing to digital maps; Mosaics creation; Adjustment of brightness/contrast; Adjustment of color palette; Digitization of over raster image.
Working with digital terrain models	Creation of DTM from 3D vector objects; Importation of DTMs from <i>PhotoMod DTM</i> module; Shed models creation of view; Profiles creation; Contour lines creation; Conversion of 2D objects to 3D objects.
Import/export	<i>DXF; MIF-MID; GRD; BMP; TIFF.</i>

***PhotoMod StereoVector* functionality.** *PhotoMod StereoVector* module is designed to allow parallel work with a digital map in *PhotoMod Vector* format. The *PhotoMod Vector* stereo window is identical to that of *PhotoMod StereoDraw*. In the mono window, maps are displayed in accordance with the selected map symbol library. This module is especially useful for updating existing maps.

Editing is simultaneously implemented in both windows. All changes performed in the stereo window are automatically displayed directly in the mono window, without any need of additional import/export operations.

In its functionality and user interface, *StereoVector* is generally similar to the *StereoDraw* module. However, there are two main differences:

- *Vector* module uses the map classifier, instead of the user-defined *PhotoMod* classifier;
- Created (edited) vector objects are stored in Vector map format, not as *PhotoMod* resources.

It is reasonable to use *PhotoMod StereoVector*, if further map work is to be continued in the Vector module or *Karta 2008* software. If created vector objects are expected to be used in other systems, it is preferable to use *StereoDraw* (Available from internet: <http://www.racurs.ru>).

***PhotoMod StereoACAD* functionality.** *PhotoMod StereoACAD* - is intended for 3D vectorization of stereopairs in *AutoCAD 2007/2008*. 3D objects created in *PhotoMod StereoACAD* are saved in *AutoCAD* format DWG/DXF. They are available for viewing and editing with using standard tools of *AutoCAD* instruments. *PhotoMod StereoACAD* works in page-flipping stereomode in following *AutoCAD OS: MS Windows 2000* and *MS Windows XP*.

PhotoMod StereoACAD provides the following image visualization functions:

- Page-flipping stereoscopic view;
- Real-time roam with fixed stereo cursor;
- Dynamic zoom;
- Two modes of marker moving – pixel and geodetic coordinates;
- 2D-3D snapping modes.

PhotoMod StereoACAD advantages:

- Easy to learn, easy to work;
- Capability to use sophisticated command set of *AutoCAD* graphic engine;
- Quality and fast stereo visualization;
- No special equipment to control stereo cursor.

***PhotoMod StereoLink* functionality.** *PhotoMod StereoLink* is a simple way to convert standard Intel-based PC with *Windows NT* (or later version) into quality stereo plotter. *StereoLink* provides effective stereo feature collection including such DTM features as break lines, height points, etc.

It allows stereoscopic view of stereo pairs, stereo pair images contrast and brightness adjustment, 3D coordinates measurements, stereoscopic feature collection, and creation of user feature tables. Stereo feature collection can be done with or without user tables.

PhotoMod StereoLink works within *MicroStation 95/SE/J* environment as an MDL-application and provides the following image visualization functions:

- Page-flipping stereoscopic view;

- Real-time roam with fixed stereo cursor;
- Dynamic zoom.

PhotoMod StereoLink advantages:

- Capability to use sophisticated command set of *MicroStation* graphic engine;
- Support of user's cell libraries and line styles;
- Quality and fast stereo visualization;
- No special equipment to control stereo cursor;
- Support of industry data formats;
- Support of hierarchical feature tables.

***PhotoMod ScanCorrect* functionality.** *PhotoMod ScanCorrect* program is designed for correction of metric errors caused by scanning of graphical data on the DeskTop Publishing (DTP) scanners.

Transformation of raster image according to the scanner distortion field is used for errors compensation. Scanner distortion field is computed from raster data obtained by scanning calibrated material (regular grid or a set of crosses).

The basic principles of working with *PhotoMod ScanCorrect* are the following:

- Inclusion of calibrated material into sequence of scanning of graphic material to obtain distortion field;
- Formation of the distortion field using raster data from the scanned calibrated material;
- Transformation of all raster data according to the distortion field.

Analysis of precision characteristics of DTP scanners shows that scanner distortion field is caused mainly by systematic scanner errors. Thus it is possible to apply the distortion field created from one image when transforming another.

If original graphic material (for example photo image) has calibrated crosses on it, the technique remains the same, but distortion field is formed from the same raster that is used in transformation. There is an option to input and reckon with the table containing coordinates of the crosses.

Input and output data of the program is 1, 4, 8, and 24-bit files in Windows BMP or TIFF formats. Auxiliary data (distortion field) is saved in ETM files.

The program allows fast converting of raster data (Available from internet: <http://www.racurs.ru>):

- From Windows BMP format to TIFF format;
- From TIFF format to Windows BMP format.

2.2. Images processing by using photogrammetric software

Images processing of object by photogrammetry method include of the following work steps (Sužiedelytė-Visockienė et al. 2011):

- Images interior orientation;
- Images relative orientation;
- Calculation of Bundle adjustment (triangulation);
- Draw the structural line of object;
- Creating Triangulated Irregular Network (TIN) of object surfaces;
- Creation of orthophoto map.

Interior orientation. The orientation procedure consists of the reconstruction of the interior orientation, which describes the geometry of the ray bundle in the camera, and the exterior orientation. The interior orientation specifies the functional dependencies between the principal point and the point, where the light ray intersects the image plain. The position of this intersection point is described by image coordinates (Wiedemann 2005). The image coordinate system defines a 2D image-based reference system of rectangular Cartesian coordinates. Its physical relationship to the camera is defined by reference points, either fiducial marks or a reseau, which are projected onto the acquired image. For a digital imaging system, the sensor matrix defines the image coordinate system. Usually the origin of the image or frame coordinates is located at the image centre (Luhmann et al. 2006). Thus, the purpose of interior orientation is to create the geometry of the projected rays that formed the image.

If the camera with the known camera calibration parameters is used, the transformation of image to the geodesy coordinate system is calculated according to the equation (Sužiedelytė-Visockienė, Bručas 2009):

$$x = x'_c + k_x(x_c \cos \varphi - y_c \sin \varphi), \quad (2.1)$$

$$y = y'_c + k_y(x_c \sin \varphi + y_c \cos \varphi), \quad (2.2)$$

where x, y – coordinates of a point in the geodesy coordinate system; x_c, y_c – coordinates of the points in digital image coordinate system; x'_c, y'_c – origin of the digital image coordinate system in the geodesy coordinate system; φ – the rotation angle of the image coordinate system in the geodesy coordinate system; k_x, k_y – the coefficients describing an image deformations along the x, y axes.

If the used camera is calibrated, the interior image orientation may be done by transforming the measured coordinates into a calibration system, defined by the fiducial marks or

the réseau crosses (Sužiedelytė-Visockienė, Bručas 2009).

If a non-calibrated camera has been used, an independent set of parameters of the interior orientation is necessary for each image. In frame cameras independent parameters of the interior orientation are only required if the zoom factor or the focus of the camera has been changed during the image acquisition (Sužiedelytė-Visockienė, Bručas 2009).

The procedure of the interior orientation using the photogrammetric system *PhotoMod* depends on the type of the camera with which the images were taken of:

- In images from an analog camera the fiducial marks on the margins of images should be measured. In this case the errors of interior orientation are calculated along both axes (Kiseleva 2002). The procedure used for the interior orientation is dependent upon the fiducial mark data and can be performed in manual, semiautomatic or fully automatic mode, as determined by the camera type (Available from internet: <http://www.racurs.ru>);

- For images from digital cameras, the interior orientation is performed in an automatic mode. It is only needed to enter the parameters of the interior orientation from the camera protocol and the axis orientation (Kiseleva 2002; Available from internet: <http://www.racurs.ru>). The parameters of the interior orientation (coordinates of the principal point, the focal length and the radial symmetric lens distortion coefficients) from the camera should be input in the same units – either pixels or millimetres (Racurs 2009).

The interior orientation should be done for each image which will be used for the data processing.

Relative orientation. The relative orientation recovers the position between the two ray bundles, creating a 3D stereo model (Ruzgienė 2008). The process of the relative orientation computes the relative orientation parameters to define the relative position of the pair of images (Racurs 2009).

The process of the relative orientation is as follows (Kiseleva 2002):

- measuring of the tie points in the stereo pairs in the overlapping areas and triplet zones (if we have three images);
- measuring of the tie points between adjacent strips;
- input and measurements of ground control points.

The following tie points position/number is considered as an optimum: tie points are grouped in the special standard zones in the images overlap, at least 2-3 points in each group (Fig.2.2) (Kiseleva 2002).

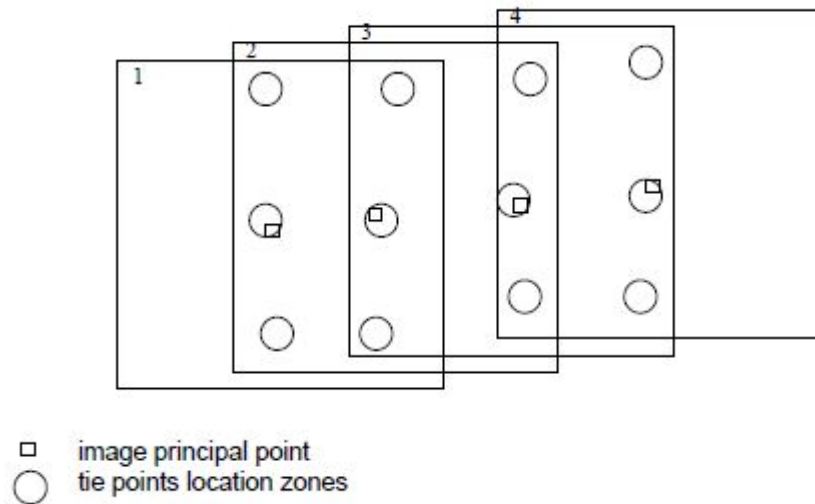


Fig. 2.2. Grouping of tie points in the images overlap

This way provides the most accurate and reliable determination of relative orientation parameters with possibility of localization of blunders. It is recommended that points in the triple overlap area were, if possible, placed uniformly in this zone (Kiseleva 2002).

Inter-strip tie points should be located in the side lap areas symmetrically relatively to its midline approximately as shown on Fig.2.3 (Racurs 2009).

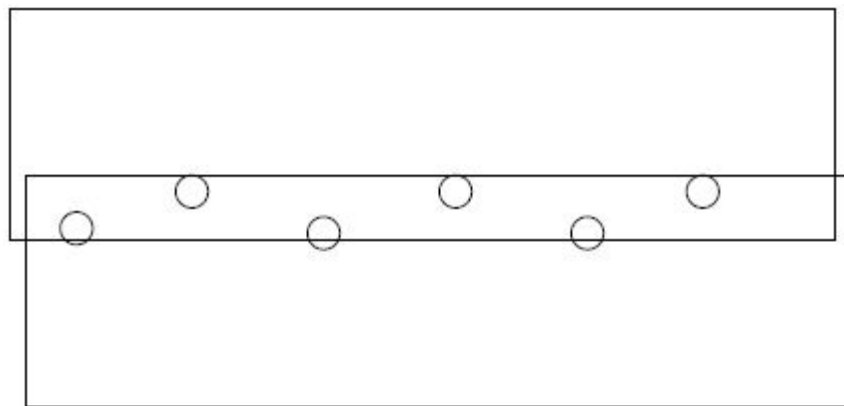


Fig. 2.3. Grouping of inter-strip tie points in the images side lap areas

It should be noticeable, that after entering a tie point in the inter-strip overlap area the results of the relative orientation procedure for the images containing this point are rejected. Thus, in this case, it should be entered such points before making orientation of stereo pairs in strips. Also, inter-strip tie points must be transferred to at least one adjacent image in each strip. Otherwise they will not be taken into account in the block adjustment by independent models method (Racurs 2009).

The measurement of a set tie points on overlapping images is needed to perform phototriangulation (Racurs 2009).

Tie points are used to create models from pairs of adjacent images and to create from these models the model of the whole strip or block in the block adjustment procedure (Racurs 2009).

Measuring points means their stereoscopic measuring on both stereo pair images (Racurs 2009).

Stereoscopic measuring can be fulfilled in three following ways (Racurs 2009):

- By manual positioning of the marker on each of two images;
- By manual positioning of the marker on one image and transferring the marked point to another image with correlation;
- By manual positioning of the marker in stereo mode.

Tie points can be measured in full automatic mode on both stereo pair images using correlation procedure (Racurs 2009).

The measurement of ground control points in photogrammetry is an essential part of producing accurate exterior orientation, DEMs and orthophotos (Available from internet: <http://www.pvts.net>). Coordinates of GCP could be entered in the software by importing the catalog of GPC (in text file) or entering values of GCP coordinates from keyboard (Racurs 2009). If the coordinates of the images projection centers is known – those could be used for block adjustment. In this case, the names of projection centers should be equal to the names of corresponding images. For the processing of single image in central projection the minimum number of control points is 3 (3 GCPs or 2 GCPs and the projection center). It is should be known that the GCP coordinates are given in the coordinate system selected, during project creation in *PhotoMod Montage Desktop* module (Racurs 2009).

After GCPs coordinates are inputed – the ground control points should be recognized and measured on the images. Ground control points must be identified and measured on one of the strip images only. If a point is imaged on more than one image it can be measured (transferred) to these images at steps 3 (Strip ties) and 4 (Tie points measurements) (Racurs 2009).

The measuring of ground control points on the images is follows (Racurs 2009):

- Selection of the point name in the list in the lower left part of the window;
- The marker positioning exactly on the ground control point on the image;
- The measurement appliance by pushing the button which is need to record the value of GCP.

When two new points are measured, selecting the third and following points in the list leads to the automatic positioning of the marker of the surrounding of selected point (Racurs 2009). Also, after coordinate values are input, points are measured on the images in semi-automatic or stereo mode (Available from internet: <http://www.racurs.ru>).

The more control and tie points are available, the better the results of the orientation

process in terms of accuracy and reliability can be obtained (Wiedemann 2005).

Bundle adjustment. During the bundle adjustment procedure the block adjustments of the strips and the image blocks takes place. The GCPs and tie points are used for the block adjustment (Racurs 2009).

PhotoMod Solver provides three algorithms to be used for the block adjustment procedure (Racurs 2009):

- **Independent strips.** This method is used to check out the gross errors, such as wrong coordinate values of control points, incorrect tie point's measurements, etc. The accuracy of this method in case of long strips (more than 10 images) may be a dozen times worse than the adjustment accuracy achieved by the other two methods.

- **Independent stereo pairs.** This method is usable for increasing the accuracy and detection of more delicate errors.

- **Bundle adjustment** is used for the final block adjustment.

In most cases, it is practical to perform adjustment alternately by method of independent stereopairs and bundle adjustment for searching and correction of delicate errors (Racurs 2009).

The break lines of object. In this part of processing of the digital images the break lines of the object are drawing (the 3D vector object is creating). Vectorization of objects could be done (Racurs 2009):

- **by stereomodes** (by using anaglyphic or shutter glasses);
- **by mono mode.**

Stereomode. Objects vectorization by stereo mode is performing by using anaglyphic or shutter glasses.

Anaglyphic glasses. Anaglyph stereoimage is formed by visualization of the left and right images of the stereopair “beyond” red and blue filters. To view such a picture you should use special anaglyph spectacles with red and blue glasses. Anaglyph stereomode requires no special equipment but it is not completely good for working with color images. Another disadvantage is that the picture gets a bit darker when viewing through filters (Racurs 2009).

Shutter glasses. Shutter glasses are liquid crystal glasses synchronized with the vertical refresh rate of the monitor. *PhotoMod* system supports two modes of working with shutter glasses (Racurs 2009):

- Interlace stereo;
- Page-flipping stereo.

Interlace stereo. Interlace (“line by line”) display mode divides the display frame into two semi-frames. The first one contains odd lines and the second one contains even lines. The right and left images of the stereopair are displayed one by one in ”odd” and “even” frames. The shutter

glasses are synchronized with the monitor vertical refresh rate and allow you to see them “simultaneously” and make stereo measurements. The interlace mode may be applied only for the whole screen, so it introduces some inconvenience when working with menus. Another disadvantage is sampling picture and, thus, reducing its resolution because of using semi-frames. The comfortable vertical refresh rate of your monitor should be at least 75 Hz “for each eye” (150 Hz for interlace mode) (Racurs 2009).

Page-flipping stereo. The page flipping (“frame by frame”) display mode provides the highest quality stereo picture because it uses full frames instead of semi-frames. The left and right images of the stereopair are displayed one by one synchronously with the frames switching. The shutter glasses are synchronized with the monitor vertical refresh rate and allows to see them “simultaneously” and make stereo measurements. For working in page-flipping mode - should be used a monitor with a good enough vertical refresh rate (at least 120 Hz) and an appropriate video adapter (Racurs 2009).

Mono mode. Monomode displays the left epipolar image of the stereopair and the left component of the stereomarker. All created in such a way vectors should be checked manually in stereomode to avoid possible correlator errors (Racurs 2009).

Triangulated Irregular Network (TIN). A triangulated irregular network (TIN) is a digital data structure used in a geographic information system (GIS) for the representation of a surface. A TIN is a vector based representation of the physical terrain surface, made up of irregularly distributed nodes and lines with three dimensional coordinates (x, y, and z) that are arranged in a network of non-overlapping triangles (Available from internet: <http://en.wikipedia.org>).

PhotoMod software provides several different strategies (algorithms) of TIN creation (Racurs 2009):

- Regular TIN;
- Adaptive TIN;
- Smooth TIN;
- TIN from vector objects;
- TIN from regions;
- TIN from pickets;
- Convex TIN from pickets.

Regular TIN. In case of regular model the program calculates Z values of all grid nodes using correlation algorithm. If the program fails to compute Z coordinate of a node in automatic mode the value of the third coordinate is calculated by interpolation between the adjacent nodes with automatically computed coordinates. The errors of automatic computations of the model can

be corrected later during the manual model editing. The final TIN is triangulated from grid nodes by modified Delaunay algorithm. It is recommended to build regular TIN when working with very heterogeneous images that can be characterized by the small-granular texture or high degree of details (Racurs 2009).

Adaptive TIN. The adaptive model is the most frequently used type of TIN. It is recommended to process images having big homogeneous or smooth parts. This method is also good for close-range photogrammetry (Racurs 2009).

The program calculates 3D coordinates using most distinctive point of image in the neighborhood of each inner grid node (the area size is 1/3 from grid step), if the option *Fixed nodes* is off. In nodes of grid boundaries the points are calculated exactly in node location. If it is impossible to calculate 3D coordinates for some node, it is skipped (except grid boundary nodes if the Rectangular boundary option is on, in this case such nodes are marked as "uncertain" and their height is calculated by interpolation of adjacent vertices) (Racurs 2009).

The final TIN is triangulated from grid nodes by modified Delaunay algorithm (Racurs 2009).

Smooth TIN. This option is suitable for smooth relief that has relatively small number of characteristic points. In the case of smooth models the polynomial interpolation function describing the surface is calculated based on 3D vector points (pickets) (Racurs 2009).

An additional parameter used for smooth model building is *Max. number of pickets* to calculate node. The total range of values is 3 – 1000. When number of pickets is not very big (500 – 1000) you should use all pickets that allow you to use all pickets and to eliminate time for searching of the closest to every node pickets whose number is equal to selected parameter value (Racurs 2009).

Smooth TIN is useful when working with smooth surfaces since it does not require editing operations related to the correlator errors (Racurs 2009).

This type of model is used for building TIN and computing contour lines for urban areas. In this case you should locate pickets on the “ground surface” to “remove” buildings, fences, trees, etc from TIN. For example you can create 3D vector lines along the town streets and use them as sets of pickets for smooth model creation. However you should keep in mind that the interpolation function may cause some residuals between real and calculated surfaces because of the smoothing (Racurs 2009).

TIN from vector objects. In this case TIN is created by triangulation of currently existing vector objects. Vector points become TIN nodes and vector lines and polygons are linked to the TIN as breaklines.

This method is very useful when you have big enough number of 3D vector objects, which completely describe the surface since it does not require editing operations related to correlator errors. As in case of smooth model you can use **TIN from vectors** algorithm to clean “noisy” elements as buildings, trees, etc. from the model just because they are not vectorized. Creating **TIN from vector objects** is more precise operation in comparison with smooth modelling, as it does not use the interpolation function (Racurs 2009).

TIN from regions. The area of the stereopair may be divided into separate regions (*local regions*) in order to use different strategies for building TIN in each region. So you can “bound” a village area by the local region and create **TIN from vectors** inside this region and **Adaptive TIN** outside this region. Prior to building TIN from regions you should create local regions and set up the parameters for each of them (Racurs 2009).

TIN from pickets. You may create a TIN by direct triangulation of pickets. Prior to TIN creation you can collect data (as 3D points – pickets) about terrain relief using different methods. *PhotoMod DTM* uses the same algorithms to build TIN and pickets. The difference is just that the pickets are not triangulated to the net of triangles and are string just as a set of XYZ points. To improve the relief model you can load the breaklines additionally to pickets (Racurs 2009).

You should start automatic pickets' extraction using regular, adaptive and smooth algorithms with rectangular grid creation (Racurs 2009).

You can also add pickets manually by positioning the marker on the place you need on stereo model (Racurs 2009).

Convex TIN from pickets. TIN is created by direct triangulation of pickets. The operation is similar to TIN creation using point vector objects, but in this case they are pickets (Racurs 2009).

The operation results in creation of TIN with convex border. It is useful if the initial pickets are distributed in such a way that they do not cover some part of a model – for instance, if there are vast water bodies (rivers and lakes) on large scale images (Racurs 2009).

Creation of orthophoto map. Orthophoto could be produced by using one image or several neighboring overlap images. Several neighboring overlap images generation into orthophotographic view is calling *mosaicking* (Shariat et al. 2008).

Types of terrain models used in orthorectification by using *PhotoMod* software could be provided by that several different strategies: (Available from internet: <http://www.racurs.ru>):

- User-defined constant height level;
- Ground control and tie points measured in the aerial triangulation step;
- DEM.

It is necessary to control the data quality in all the above-mentioned work stages, particularly the results of the triangulation. Thus, in the next section will be described accuracy of photogrammetric measurements data.

2.3. Accuracy control of photogrammetric work stages

The accurate measurements of ground control points and tie points in the digital images leads to the accurate results of triangulation (bundle adjustment). Thus, the measurements quality should be observed at every work step.

The measurement quality of tie and ground control points by using this photogrammetric software can be checked by the following ways (Sužiedelytė-Visockienė et al. 2011):

1) Accuracy control using correlation coefficient (if points are added by correlator). The acceptable value of the correlation coefficient can be determined from images quality. For contrast and high quality images the threshold is 0.9–0.95, for unclear images the threshold can be 0.8 at well recognized points.

2) Accuracy control using vertical parallax residual. After measuring 5 points on the stereopair, the relative orientation parameters of images pairs are calculated and then recomputed more exactly by software while points being added. The program calculates the maximum error (E_{\max}) of vertical paralallax residuals and the root mean squared error (RMS) (Sužiedelytė-Visockienė et al. 2011):

$$E_{\max} = 2 \times E_{\text{mean}} , \quad (2.3)$$

$$\text{RMS} = \sqrt{2} \times E_{\text{mean}} , \quad (2.4)$$

where E_{mean} – mean error of measurement points in the model. This error should not be greater than half of the scanning pixel size for analog camera and half of matrix pixel size for digital camera.

Measurement units are pixels or millimetres depending on camera units.

The images of the object were taken by using the digital camera *Canon EOS 1D Mark III* with the matrix pixel size of 6.4 μm . Thus, the mean value should not be more than 3.2 μm (Sužiedelytė-Visockienė et al. 2011). The maximum error and the root mean squared error of measured tie and ground control points should not exceed the values given in table 2.4.

Table 2.4. Calculated maximum error and root mean squared error to the digital camera *Canon EOS 1D Mark III*

$E_{max}, \mu\text{m}$	RMS, μm
6.4	4.5

3) Accuracy control by adjacent models (in overlapping or triplets). After measuring the tie and ground control points on stereo pairs (models) they should be transferred to the geodetic coordinate system. The relative orientation accuracy can be checked by comparing the discrepancies of the points measurements on the adjacent models (in triplets). Triplet errors: E_X, E_Y, E_Z in their X, Y, Z coordinates were calculated on two adjacent models. Mean triplet errors in XY plane and Z coordinates are calculated by following formulas (Sužiedelytė-Visockienė et al. 2011):

$$E_{mean}^{XY} = \sqrt{2} * 0,5 \times p_{xl}, \quad (2.5)$$

$$E_{mean}^Z = \frac{c}{b_x} E_{mean}^{XY}, \quad (2.6)$$

where p_{xl} – is the matrix pixel size for a digital camera (6.4 microns); c – is the focal length of a camera (Table 2.5, 2.6), b_x – is base in the image scale.

Approximate base in the image scale (b_x) was calculated by using the following formula (Kiseleva 2002) :

$$b_x = l_x \times (100\% - p_x) \times m/100\%, \quad (2.7)$$

where: b_x - survey basis (13.2 mm); l_x - image size along the X axis (35.9 mm); p_x - size of the overlapping zone (60 %); m –scale denominator of the image (0.92).

The discrepancies of E_{mean}^{XY} and E_{mean}^Z should not exceed the values given in table 2.5 (Sužiedelytė-Visockienė et al. 2011).

Table 2.5. Quality of measurements of GCP and tie points

Point	$E_{mean}^{XY}, \mu\text{m}$	$E_{mean}^Z, \mu\text{m}$
<i>GCP, Tie</i>	4.5	17.3

After relative orientation and triplet accuracy control the next stage – bundle adjustment can be performed. According software manufacturers, acceptable errors on bundle adjustment are dependent on different products: topographic maps or orthophoto creation (Kiseleva 2002).

Accuracy control of bundle adjustment for topographic maps creation. Accuracy control for topographic maps creation on ground controls points (GCP) after adjustment should not be greater than 0.2 mm in XY plane (in output map (plane) scale) and $0.15 \times h_{int}$ by Z, where h_{int} – contours interval of the output map (Kiseleva 2002).

Acceptable mean residuals on tie points – 0.3 mm in the output map scale. Also acceptable mean residuals on tie points by Z (Kiseleva 2002):

- $0.2 \times h_{int}$ – for contour interval of 1 m and also for scale 1:1000, 1:500 with the contour interval of 0.5 m;
- $0.25 \times h_{int}$ – for contour interval of 2.5 m and also scale – 1:2000 and 1:500 with the contour interval of 0.5 m;
- $0.35 \times h_{int}$ – for contour interval of 5 m and 10 m.

Accuracy control of bundle adjustment for orthophoto creation. Accuracy of adjustment for orthophoto creation is actual for architecture objects or orthophoto maps creation. In the *PhotoMod* software acceptable mean residuals of GCP in XY plane are 0.2 mm in output map scale and in Z – $1/3 \Delta h_{DTM}$, where Δh_{DTM} is mean residuals of Digital Terrain model (DTM). Calculation formula of Δh_{DTM} is (Kiseleva 2002):

$$\Delta h_{DTM} = 0.3mm \times c \times \frac{M}{r} , \quad (2.8)$$

where M – output map (plane) scale; r – maximum distance from the image point to the nadir point (mm), which equals to the half of diagonal of “working area”.

As it is seen from above by software manufacturers given information about bundle adjustment accuracy results - the program does not calculate σ_0 value for final evaluation of triangulation. In this case, the accuracy result of bundle adjustment should be calculated by using 1.1 or 1.2 formulas, given in section 1.3.

Further in next section will be described the images processing procedure and the results of images processing. Also the brief discussion about the processing results will be given.

2.4. Processing of the images by using digital photogrammetric software *PhotoMod*

The object of analysis is the North wall of the Vilnius University yard in the Vilnius old town (Fig. 2.4) (Sužiedelytė-Visockienė et al. 2011).



Fig. 2.4. Three overlapping images (P915-P912-P918)

The images were taken by using the *Canon EOS 1D Mark III* digital photo-camera. The characteristics are listed in Table 2.6 (Sužiedelytė-Visockienė et al. 2011).

Table 2.6. Characteristics of digital camera *Canon EOS 1D Mark III*

	Characteristics	Value
	Focal lengths (mm)	50
	Resolution (pixel)	21 mln.
	Pixel size, <i>pxl</i> (μm)	6.4×6.4
	Image size (mm)	35.9×23.9
	Image size (pixel)	5616×3744

This camera is calibrated (its optics distortions determined and evaluated) by using Tcc software at the Institute of Photogrammetry of University of Bonn (Germany) in 2008 (Sužiedelytė-Visockienė, Bručas 2009). The camera parameters are given in Table 2.7 (Sužiedelytė-Visockienė, et al. 2011).

Table 2.7. Result of camera *Canon EOS 1D Mark III* calibration (2008)

Parameter	Result
Focal length (mm)	
c	50.7583
Scale of image (constant)	
S_{xy}	0.99
The base point corrections of the photo-camera (mm)	
x_0	-0,0495
y_0	-0,2559
Radial-symmetrical distortion of the photo-camera	
A_1	-1.789E-09
Radial-asymmetrical distortion of the photo-camera	
B_1	1.017E-8
B_2	-1.655E-8

The images of the object were corrected for the digital camera objective distortions by using the special software *Tcc Distortion Correct* made in Germany. In the figure 2.4 were correct three overlapping images.

The calculated accuracy results of the prime step of images processing (relative orientation) is already known (see section 2.3). In this case the images processing could be started. The accuracy results of images processing are always observing with already known measurement discrepancies during the images processing procedure.

The first step of the processing of scanned images is the interior orientation. Because of the images were taken with digital camera, the first step of images processing was performed by software in automatic mode. The coordinates of principal point are known from camera definition where the parameters of sensor geometry during new project creation were entered. The coordinates of principal point are $x' = 2808$ and $y' = 1872$ given in the unit pixels (Sužiedelytė-Visockienė, Bručas 2009).

The next step of images processing was the relative orientation. During this procedure, first of all, the 8 tie points were placed uniformly in the triple overlap area and measured. Further, values of 10 ground control points coordinates were entered and ground control points were measured in stereo mode. The coordinates of ground control points are in the relative coordinate system of the building. The tie and ground control points were measured manually.

We had the three images and made two models P915-P912 and P912-P918 (triplets) during procedure of relative orientation. In this case the accuracy control of relative orientation by using digital photogrammetric software *PhotoMod* can be checked in followed ways:

- separately in each model (according formulas 2.3 and 2.4). In this case the accuracy control of the final result of relative orientation is computed;
- in all models together (according formulas 2.5 and 2.6). In this case the accuracy control could be observed separately for tie and ground control points in triplets after transference to the relative coordinate system of the building.

The final result of relative orientation was evaluated for two model separately according given formulas 2.3 and 2.4 (see section 2.4). Accuracy control result present in the table 2.8.

Table 2.8. Relative orientation result

Model	E_{max}, μm	RMS, μm
P915-P912	3.5	1.7
P912-P918	3.3	1.9
Average	3.4	1.8

This step of accuracy control using by manufacturer given formulas was successful: the average of maximum vertical parallax error (E_{max}) and root mean square error (RMS) for both model does not exceed computed values in table 2.4.

Also, this step of images processing was evaluated according given formulas 2.5 and 2.6 in triplets for tie and ground control points separately. The accuracy result of tie and GCP in triplet of relative orientation (mean triplet errors in XY plane and Z coordinates) is shown in table 2.9.

Table 2.9. Quality of triplets

Point	E_{mean}^{xy}, μm	E_{mean}^z, μm
GCP	3.0	8.0
Tie	4.0	16.0
Average	3.5	12.0

The second step of accuracy control using by manufacturer given formulas was also successful: the average of mean triplet errors in XY plane and Z coordinates do not exceed values which were computed according 2.4 and 2.5 formulas.

In order, to control accuracy results independent of software manufacturers given formulas, the results of this step of images processing were observed by looking for residuals of

each points and computing standard deviation. The displacement of the projection of the adjusted ground coordinate into the image compared to the measured image coordinate is given in table 2.10:

Table 2.10. Residuals between adjusted coordinates and between measured coordinates in the images

Point ID	Point type	Number of images the point was measured in	Image ID	Residuals x, μm	Residuals y, μm
102	GCP	2	P915	-0,1	-0,1
			P912	0,0	1,0
105	GCP	3	P918	0,1	0,8
			P915	-0,6	-0,6
			P912	0,8	0,8
106	GCP	3	P915	-0,1	-0,1
			P912	0,0	0,4
			P918	-0,1	0,7
107	GCP	2	P912	0,1	0,0
			P918	-0,2	0,3
109	GCP	3	P915	0,3	0,9
			P918	0,2	0,0
			P912	0,0	-0,7
110	GCP	2	P915	-0,4	-0,1
			P912	-0,1	-2,5
111	GCP	3	P918	-0,1	-5,1
			P915	0,0	0,6
			P912	0,0	-0,1
600	GCP	2	P912	0,1	-1,2
			P915	0,3	-0,2
602	GCP	3	P912	0,0	-1,2
			P918	-1,4	-1,5
			P915	-1,5	1,5
603	GCP	2	P918	0,3	0,0
			P912	-0,2	0,0

Table 2.10. continuation:

Point ID	Point type	Number of images the point was measured in	Image ID	Residuals x, μm	Residuals y, μm
901	TP	2	P918	-0,5	-0,5
			P912	0,2	0,1
902	TP	2	P912	0,0	1,0
			P915	-0,2	-0,2
903	TP	3	P915	-0,6	-0,8
			P918	-0,6	0,3
			P912	0,0	1,0
904	TP	3	P918	0,4	0,3
			P915	0,4	-0,3
			P912	0,0	0,6
905	TP	2	P912	-0,2	0,1
			P918	0,3	0,2
906	TP	2	P912	-0,1	0,0
			P918	0,2	0,4
907	TP	2	P912	0,0	0,0
			P918	-0,1	-0,4
908	TP	2	P912	0,0	1,1
			P915	-0,1	0,2
Standard deviation				0,4	1,1

As it is seen from table 2.10, the standard deviation is: $x = 0,4$ and $y = 1,1$ given in the units micron. This step of images processing was successful and results are great.

As was written in previous section - the program does not calculate σ_0 value for final evaluation of triangulation. In this case, for computation of triangulation result, the residuals of measured the image points of the ground control points (X, Y and Z) is shown in table 2.11:

Table 2.11. Residuals of measured the image points of the ground control point

Point ID	Number of images the point was measured in	Residuals X, m	Residuals Y, m	Residuals Z, m
102	2	-0,003	-0,002	-0,004
105	3	0,001	0,000	0,007
106	3	0,001	-0,001	0,004
107	2	0,001	-0,001	-0,007
109	3	0,001	0,007	0,007
110	2	0,002	-0,002	-0,005
111	3	-0,002	-0,002	0,004
600	2	0,001	0,002	0,004
602	3	-0,002	-0,004	-0,019
603	2	0,000	0,003	0,010
RMS		0,002	0,003	0,008

As can be see from previous table, the residuals of measured the image points of the ground control points are very trifling. The values of RMS shows the final result of aerial triangulation (see section 1.3). The final result of aerotriangulation is great. The triangulation report is given in appendix 1.

After the bundle adjustment the TIN data of an object is available for compiling break lines and orthophoto map. The accuracy of all these results is determined by the received accuracy of the aerial triangulation (Table 2.11) (Sužiedelytė-Visockienė et al. 2011).

The created break lines of the object were drawn in stereomode by using shutter glasses (Fig. 2.5).

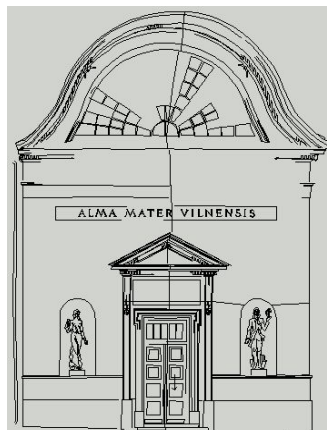


Fig. 2.5. Break lines of the object

The TIN of the object was created by using these strategies of the TIN creation:

- Regular TIN. By using this algorithm the smallest step of the grid was selected (0.5 mm). The result has obtained of a cloud of 341 550 points;
- Adaptive TIN. The result has obtained of cloud of 131 830 points by using this algorithm.
- Smooth TIN. Creating TIN of the object by using this algorithm the photo triangulation and break lines data was used. Also, the maximum number of pickets was carried out. Pickets are needed for the calculation of nodes highs. The result has obtained of 334 756 nodes.

The orthophoto of the object was created by using one image P912 (Fig. 2.4). The view of the object is captured from front on it. The image P912 was rectified with reference to ground control points and tie points. The smallest cell size of the ortophotographic view was set to 1 mm. The orthophoto was created for the statue on the left side (Fig.2.6).



Fig. 2.6 Orthophoto of the object

The orthophoto has a reference to a geodetic coordinate system and looks like a picture. In the orthophoto it is possible to measure the position and dimensions of the object.

3. DIGITAL PHOTOGRAMMETRIC SYSTEM *INPHO*

Inpho is a digital photogrammetric system which was founded in 1980 by Friedrich Ackermann, the retired head of the Institute of Photogrammetry of Stuttgart University. *Inpho* is designed for processing a wide range of digital imagery: scanned aerial film frames, images from digital aerial cameras as well as images from various satellite sensors for all standard tasks in a digital photogrammetric project, including geo-referencing, DTM generation, orthophoto production and 3D feature collection (Lothhammer 2005 ; Available from internet: <http://www.inpho.de>).

The main advantages of *Inpho*'s system are its rigorous mathematical modeling for top accuracy, and its smooth workflow and high degree of automation for supreme productivity (Available from internet: <http://www.inpho.de>).

The digital photogrammetric system *Inpho* as well as the digital photogrammetric system *PhotoMod* (see section 2.1) consist of several modules. The brief description about the main functions of each component will be given in further section.

3.1. The components of digital photogrammetric system *Inpho*

Inpho's digital photogrammetric workflow components are given in figure 3.1.

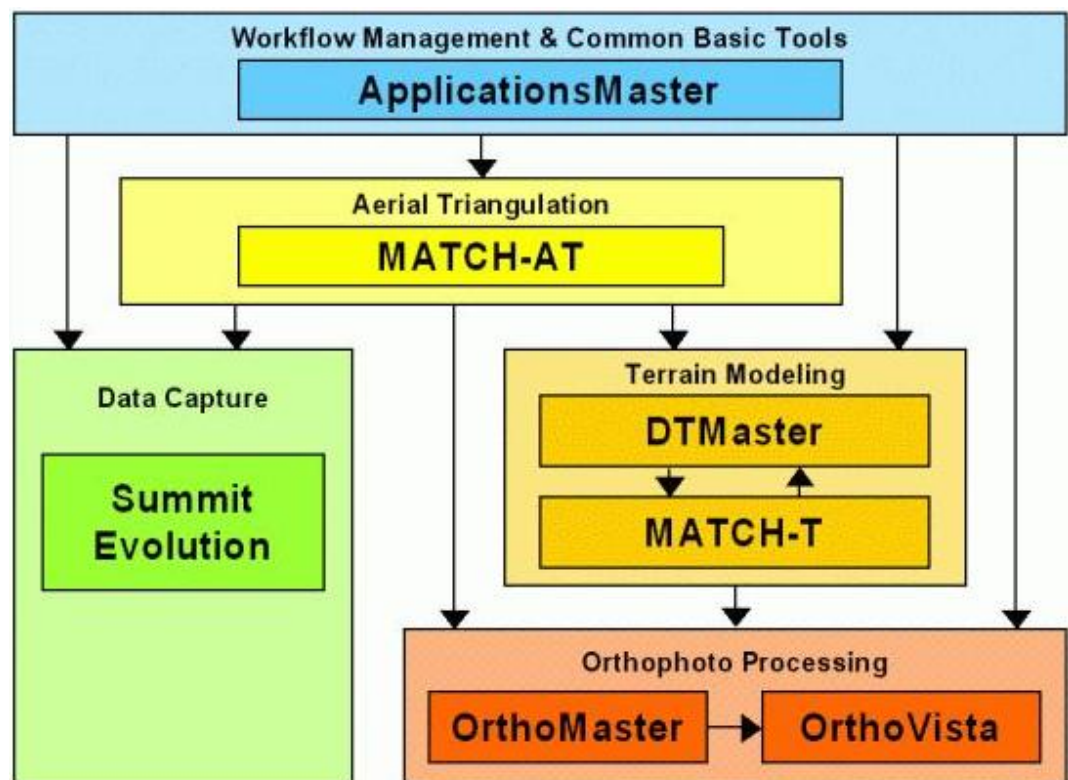


Fig. 3.1. *Inpho*'s modules

The components of a digital photogrammetric workflow (see fig. 3.1) guarantee a high degree of automation (Lothhammer 2005).

ApplicationsMaster. The *ApplicationsMaster* is the core component of *Inpho's* photogrammetric system which integrates project generation and handling tools as well as application programs (*inBLOCK*, *MATCH-AT*, *MATCH-T DSM*, *DT-Master* and *OrthoMaster*) into one working environment (Inpho 2010).

The ApplicationsMaster provides by using tools to setup and edit a project, to generate image pyramids, to determine interior orientation parameters and to import and export exterior orientations and image coordinates from and into various formats. Furthermore, conversion modules allow translating 3rd party project files (e.g. BAE SocetSet projects) into *Inpho* files as well as converting TIFF-images into another format (e.g. scanline TIFF into tiled TIFF). Finally, single points/files or whole projects can be transformed into a different coordinate system using the transform tool just as digital elevation models can be tiled, filtered, interpolated, merged or converted into different formats utilizing the DTMTToolkit (Inpho 2010).

MATCH-AT. By using this module of *Inpho's* digital photogrammetric software the full aerial triangulation for geo-referencing of any frame imagery from digital or analogue cameras in one automatic process, including point selection, point transfer and block adjustment could be done (Sigle, Heuchel 2001.; Available from internet: <http://www.inpho.de>).

MATCH-T (also named *MATCH-T DSM*). This module of *Inpho* is usable for an automated terrain and surface extraction providing highly precise digital terrain models and digital surface models derived from aerial or satellite imagery. The high dense of point clouds in urban and forest areas by using *MATCH-T* could be achieved. This module is designed for processing the most demanding photogrammetric projects with block sizes of 20000 images and even more (Available from internet: <http://www.inpho.de>).

DTMaster. *DTMaster* is designed for fast and precise DTM editing. *DTMaster* is available stand-alone, or as part of complete solutions for DTM generation by photogrammetry or *LIDAR* (Available from internet: <http://www.inpho.de>):

- *DTM Box* combines *DTMaster Stereo* with *MATCH-T*, *Inpho's* product for automatic DTM generation from aerial or satellite imagery;
- *LIDAR Box* combines *DTMaster* with *SCOP++ Kernel* and *SCOP++ LIDAR*, *Inpho's* products for advanced DTM processing and robust filtering of *LIDAR* data.

OrthoMaster. By using this module of *Inpho's* digital photogrammetric software the high quality orthophotos could be generated. The orthophoto could be generated from single image or blocks of images. In combination with *OrthoVista*, *OrthoMaster* is able to generate true orthophotos and true orthomosaics, in which all man-made 3D objects (e.g. buildings and bridges) are presented

in their true locations, without disturbing relief displacements (Available from internet: <http://www.inpho.de>).

OrthoVista. This module of Inpho is usable for automatic compensation of image intensity and color variations originated from the imaging process. *OrthoVista* computes radiometric adjustments that compensate for visual effects within individual images, such as hot spots, lens vignetting and color variations. Further, *OrthoVista* performs a blockwide color balancing by adjusting adjacent images to match in color and brightness. Multiple orthophotos are combined into one seamless, color balanced and geometrically perfect orthomosaic (Available from internet: <http://www.inpho.de>).

Summit Evolution. This module of *Inpho* is a digital photogrammetric stereo workstation and usable for vector data collection. Vector data could be collected directly into *ArcGIS*, *AutoCAD* or *MicroStation* softwares which are integral parts of *Summit Evolution* (Available from internet: <http://www.inpho.de>).

3.2. Accuracy control of photogrammetric work stages

The resolution of digital images has a direct influence on the accuracy of photogrammetric processes. In this case, all accuracy check thresholds are dependent on image resolution.

In general, the higher the resolution, the better the image quality and the better the results of photogrammetric processes.

As was mentioned before, the digital photogrammetric system is designed for aerial and satellite images processing. In this case, the following formulas of accuracy control are usable for aerial images (for satellite images the processing of those formulas is not advisable).

The accuracy control of measured tie points and ground control points in the image.

The residuals of the measurements in the images shows the displacement of the projection of the adjusted ground coordinates into the image compared to the measured image coordinate. The residuals of the image measurement on manual mode should correspond to the standard deviation ($SD_{x,y}$) (Inpho 2010):

$$SD_{x,y} = 1/3 \times \text{pixel} , (3.1)$$

where: pixel – pixel size of the camera (6.4 in units micron).

Accuracy control of ground control points measurements. The accuracy control of ground control points is based on calculation of residuals from given ground control points in terrain units (m) and from the adjusted ground control points.

In digital aerial triangulations (for processing aerial images), the achievable accuracy between adjusted ground control points planimetric coordinates and given ground control points coordinates can be calculated by followed formula (Inpho 2010):

$$\text{OBJECT}(X,Y) = 1/3 \times \text{pixel} \times \text{image scale}, \quad (3.2)$$

The accuracy in height could be computed according to the base/height ratio as a factor of the planimetry (Inpho 2010):

$$\text{HEIGHT ACCURACY} = \text{OBJECT}(X,Y) \times h/b, \quad (3.3)$$

where: h = focal length of the camera (mm); b = survey basis (mm).

Also the program calculate Root Mean Square (RMS) error with taking into account the residuals of adjusted ground control points and ground control points with given coordinates (see section 1.3).

Accuracy control of triangulation. The value of the standard deviation of unit weight (σ_0) shows the final result of aerial triangulation (see section 1.3) by making images processing with *Inpho* software. Standard deviation of unit weight at least should correspond to 1/3 pixel (Inpho 2010).

As is seen, the main formulas of accuracy control (3.1, 3.2 and 3.3) are based on image resolution.

The resolution of digital images (taken directly from digital camera) is much higher then the analogue images. As a result, the object surface (e.g. building facade) is represented by too many pixels. The tests have shown, that the in consequence of this, the matching of points could be failed and the accuracy results are not improved and might be made less by using this software. In this case, the accuracy control of using high resolution digital images could be less by changing the pixel identification accuracy in formulas 3.1 and 3.2. To made this, there is always need to keep a close watch on results during images processing for finding the best accuracy result of processed images.

Further in next section will be described the images processing procedure and the results of images processing. Also the brief discussion about the processing results will be given.

3.3. Processing of the images by using digital photogrammetric software *Inpho*

The digital images processing by using digital photogrammetric software *Inpho* was performed with that same images of the object, which were used for processing by digital photogrammetric software *PhotoMod* (see section 2.4) and with original images of that same object using new camera calibration parameters obtained with using scale bars after the camera calibration procedure (see section 6.4).

As we already know – the first step of the processing of scanned images is the interior orientation. Using *Inpho* photogrammetric software the determination of interior orientation is only required for digitized analogue images. While using digital images, the principal point coordinates are given directly from digital camera. The object images were taken by a digital camera and thus no interior orientation was necessary. The same applied to the *PhotoMod* photogrammetric software.

The coordinates of principal point are known from camera definition where the parameters of sensor geometry during new project creation were entered. The images which were used for processing were taken with that same digital camera *Canon EOS 1D Mark III*. In this case, the principal point coordinates are the same in both cases for corrected from the camera objective distortions images and for original images. The coordinates of principal point are $x' = 2807.50$ and $y' = 1871.50$ given in the unit pixels. The results of interior orientation is stored and can be seen only in project files (*.prj).

In the next step of the images processing the image points of the ground control points and tie points were measured (but not in stereo mode like it was done by using *PhotoMod* software) in corrected from the camera objective distortions images and in the original images. In order to reach an equivalent comparison of the results, the same 10 ground control points and the 8 tie points were measured in manual mode like it was done by using *PhotoMod* software.

After the points were measured the computations of the aerial triangulation were made. In the first step of the aerial triangulation the a-priori accuracy of the image and the object point was set according to the above mentioned formulas provided by the system manufacturer (see 3.2 section) in both cases for corrected from camera objective distortions images and for original images. In this case, the results still indicated a slightly unbalanced weight of the involved observation types, image and object point measurements.

The images were taken with a 21MPixel camera. This high number of pixels leads to a far too high resolution of the object and does not correspond to the lower definition accuracy of points on the rough surface of the building's facade. As a consequence details on the facade are never better defined than within a few pixel and thus the formula given in section 3.2 does not hold.

In order to analyse the quality of the bundle adjustment, it is possible to calculate image coordinate residuals (corrections), standard deviations of object points and orientation data, correlations between parameters and reliability numbers for the detection of gross errors and also for results observing (Luhmann et al. 2006). In the followed tables the accuracy results of basic images processing steps for corrected from camera objective distortions images and for original images are given. These results lead to final result of the aerial triangulation. The accuracy of the image and the object point was set irrespective of the formulas given in section 3.2.

The displacement of the projection of the adjusted ground coordinate into the image compared to the measured image coordinate for corrected from camera objective distortions images and for original images is given in table 3.1.

Table 3.1. Residuals between adjusted coordinates and between measured coordinates in the images

General information				Results			
				Before camera calibration		After camera calibration	
Point ID	Point type	Number of images the point was measured in	Image ID	Residuals x, μm	Residuals y, μm	Residuals x, μm	Residuals y, μm
102	GCP	2	P915	0,2	0,0	-0,8	-1,8
			P912	-0,5	-0,2	0,4	1,8
105	GCP	3	P918	0,4	0,8	-0,5	0,9
			P915	0,3	0,0	-0,2	-0,5
			P912	-0,8	-0,9	0,5	-0,3
106	GCP	3	P915	0,4	-0,5	0,5	-1,2
			P912	-0,1	-0,2	-0,6	-0,2
			P918	-0,2	0,7	0,2	1,6
107	GCP	2	P912	-3,7	-1,3	-0,9	0,3
			P918	3,9	1,7	1,1	0,4
109	GCP	3	P915	-1,8	-2,1	-0,1	1,0
			P918	-0,1	-0,1	-0,7	-2,1
			P912	3,2	0,8	1,8	-0,5
110	GCP	2	P915	0,3	1,7	-0,5	1,0
			P912	-0,6	-1,3	-1,2	0,8

Table 3.1. continuation:

General information				Results			
				Before camera calibration		After camera calibration	
Point ID	Point type	Number of images the point was measured in	Image ID	Residuals x, μm	Residuals y, μm	Residuals x, μm	Residuals y, μm
111	GCP	3	P918	-2,9	-1,8	-1,1	-1,0
			P915	0,5	1,4	-0,5	0,8
			P912	2,1	0,9	1,2	0,3
600	GCP	2	P912	0,2	-2,0	0,0	0,1
			P915	-0,1	2,0	-0,1	0,1
602	GCP	3	P912	-0,5	1,6	-0,5	-0,8
			P918	0,1	-1,9	0,1	0,4
			P915	0,1	0,5	0,4	0,5
603	GCP	2	P918	-1,3	0,4	0,8	2,1
			P912	1,0	-0,3	-0,7	-2,2
901	TP	2	P915	0,0	-0,8	0,0	-0,7
			P912	0,0	0,8	0,0	0,7
902	TP	3	P918	1,7	1,4	0,9	1,0
			P915	-0,1	-1,0	0,9	0,3
			P912	0,3	-0,4	-1,7	-1,3
903	TP	3	P915	0,0	0,2	-1,0	-1,1
			P918	-0,1	0,2	-1,1	-3,0
			P912	0,1	-0,5	2,0	1,9
904	TP	2	P918	0,0	0,4	0,0	-1,3
			P912	0,0	-0,4	0,0	1,3
905	TP	3	P915	1,1	0,4	-0,2	0,3
			P918	1,1	-2,2	-0,2	-1,2
			P912	-2,3	1,8	0,3	0,9
906	TP	3	P912	1,7	1,5	1,2	-0,2
			P915	-0,9	-1,5	-0,6	0,8
			P918	-0,8	0,0	-0,6	-0,8

Table 3.1. continuation (1):

General information				Results			
				Before camera calibration		After camera calibration	
Point ID	Point type	Number of images the point was measured in	Image ID	Residuals x, μm	Residuals y, μm	Residuals x, μm	Residuals y, μm
908	TP	2	P912	0,0	0,0	0,0	0,8
			P915	0,0	0,0	0,0	0,7
909	TP	3	P915	0,0	-0,5	0,9	-1,6
			P912	0,0	0,4	-1,8	-0,7
			P918	0,0	0,2	0,9	1,0
Standard deviation				1,3	1,1	0,8	1,2

As it is seen from table 3.1, the maximum residuals (the worst points) of measured in corrected from camera objective distortions images are: $x = 3,9$ and $y = -2,2$ given in the units micron. These residuals are in points 107 and 905 (in images P918) respectively. Nevertheless of those maximum residuals in previous mentioned points, the standard deviation of all residuals is acceptable. The result of standard deviation of all measured points in corrected from the camera objective distortions images is: $x = 1,3$ and $y = 1,1$ given in the units micron. It could be stated that this step of images processing was successful and results are great.

The maximum residuals between adjusted and in the image space measured points in the original images which were used after camera calibration procedure are: $x = 2,0$ and $y = -3,0$ given in the units micron. These residuals are in point 903 (in the image P912 and P918) respectively. Despite the fact that residuals of those points are slightly higher from the other points - the result of standard deviation of all measured points in corrected from camera distortions images is: $x = 0,8$ and $y = 1,2$ given in the units micron. It could be stated that this step of images processing was successful and results are great.

The table 3.2 shows the residuals of measured the image points of the ground control points (X, Y, and Z) also for corrected from camera objective distortions images and also for original images.

Table 3.2. Residuals of measured the image points of the ground control point

General information		Results					
		Before camera calibration			After camera calibration		
Point ID	Number of images the point was measured in	Residuals X, m	Residuals Y, m	Residuals Z, m	Residuals X, m	Residuals Y, m	Residuals Z, m
102	2	-0,004	-0,002	0,002	-0,007	0,001	0,000
105	3	-0,002	-0,002	0,000	-0,004	0,002	0,002
106	3	0,001	-0,001	0,002	0,002	0,002	0,001
107	2	0,002	0,010	-0,010	0,005	0,011	0,000
109	3	0,016	-0,021	-0,017	0,016	-0,025	0,011
110	2	-0,004	0,007	0,006	-0,004	0,001	0,005
111	3	-0,002	0,007	0,014	-0,004	0,002	0,003
600	2	0,003	0,000	-0,002	-0,003	0,004	0,001
602	3	-0,004	0,003	0,000	-0,001	0,002	0,001
603	2	-0,005	0,001	0,005	0,001	-0,001	0,003
RMS		0,006	0,008	0,008	0,006	0,009	0,004

From previous table, the biggest discrepancy between adjusted ground control points planimetric coordinates and between given ground control points coordinates in the 109 point is seen. The biggest discrepancy in height accuracy is seen in the 109 point also. This high discrepancy in X, Y and Z coordinates in 109 point is in corrected from camera objective distortions images and in the original images. In consequence of the high discrepancies in the 109 point the values of RMS are higher. But the residuals calculated in the adjustment should not be used directly for the detection of outliers (Luhmann et al. 2006). In this case and in order to reach an equivalent comparison of the results, the 109 point was not eliminated from adjustments.

Despite the fact that the 109 point was not eliminated from adjustments, the value of the standard deviation (σ_0) which shows the final result of aerial triangulation is 0.5 in units micron (0.1 pixel size) for corrected from camera objective distortions images (before camera calibration) and in the original images (after camera calibration). The final result of aerial triangulation is great. The triangulation statistics and report of corrected from camera objective distortions images are given in appendix 2 and 3 respectively. The triangulation statistics and report of the original images are given in appendix 4 and 5 respectively.

4. BUNDLE BLOCK ADJUSTMENT *BLUH*

The work with a bundle triangulation program is an optimization process that finds the optimum positioning of the “image-network” in relation to the control point provided. As a result of diverse requirements and applications there are many different bundle adjustment packages on the market. As examples, for aerial applications there are (Luhmann et al. 2006):

- *PAT-B (PAT-M)* (University of Stuttgart, Germany) (Ackermann et. al. 1970);
- *BLUH* (University of Hannover, Germany) (Jacobsen 1982);
- *ORIMA* (Leica Geosystems, Switzerland)

and for close range photogrammetry (Luhmann et al. 2006):

- *BINGO (GIP, Germany)* (Kruck 1983);
- *STARS (GSI, USA)* (Fraser and Brown 1986);
- *CAP (K² Photogrammetry, Germany)* (Hinsken 1989);
- *ORIENT* (Technical University of Vienna, Austria) (Kager 1989);
- *PHIDIAS/BUN (PHOCAD, Germany)* (Benning and Schwermann 1997);
- *AX. ORI (AXIOS 3D, Germany)* (Hemken and Luhmann 2002).

The most famous ones for aerial applications are *PAT-B* and *BLUH* (Wiedemann et al. 2001).

The program system *BLUH* is optimized for aerial triangulation but not limited to this. Even close range images taken from all directions (with exception of $\omega = 80 - 120$ grads) can be handled. *BLUH* software is based on the collinearity equation. Observations are photo coordinates, control point coordinates and (if available) coordinates of the projection centres (usually determined by relative kinematic GPS positioning). Unknowns are the photo orientations, object coordinates and additional parameters (if self calibration with additional parameters is specified for the program run) (Jacobsen 2009).

By using software package *BLUH* the bundle block adjustment of the images was done.

4.1. Purpose of bundle block adjustment

Bundle block adjustment (bundle triangulation, multi-image triangulation, multi-image orientation) is a method for the simultaneous numerical fit of an unlimited number of spatially disturbed images (bundle of rays). It makes use of photogrammetric observations (measured image points), survey observations and an object coordinate system. Using tie points, single images are merged into a global model in which the object surface can be reconstructed in three dimensions. The connection to a global object coordinate system can be provided by a minimum number of

ground control points. In this case, at least three control points should be used (Atkinson 2001). Larger areas without ground control points can be bridged by tying the images to a photogrammetric block. The corresponding (homologous) point are called tie points and represent image rays that should intersect in their corresponding object point with minimum inconsistency (Luhmann et al. 2006).

In an over-determined system of equations, an adjustment technique estimates 3D object coordinates, image orientation parameters and any additional model parameters, together with related statistical information about accuracy and reliability. Since all observed (measured) values, and all unknown parameters of a photogrammetric project are taken into account within one simultaneous calculation, the bundle triangulation is the most powerful and accurate method of image orientation and point determination in photogrammetry (Luhmann et al. 2006).

By block adjustment the exterior orientation parameters of a block of images, as well as the ground coordinates of tie points, are determined simultaneously (Albertz, Wiggenhagen 2009).

The method is based on the mathematical model of perspective geometry, and uses directly the image coordinates as observations. For the computation the bundles of rays from the projection centres to the image points are established, according to the collinearity equations (Albertz, Wiggenhagen 2009):

$$x'_i = C_k \frac{a_{11}(X_i - X_0) + a_{21}(Y_i - Y_0) + a_{31}(Z_i - Z_0)}{a_{13}(X_i - X_0) + a_{23}(Y_i - Y_0) + a_{33}(Z_i - Z_0)}, \quad (4.1)$$

$$y'_i = C_k \frac{a_{12}(X_i - X_0) + a_{22}(Y_i - Y_0) + a_{32}(Z_i - Z_0)}{a_{13}(X_i - X_0) + a_{23}(Y_i - Y_0) + a_{33}(Z_i - Z_0)}, \quad (4.2)$$

where given are: C_k - focal length; X_i, Y_i, Z_i – coordinates of the ground control points;

measured: x_i, y_i – image coordinates;

unknowns: $X_0, Y_0, Z_0, \varphi, \omega, \kappa$ (the angles are included in the rotation matrix a_{ii}), X_i, Y_i, Z_i of the tie points.

$$v = A_1 \times x_1 + A_2 \times x_2 - l, \quad (4.3)$$

Adjustment with x_1 = object coordinates and x_2 = image orientation parameters.

In the followed sections the brief discussion about bundle adjustment by using for this purpose suitable software will be given.

4.2. The modules of *BLUH*

The program system *BLUH* has been written for handling in the command window (CMD). The program system has no dialogue and is subdivided into several program modules to ensure a flexible handling (Jacobsen 2009):

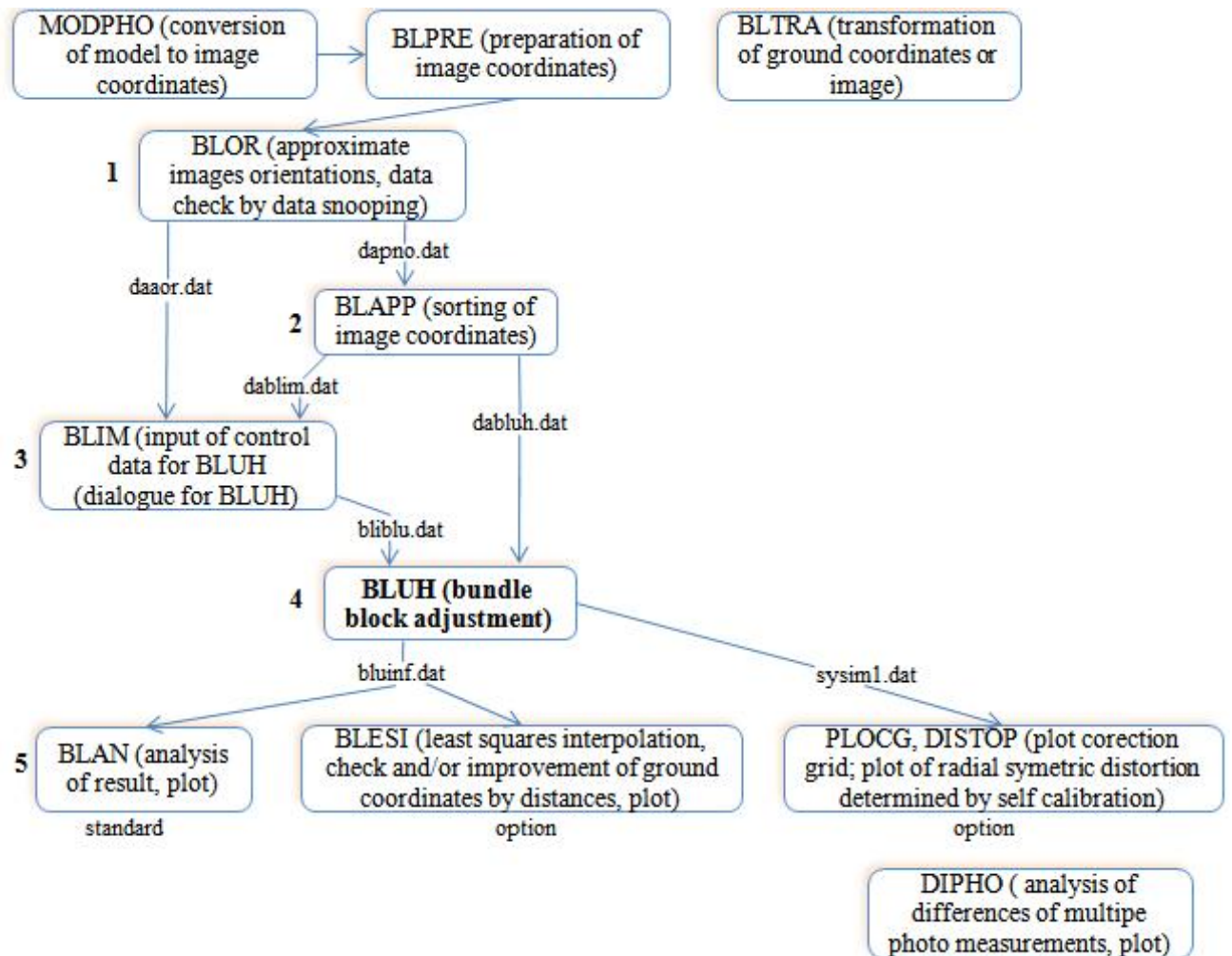


Fig. 4.1. The modules of *BLUH*

For the computation of a bundle block adjustment only the modules *BLOR*, *BLAPP*, *BLIM* and *BLUH* are necessary, they can be handled as one unique set or separately (in figure 4.1. they are marked with different colour). Even a batch handling of this group is possible or in can be included into a shell because the control data can be introduced not only by dialogue, it is also possible to introduce it by support files. The other modules can be used for special conditions, for analysis of the data and for other support of the data handling (Jacobsen 2009).

4.3. Results of the *BLUH* processing

After the adjustment in *Inpho* when the corrected from camera objective distortions images and the original images were processed, all measured image co-ordinates of each sub-block and ground control points coordinates were exported in a *BLUH* format. The two separate files for exportation were created. All observations (image coordinates, original ground control points coordinates) were adjusted in a bundle block adjustment.

In order to analyse the quality of the bundle block adjustment, the basic steps of computed results were observed (table 4.1, 4.2). The same manner the results for corrected from camera objective distortions images and for the original images were observed by processing images with digital photogrammetric softwares *PhotoMod* and *Inpho*.

Table 4.1. Residuals between adjusted coordinates and between measured coordinates in the images

General information				Result			
				Before camera calibration		After camera calibration	
Point ID	Point type	Number of images the point was measured in	Image ID	Residuals x, μm	Residuals y, μm	Residuals x, μm	Residuals y, μm
102	GCP	2	P915	0,0	0,2	0,0	-1,0
			P912	0,0	-0,2	0,0	1,1
105	GCP	3	P918	0,4	0,8	-1,3	-1,0
			P915	0,4	0,0	-1,3	-1,4
			P912	-0,8	-0,8	0,5	0,5
106	GCP	3	P915	0,1	-0,6	1,5	-1,2
			P912	-0,1	-0,1	-0,6	0,8
			P918	0,1	0,7	1,3	2,4
107	GCP	2	P912	0,0	-1,3	0,0	0,7
			P918	0,0	1,3	0,0	-0,7
109	GCP	3	P915	-1,2	-1,6	-0,6	1,1
			P918	-1,1	0,4	-0,7	0,4
			P912	2,3	1,2	1,3	-1,8
110	GCP	2	P915	0,0	1,5	-0,2	0,5
			P912	0,0	-1,6	0,2	-1,7

Table 4.1. continuation:

General information				Result			
				Before camera calibration		After camera calibration	
Point ID	Point type	Number of images the point was measured in	Image ID	Residuals x, μm	Residuals y, μm	Residuals x, μm	Residuals y, μm
111	GCP	3	P918	-0,8	-2,0	-1,4	-1,9
			P915	-0,8	1,4	-0,8	1,1
			P912	1,6	0,5	1,4	-0,3
600	GCP	2	P912	-0,1	-2,0	0,0	-1,4
			P915	0,1	2,0	0,0	1,4
602	GCP	3	P912	-0,3	1,7	-0,6	1,5
			P918	0,1	-1,9	1,2	-1,7
			P915	0,2	0,2	1,4	-1,9
603	GCP	2	P918	0,0	0,1	0,0	1,3
			P912	0,0	-0,1	0,0	-1,3
901	TP	2	P915	0,0	-0,6	-0,1	0,9
			P912	0,0	0,7	-0,1	-0,9
902	TP	3	P918	-0,2	1,5	-0,4	-1,6
			P915	-0,2	-1,2	-0,4	1,2
			P912	0,5	-0,3	0,5	0,9
903	TP	3	P915	-0,1	-0,1	0,0	-0,9
			P918	-0,1	0,3	-0,1	-0,8
			P912	0,2	-0,2	0,0	0,4
904	TP	2	P918	0,0	0,2	0,0	1,2
			P912	0,0	-0,2	0,0	-1,2
905	TP	3	P915	1,2	0,4	1,7	-0,6
			P918	1,2	-2,3	1,6	1,3
			P912	-2,4	1,9	-2,2	1,3
906	TP	3	P912	1,5	1,5	1,0	-1,1
			P915	-0,8	-1,5	-0,4	-1,8
			P918	-0,7	-0,1	-0,5	0,9

Table 4.1. continuation (1):

General information				Result			
				Before camera calibration		After camera calibration	
Point ID	Point type	Number of images the point was measured in	Image ID	Residuals x, μm	Residuals y, μm	Residuals x, μm	Residuals y, μm
908	TP	2	P912	0,0	-0,1	0,1	-1,4
			P915	0,0	0,1	-0,1	0,3
909	TP	3	P915	0,4	-0,7	1,6	-1,1
			P912	0,0	-0,1	-3,0	0,1
			P918	0,4	0,6	1,3	1,3
Standard deviation				0,8	1,1	1,0	1,2

As it is seen from previous table, the maximum residuals (the worst points) measured in corrected from camera objective distortions images are: $x = -2,4$ and $y = -2,3$ given in the units micron. These residuals are in the points 905 (in the images P912 and P918) respectively. Nevertheless of those maximum residuals in previous mentioned points, the standard deviation of all residuals is acceptable. The result of standard deviation of all measured points in corrected from camera objective distortions images is: $x = 0,8$ and $y = 1,1$ given in the units micron. This step of images processing was successful and results are great.

The maximum residuals between adjusted and in the image space measured points in the original images which were used after camera calibration procedure are: $x = -3,0$ and $y = 2,4$ given in the units micron. These residuals are in the points 909 and 106 (in the images P912 and P918) respectively. The residuals in the other points are less. Nevertheless the result of standard deviation of all measured points in the original images is: $x = 1,0$ and $y = 1,2$ given in the units micron. This step of images processing was successful and results are great.

The table 4.2 shows the residuals of measured the image points of the ground control points (X, Y, and Z) for corrected from camera objective distortions images and for original images.

Table 4.2. Residuals of measured the image points of the ground control point

General information		Result					
		<i>Before camera calibration</i>			<i>After camera calibration</i>		
Point ID	Number of images the point was measured in	Residuals X, m	Residuals Y, m	Residuals Z, m	Residuals X, m	Residuals Y, m	Residuals Z, m
102	2	0,004	0,002	-0,009	-0,010	0,014	0,006
105	3	0,001	0,002	-0,001	0,007	-0,002	0,020
106	3	-0,002	0,001	-0,003	0,002	-0,011	0,009
107	2	0,001	-0,02	0,043	0,007	0,015	-0,009
109	3	-0,015	0,019	0,021	0,005	-0,011	0,010
110	2	0,004	-0,006	-0,012	-0,005	-0,012	-0,018
111	3	0,002	-0,005	-0,016	-0,005	-0,023	-0,013
600	2	-0,003	0,001	-0,002	-0,003	0,017	-0,021
602	3	0,003	-0,003	-0,001	0,006	-0,006	-0,006
603	2	0,004	-0,001	-0,011	0,015	0,006	-0,019
RMS		0,005	0,009	0,017	0,007	0,013	0,014

As can be seen from previous table, the residuals of measured the image points of the ground control points are very trifling for images which are corrected from camera objective distortions. Those same residuals for the original images are small to. The final result of bundle adjustment (σ_0) is 1.36 in units micron (0.3 pixel size) for corrected from camera objective distortions images (before camera calibration) and for the original images (after camera calibration). The bundle triangulation report of corrected from camera objective distortions images and of the original images are given in appendix 6 and 7 respectively.

5. ANALYZING PHOTOGRAMMETRIC SOFTWARE *AICON 3D STUDIO*

The analyzing software *AICON 3D Studio* is the one more software which was introduced and with which the digital camera *Canon EOS 1D Mark III* calibration procedure during Master thesis was done. Brief discussion about this system is given in followed sections.

5.1. Purpose of *AICON 3D Studio*

AICON 3D Studio is an analyzing software which is able to receive 3D data from different measuring systems and process them further. The *AICON 3D Studio* is a modular software. According to application range, the different modules of *AICON 3D Studio* are used. Due to the integration of different measuring modules, the *AICON 3D Studio* is an efficient control panel for different measuring instruments (Available from internet: <http://www.aicon3d.de>).

5.2. The modules of the analyzing photogrammetric software *AICON 3D STUDIO*

The analyzing photogrammetric software *AICON 3D Studio* consist of followed modules (Available from internet: <http://www.aicon3d.de>):

- *Digital Photogrammetric Analysis (DPA)* system;
- *DPS* system.

DPA system. One of integrated measuring module into the *AICON* software is a *Digital Photogrammetric Analysis (DPA)* system. The *AICON's DPA* system is 3D measurement system using for following applications (AICON 3D Systems GmbH 2009; Available from internet: <http://www.qfp-service.it>):

3D inspection

- Inspection of sheet metal parts and tolerance analysis;
- Fixture inspection;
- Comparison with *CAD*;
- Roundness inspection, e.g. tunnels or tanks;
- Measurement of large steel fabricated structures.

3D process analysis

- Deformation analysis in vehicle safety tests;
- Deformation analysis of sheet metal and plastic parts, e.g. in environmental chambers or strain tests;
- Motion analysis, e.g. of components under loa.

Measuring principle. *AICON's DPA* system are portable 3D measuring machine that use a high resolution digital camera for data collection. The part, which may be of any size, is photographed from a number of directions. The images could be processed and above mentioned tasks could be made either simultaneously with data collection (online processing) or after data collection (offline processing) with *AICON's* software. The *AICON* software automatically calculates the 3D coordinates of all targeted points. The calculation is based on the principle of spatial image triangulation and is processed completely automatic. In addition to 3D coordinates, *DPA* provides statistical analysis of the results with specific accuracy information about each coordinate (Available from internet: <http://www.qfp-service.it>).

DPS system. *DPS* system is the other one of integrated measuring module into the *AICON* software. Combined with the *DPS* system, it serves as optical 3D positioning equipment that controls the 3D position of the dummy relative to the vehicle during the positioning process. With the help of measuring points or adapters, the current dummy position is recorded in real time, and compared to nominal data.

With all points on the dummy measured and displayed simultaneously in vehicle coordinates, the technician can quickly put the dummy into its target position. Movements of the vehicle that are caused by the positioning of the dummy are compensated automatically because of continuous monitoring of a set of targeted reference points.

The system allows for the measurement of additional coordinates of single points, lengths or angles with the probe according to a predefined measuring plan. The results are shown in a measurement report. Further individual processing via an XML export is available (Available from internet: <http://www.aicon3d.de>).

By using *AICON's DPA* system the digital camera *Canon EOS 1D Mark III* calibration procedure was done. About camera calibration procedure is written in chapter 6.

6. CAMERA CALIBRATION

The primary objective of photogrammetry is to generate spatial and descriptive information from two-dimensional imagery (Habib et al. 2005). The accuracy obtainable in digital images processing depends on the scale and type of image, the instruments used, the skill of the compiler, the density of ground control points, the amount of terrain surface, and the nature of the vegetative cover. These factors relate to the data taken from the images (Available from internet: <http://www.blm.gov>). Thus, the images acquisition is the first step which leads to a high accuracy of images processing.

The images for photogrammetric purpose are taken by the analogue or digital photo cameras. In order to generate reliable and accurate information from images, photo cameras usually are calibrated before using them (Sužiedelytė-Visockienė, Bručas 2009).

Next in this chapter will be discussed about the purpose of camera calibration and the calibration procedure of non-metric digital photo-camera *Canon EOS 1D Mark III*. The calibration results will be given in the last section.

6.1. The goal of a camera calibration

The purpose of camera calibration is to determine the geometric camera model described by the parameters of interior orientation (Luhmann et al. 2006; Schenk 2005):

- Principal distance;
- Focal length of the camera;
- Image coordinates of principal points;
- Radial distortion;
- Tangential (asymmetric or decentring) distortion;
- Affinity and shear of the image coordinate system;
- Other additional parameters.

There are 3 different camera calibration methods characterised by the reference object used and by the time and location of calibration (Luhmann et al. 2006; Sužiedelytė-Visockienė, Bručas 2009):

- Laboratory calibration. Interior orientation parameters are determined by goniometers, collimators or other optical alignment techniques where imaging direction or angles of light rays are measured through the lens of the camera. The advantage of this method is that the calibration takes place under laboratory conditions and hence better accuracy at defining of

unknown quantities is achieved. Laboratory calibration is generally only used for metric cameras and is using before surveying.

- Test field calibration. This type of calibration is based on a suitable targeted field of object points with known coordinates and distances. The images of a test-field are taken from different positions and directions from several camera stations (the number of cameras stations depends on test field size), ensuring good ray intersection and filling the image format. The neighbour images should be overlapped. Measured image coordinates and approximately known object data are processed by bundle adjustment to give the parameters of the camera model (interior orientation) as well as the adjusted test field coordinates and the parameters of exterior orientation. Test fields can be mobile, or stationary.

- Self-calibration. For this type of calibration the images acquired for the actual object measurement are used. In this case the test field is replaced by the actual object which must be imaged under conditions similar to those required for test field calibration itself (spatial depth, tiled images and suitable ray intersections). Self-calibrations do not require coordinates of known reference points. The parameters of interior orientation can be calculated solely by the photogrammetric determination of the object shape. If employed, reference points can be used to define a particular global coordinate system for the parameters of exterior orientation.

The camera calibration procedure can be divided into several stages: test-field target images making, processing of the resulting images and estimation of the camera parameters (Sužiedelytė-Visockienė, Bručas 2009).

Determining the parameters of photo cameras (cameras calibration) is absolutely necessary for the successful images processing (Sužiedelytė-Visockienė, Bručas 2009).

In the next section will be written about non-metric camera *Canon EOS 1D Mark III* calibration procedure.

6.2. Measurements for the digital camera calibration

The non-metric camera *Canon EOS 1D Mark III* (see section 2.4) calibration was performed in the photogrammetric laboratory at Neubrandenburg University of Applied Sciences (Germany) using 3D test-field (fig. 6.1).



Fig. 6.1.Test-field for the camera calibration

The field consists of retroreflective targets with known coordinates and distances and of two calibrated scale bars with precisely known distance between points. In order to get spatial information some points are arranged on a stamp at the top of the plane (Abraham 2004).

In order to capture all types of distortions and stabilize the determination of the focal length (especially when using longer focal lengths) the images were taken:

- in different orientations. At each station, the camera was rotated around its optical axis by 0° , 90° and -90° ;
- in different inclinations.

The cameras position with used different orientations and inclinations is given in figure 6.2.

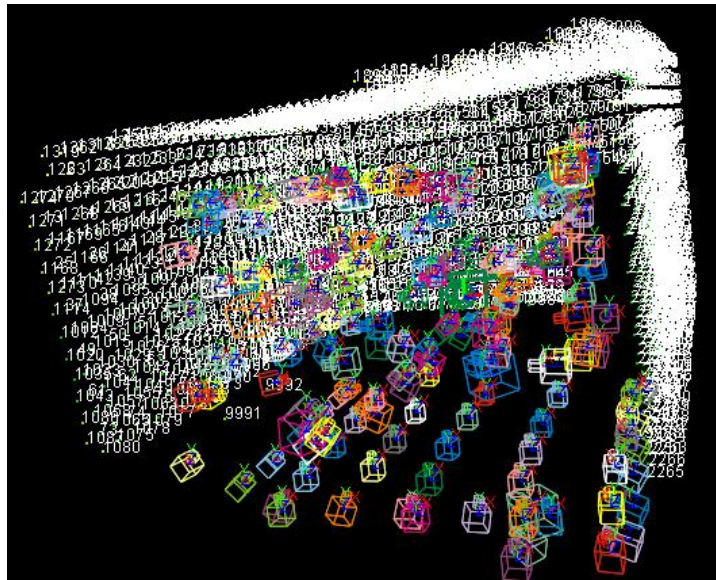


Fig. 6.2. Photo camera position

All automated camera parameters (zoom, auto focus, aperture, white balance, etc.) were kept constant during data capture (were turned off) (Wojtas 2010; Sanz-Ablanedo et al. 2010). The 185 images taken in that case for successful processing of calibration were used.

6.3. Computation of the digital camera calibration parameters

The images were processed and computations of camera calibration parameters were made with software *AICON* (see chapter 5). In order to evaluate the differences between calibration parameters and to estimate the necessity of using scale bars, the images were processed in two different ways:

- including scale bars for the images processing;
- not including scales bars in the images processing.

During the adjustment procedure the software created an approximate 3D model of the points marked on the test-field. The coordinates are required to number the retroreflective targets (including the scale bars), that are detected in the image and to set up correspondences between the targets in different images (fig. 6.3.).



Fig. 6.3. Numbered targets

The numbers of the points are always unique, otherwise the result of the bundle adjustment alignment will be inadequate (Sužiedelytė-Visockienė, Bručas 2009).

The accuracy of the result is defined by the mean value in the coordinate list for X, Y and Z in units mm, RMS also for X, Y and Z in units mm and standard deviation of the weight unit (σ_0) in units micron. The standard deviation (σ_0) shows the mean point measurement accuracy for all images of the adjustment statistics. The accuracy results of calibration are given in table 6.1.

Table. 6.1. Results of bundle block adjustment

Accuracy, μm	Calibration with using scale bars	Calibration without using scale bars
E_{mean}^{XY}	4.5	3.2
E_{mean}^Z	2.5	2.1
RMS xy	5.0	4.0
RMS z	3.4	3.1
σ_0	5	5

The software manufacturers have not listed the value which shows the successful adjustment. It is only stated, that the mean values and the RMS values should have similar sizes for X, Y and Z. The RMS value should be slightly higher than the mean value. However, the final result of bundle adjustment of all images (with scale bars and without it) is 5 in units micron. According the estimated σ_0 value it could be stated that the results of camera calibration in both ways are great (AICON 3D Systems GmbH 2009).

6.4. Results of the digital camera calibration

The interior orientation and lens distortion parameters of the camera, i.e. principal distance c , principal point offset x_0/y_0 , radial-symmetric and tangential distortion coefficients were calculated simultaneously with the numerical 3D reconstruction process by bundle adjustment (Peipe, Stephani 2003). Calibration results and precision parameters of camera are given in table 6.2.

Table. 6.2. The new calibration results of the digital camera *Canon EOS 1D Mark III*

<i>Parameters</i>	<i>Results</i>	
	<i>With using scale bars</i>	<i>Without using scale bars</i>
Focal length (mm)		
c	50,7930	50,7931
The base point corrections of the photo-camera		
x_0	-0,2282	-0,2324
y_0	0,2019	0,2026

Table. 6.2. continuation:

<i>Parameters</i>	<i>Results</i>	
	<i>With using scale bars</i>	<i>Without using scale bars</i>
Radial-symmetric distortion of the photo-camera		
A1	-6,4466E-05	-6,4508E-05
A2	4,1312E-08	4,1565E-08
A3	2,8812E-11	2,8407E-11
Radial-asymmetric distortion of the photo-camera		
B1	-7,1262E-05	-7,2810E-06
B2	-2,5987E-06	-2,5725E-06
Affinity/Orthogonality		
C1	1,3696E-03	1,3715E-03
C2	-2,5531E-05	-2,6262E-05

As can be seen from the previous table, the values of cameras interior orientation parameters which are estimated using scale bars and without them are very similar: differences between the focal length (c) in both cases is $\pm 0,0001$ in units mm; $x_0 = \pm 0,0042$ in units mm; $y_0 = \pm 0,0007$ in units mm. The differences between the radial-symmetric and between the radial-asymmetric distortions are very small: $A1 = \pm 4,2000e-08$; $A2 = \pm 2,5300E-10$; $A3 = \pm 4,0500E-13$; $B1 = \pm 6,3981E-05$; $B2 = \pm 2,6200E-08$; $C1 = \pm 1,9000E-06$; $C2 = \pm 7,3100E-07$. The previous values have no dimension.

Thus, both camera calibration parameters (see table 6.2) could be used for correction of the camera optical errors in images.

However, digital cameras are not manufactured specifically for the purpose of photogrammetric mapping, and thus have not been built to be as stable as traditional mapping cameras. If a camera is stable, then the derived internal orientation parameters should not vary over time. The test, which were made with digital cameras showed, that the internal orientation parameters was stable as long as no zoom and no auto focus were used after the camera calibration (Habib et al. 2008; Läbe, Förstner 2004).

7. THE RESULTS ANALYSIS OF PROCESSED IMAGES AND THE DIGITAL CAMERA CALIBRATION PARAMETERS

The corrected from camera objective distortions digital images and the original digital images after camera calibration procedure during the research work were processed. The digital images were processed by using digital photogrammetric softwares *PhotoMod* and *Inpho* which are developed for processing a wide range of digital imagery such as scanned aerial film frames, images from digital aerial cameras as well as images from various satellite sensors. By using those systems not only the bundle adjustment but also DTM, digital maps and orthophotos creation could be performed. The other one system by using which the bundle adjustment procedure was performed is *BLUH*. *BLUH* system is developed only for bundle triangulation and can be used for close range images taken from all directions.

It should be noted that the corrected from camera objective distortions digital images were processed by using both digital photogrammetric softwares (*PhotoMod* and *Inpho*) and the original images after camera calibration procedure were processed by using just digital photogrammetric software *Inpho*. The system *BLUH* was used for both types of the images processing.

Further in next sections the result analysis of processed images will be performed. Also, the comparison between old camera calibration parameters and between new camera calibration parameters will be given.

7.1. Aerial triangulation results analysis before camera calibration

In this section the results analysis of processed digital images which were corrected from camera objective distortions is performed.

The results of standard deviation between adjusted and measured points in image space were observed. The summerised results of calculated discrepancies (residuals) between adjusted points coordinates and between measured coordinates in image space is given in tabale 7.1.

Table. 7.1. Comparison of standard deviation between adjusted and between measured points in image space

Software	Images	Tie points	Control points	Standard Deviation, x (μm)	Standard Deviation, y (μm)
<i>PhotoMod</i>	3	8/8	10/10	0,4	1,1
<i>Inpho</i>	3	8/8	10/10	1,3	1,1
<i>BLUH</i>	3	8/8	10/10	0,8	1,1

As it can be seen from previous table, the results have slight differences only in x plane. The best result in image measurements was achieved with *PhotoMod*. Nevertheless the results reached with *PhotoMod*, *Inpho* and *BLUH* correspond accuracy requirements for measurements in image space: the values do not exceed 1,0 in units micron.

In order to make comparison of bundle triangulation results the same three images for processing were used. Also the 10 GCP were measured in manual mode. As a priori value, the standard deviation of the ground control points were set as 0,02 in units meters for X, Y and Z to guarantee the same conditions for all adjustments. The results of bundle triangulation are summarised in table 7.2.

Table. 7.2. Bundle triangulation results

Software	Images	Control points	σ_0 , μm	RMS X, m	RMS Y, m	RMS Z, m
<i>PhotoMod</i>	3	10/10	-	0,002	0,003	0,008
<i>Inpho</i>	3	10/10	0,5	0,006	0,008	0,008
<i>BLUH</i>	3	10/10	1,36	0,005	0,009	0,017

The *PhotoMod* does not show (compute) the σ_0 value. In this case, the comparison of results could be done to the RMS values which also show the triangulation result. Thus, the results were similar for all systems, but with slight differences in the planimetry and heights. The best results with respect to the RMS of the control points were achieved with *PhotoMod*.

Performing comparison to σ_0 value, best result was achieved with *Inpho* software (0,5 in units micron). The result for *BLUH* is slightly worse (1,36 in units micron). Nevertheless the result of bundle adjustment is good for both softwares, because the accuracy reaches 0,1 and 0,3 pixel size respectively. Also, according to the RMS values given in table 7.2, the assumption about dependence between RMS values and between the results of σ_0 could be made. In this case, the result of σ_0 with *PhotoMod* could be better than with *Inpho* and *BLUH*.

7.2. Aerial triangulation results analysis after camera calibration

In this section the results analysis of processed original digital images which were used after camera calibration is performed.

The results of standard deviation between adjusted and measured points in image space were observed. The summerised results of calculated discrepancies (residuals) between adjusted coordinates and measuerd coordinates in image space is given in tabale 7.3.

Table. 7.3. Comparison of standard deviation between adjusted and between measured points in the image space after camera calibration procedure

Software	Images	Tie points	Control points	Standard Deviation, x (μm)	Standard Deviation, y (μm)
<i>Inpho</i>	3	8/8	10/10	0,8	1,2
<i>BLUH</i>	3	8/8	10/10	1,0	1,2

As it can be seen from table 7.3, the results achieved with *Inpho* and *BLUH* correspond accuracy requirements for measurements in image space: the values do not exceed 1,0 in units micron. The better result is achieved with *Inpho*.

In order to make comparison of bundle triangulation results using original digital images after camera calibration procedure the 10 GCP were measured in manual mode. As a priori value, the standard deviation of the ground control points were set as 0,02 in units meters for X, Y and Z to guarantee the same conditions for all adjustments. The results of bundle triangulation are summarised in table 7.4.

Table. 7.4. Bundle triangulation results after the camera calibration procedure

Software	Images	Control points	σ_0 , μm	RMS X, m	RMS Y, m	RMS Z, m
<i>Inpho</i>	3	10/10	0,5	0,006	0,009	0,004
<i>BLUH</i>	3	10/10	1,36	0,007	0,013	0,014

The final result of aerial triangulation (σ_0) was achieved 0.5 in units micron (0.1 pixel size) and 1,36 in units micron (0.3 pixel size) by using digital photogrammetric software *Inpho* and system *BLUH* respectively. The accuracy result reached with *Inpho* and *BLUH* meets the accuracy requirements.

7.3. Comparison of aerial triangulation results before camera calibration and after camera calibration

In this section the results comparison of processed digital images before camera calibration (by using corrected from camera objective distortions digital images) and after camera calibration (by using the original digital images) is given. Because of the original digital images was not processed by using digital photogrammetric system *PhotoMod* – the system in results comparison was not involved.

The results of standard deviation between adjusted and measured points in image space during digital images processing were observed. The summerised results of calculated discrepancies (residuals) between adjusted coordinates and measuerd coordinates in image space before camera calibration and after camera calibration is given in tabale 7.5.

Table. 7.5. Comparison of standard deviation between adjusted and between measured points in image space before and after camera calibration

General information				Result			
				Before camera calibration		After camera calibration	
Software	Images	Tie points	Control points	Standard Deviation, x (μm)	Standard Deviation, y (μm)	Standard Deviation, x (μm)	Standard Deviation, y (μm)
<i>Inpho</i>	3	8/8	10/10	1,3	1,1	0,8	1,2
<i>BLUH</i>	3	8/8	10/10	0,8	1,1	1,0	1,2

As it can be seen from previous table, the results of this measurement step achieved by using digital photogrammetric softwares *Inpho* and *BLUH* are very similar in both cases: before camera calibration in corrected from camera objective distortions images and after camera calibration in the original images. But the better result in x and y planes is achieved by using the original digital images after camera calibration procedure which were processed with *Inpho* software. The result achieved with *BLUH* system by using the original digital images after camera calibration procedure is slightly higher in x plane.

In this step of images processing the best result was achieved with *BLUH* system by using corrected from camera objective distortions digital images before camera calibration procedure.

The summarized bundle triangulation results by using corrected from camera objective distortions digital images and the original digital images are given in the table 7.6

Table. 7.6. Comparison of bundle triangulation results before and after camera calibration procedure

General information			Result							
			Before camera calibration				After camera calibration			
Software	Images	Control points	σ_0 , μm	RMS X, m	RMS Y, m	RMS Z, m	σ_0 , μm	RMS X, m	RMS Y, m	RMS Z, m
<i>Inpho</i>	3	10/10	0,5	0,006	0,008	0,008	0,5	0,006	0,009	0,004
<i>BLUH</i>	3	10/10	1,36	0,005	0,009	0,017	1,36	0,007	0,013	0,014

As it is seen from table 7.6, the results of RMS achieved by using digital photogrammetric software *Inpho* are very similar in both cases: before camera calibration in corrected from camera objective distortions images and after camera calibration in the original images. Though, the better result in planimetry is achieved by using corrected from camera objective distortions digital images (before camera calibration procedure) and the twice better result in height is achieved by using the original digital images (after camera calibration procedure). The final result of bundle adjustment is the same before camera calibration procedure and after camera calibration procedure.

Very similar distribution of the results of RMS and of the final adjustment result is achieved by using system *BLUH* (see table 7.6). The better result in planimetry is achieved by using corrected from camera objective distortions digital images (before camera calibration procedure) and the better result in height is achieved by using the original digital images (after camera calibration procedure). The final result of bundle adjustment is the same before camera calibration procedure and after camera calibration procedure.

The best result of bundle adjustment was achieved with digital photogrammetric software *Inpho* after camera calibration procedure by using the original digital images.

7.4. Comparison of camera calibration parameters

In this section the comparison between the old digital camera *Canon EOS 1D Mark III* calibration results and between the results which were got during research work is made. Comparison of camera calibration parameters is given in table 7.7.

Table. 7.7. Comparison of camera calibration parameters

<i>Parameters</i>	Results		
	<i>The old calibration</i>	<i>Calibration performed during research work</i>	
		<i>With using scale bars</i>	<i>Without using scale bars</i>
Focal length (mm)			
c	50,7583	50,7930	50,7931
The base point corrections of the photo-camera (mm)			
x_0	-0,0495	-0,2282	-0,2324
y_0	-0,2559	0,2019	0,2026
Radial-symmetric distortion of the photo-camera			
A1	-1.789E-09	-6,4466E-05	-6,4508E-05
A2	-	4,1312E-08	4,1565E-08
A3	-	2,8812E-11	2,8407E-11

Table. 7.7. continuation:

<i>Parameters</i>	Results		
	<i>The old calibration</i>	<i>Calibration performed during research work</i>	
		<i>With using scale bars</i>	<i>Without using scale bars</i>
Radial-asymmetric distortion of the photo-camera			
B1	1,0170E-05	-7,1262E-05	-7,2810E-06
B2	-1.655E-8	-2,5987E-06	-2,5725E-06
Affinity/Orthogonality			
C1	-	1,3696E-03	1,3715E-03
C2	-	-2,5531E-05	-2,6262E-05

The camera calibration procedure was performed at the Institute of Photogrammetry in Bonn University (Germany) in 2008 before (the results of this calibration are listed in column named “The old calibration”). As can be seen from the previous table, the values between the old camera calibration interior orientation parameters and between the new calibration interior orientation parameters are very differ. Also, the difference between amount of computed parameters is seen. However, the differences between the proportion of the obtained values of calibration parameters and between amount of computed calibration parameters in both cases (in old calibration and in new calibration) do not mean bad result, because the computations of parameters were performed by using different softwares and different technique during images taking process. Also, there are no standards for calibration reports of digital cameras at the moment. In this case, the camera calibration parameters which should be entered during project creation process depending on the software which is using for images processing. The camera calibration parameters which were need to enter in the digital photogrammetric softwares *PhotoMod* and *Inpho* during project creation process and the camera calibration parameters which were need to enter in system *BLUH* are given in table 7.8.

Table. 7.8. Camera calibration parameters in *PhotoMod*, *Inpho* and *BLUH*

Software	Camera calibration parameters								
	Focal length (c)	The base point corrections of the photo-camera (x_0, y_0)	Radial-symmetric distortion of the photo-camera			Radial-asymmetric distortion of the photo-camera		Affinity/Orthogonality	
			A1	A2	A3	B1	B2	C1	C2
<i>PhotoMod</i>	+	+	+	+	+	-	-	-	-
<i>Inpho</i>	+	+	+	+	+	-	-	-	-
<i>BLUH</i>	+	-	-	-	-	-	-	-	-

As it is seen from previous table, the same number of introduction of camera calibration parameters is required for *PhotoMod* and *Inpho* softwares.

It should be noted when the corrected from camera distortions digital images were used – only calibrated focal length (c) was need to enter during project creation in *PhotoMod* and *Inpho* softwares. Also, because the points measurements in the images were performed with digital photogrammetric system, the system *BLUH* requires to enter only calibrated focal length (c).

CONCLUSIONS

1. The digital images of the culture heritage facade which were corrected from the digital camera *Canon EOS 1D Mark III* objective distortions were processed using digital photogrammetric system *PhotoMod*. After aerial triangulation was done, the root mean square between in images by stereo mode measured ground control points and between in geodetic method measured ground control points were detected: RMS X = 0,002 in units metres, RMS Y = 0,003 in units metres and RMS Z = 0,008 in units metres. Using this software in addition, the break lines of the object were plotted and the orthophoto was generated.

2. The digital images of that same object which were corrected from the digital camera *Canon EOS 1D Mark III* objective distortions were processed using digital photogrammetric system *Inpho*. After aerial triangulation was done, the root mean square between in images not by stereo mode measured ground control points and between by geodetic method measured ground control points were detected: RMS X = 0,006 in units metres, RMS Y = 0,008 in units metres and RMS Z = 0,008 in units metres. The value of σ_0 is equal to 0.5 in units micron.

3. The tie points which were measured in that same digital images of the object which were corrected from the digital camera *Canon EOS 1D Mark III* objective distortions using software *Inpho* and by geodetic method measured ground control points for further processing were transformed to bundle adjustment designed software *BLUH*. After aerial triangulation was done, the root mean square between in images not by stereo mode measured ground control points and between by geodetic method measured ground control points were detected: RMS X = 0,005 in units metres, RMS Y = 0,009 in units metres and RMS Z = 0,017 in units metres. The value of σ_0 is equal to 1.36 in units micron.

4. The calibration of the digital camera *Canon EOS 1D Mark III* (50 mm objective-lens) was performed in a specially designed calibration laboratory at Neubrandenburg University of Applied Sciences in Germany. Significant differences between the old calibration parameters (obtained three years ago) and between the new results, obtained by the author in this master work, were not found. It means that the parameters which were set during camera calibration procedure three years ago were not changed during all the time the camera was used in this work.

5. By using new camera calibration parameters the aerial triangulation procedure was repeated using digital photogrammetric system *Inpho*. For this purpose the original digital images (not corrected from the digital camera *Canon EOS 1D Mark III* objective distortions) of that same object were used. After aerial triangulation was done using software *Inpho*, the root mean square between in images not by stereo mode measured ground control points and between by geodetic method measured ground control points were detected: RMS X = 0,006 in units metres, RMS Y =

0,009 in units metres and RMS Z = 0,004 in units metres. The value of σ_0 is equal to 0,5 in units micron.

6. By using the new camera calibration parameters the tie points, which were measured in that same original digital images of the object using software *Inpho* and by geodetic method measured ground control points for further processing were transformed to bundle adjustment designed software *BLUH*. After aerial triangulation was done, the root mean square between in images not by stereo mode measured ground control points and between by geodetic method measured ground control points were detected: RMS X = 0,007 in units metres, RMS Y = 0,013 in units metres and RMS Z = 0,014 in units metres. The value of σ_0 is equal to 1.36 in units micron.

7. The results of aerial triangulation which were obtained by using all examined softwares meet accuracy requirements. According to this, it can be stated that the digital photogrammetric systems *PhotoMod* and *Inpho* which are developed for processing scanned aerial film frames, images from various satellite sensors could be used for close-range digital images processing too.

8. During the digital images processing procedure it was established that formulas given for accuracy control by software's manufacturers not allways hold on. Thus, there are an importance for operator experience and skills during digital close-range images processing procedure.

REFERENCES

- Abraham S. 2004. Tcc – a software for test field based self-calibration of multi-camera-systems. Institut für Photogrammetrie, Universität Bonn. 39 p.
- AICON 3D Systems GmbH. 2009. AICON 3D Studio user Manual. Braunschweig, Germany. 14-9.
- Albertz J.; Wiggenhagen M.. 2009. Guide for Photogrammetry and Remote Sensing. Hamburg, Germany. 334.
- Atkinson, K.B. 2001. Close Range Photogrammetry and Machine Vision. Scotland, UK. 363.
- Habib A.; Jarvis A.; Datchev I.; Stensaas G.; Moe D.; Christopherson J. 2008. Standards and specifications for the calibration and stability of amateur digital cameras for close-range mapping applications. *The International Archives of the Photogrammetry, Remote Sensing and Spatial Information Sciences*, Vol. XXXVII. Part B1. Beijing. 1059 – 1064.
- Habib A. F.; Pullivelli A. M.; Morgan M. 2005. Quantitative measures for the evaluation of camera stability. *Society of Photo-Optical Instrumentation Engineers*. Calagary, Canada.
- Inpho. 2010. ApplicationsMaster Manual for Version 5.3 and higher. 363.
- Inpho. 2010. Match-AT Manual for Version 5.3 and higher. 244.
- Jacobsen, K. 2001. PC-Based Digital Photogrammetry. Damaskus, GORS.
- Jacobsen K. 2009. Program system *BLUH*: User Manual. Hannover, Germany. 21.
- Kersten, T. 1999. Results of digital aerial triangulation using different software packages. *OEEPE Workshop on Automation in Digital Photogrammetric Production*, No. 37, 241-256.
- Kiseleva, A.S. 2002. Accuracy control at various stages of photogrammetric processing in *PhotoMod* system. Moscow.
- Läbe, T.; Förstner, W. 2004. Geometric stability of low-cost digital consumer cameras. *The International Archives of the Photogrammetry, Remote Sensing and Spatial Information Sciences*, 35(B1). 528 – 534.
- Lothhammer, K. L. 2005. Photogrammetric workflow: the *Inpho* approach. Bogotá, Colombi.
- Luhmann T.; Robson S.; Kyle S.; Harley I. 2006. Close range photogrammetry: principles, Methods and Applications. Scotland, United Kingdom. 510.
- Madani, M. 2001. Importance of Digital Photogrammetry for a complete GIS. 5th Global Spatial Data Infrastructure Conference. Cartagena, Columbia.

- Peipe J.; Stephani M. 2003. Performance evaluation of a 5 Megapixel digital metric camera for use in architectural photogrammetry. *The International Archives of the Photogrammetry, Remote Sensing and Spatial Information Sciences*, Vol. XXXIV, Part 5/W12. 259-261.
- Racurs. 2009. Software *PhotoMod* 4.4 Module Aerial Triangulation user manual. Moscow. 161.
- Racurs. 2009. Software *PhotoMod* 4.4 Module *PhotoMod* DTM user manual. Moscow. 75.
- Racurs. 2009. Software *PhotoMod* 4.4 Module *PhotoMod* Solver user manual. Moscow. 77.
- Racurs. 2009. Software *PhotoMod* 4.4 Module *PhotoMod* Stereo Draw user manual. Moscow. 123.
- Ruzgienė B. 2008. Fotogrametrija. Vilnius: Technika. 2008. 204.
- Sanz-Ablanedo E.; Rodríguez-Pérez J. .; Armesto J.; Taboada M. F. Á. 2010. Geometric Stability and Lens Decentering in Compact Digital Cameras. *MDPI journal: Sensors*. 1553-1572.
- Schenk, T. 1999. Digital photogrammetry, Volume 1. Dayton, Ohio, USA. 421.
- Schenk T. 2005. Introduction to Photogrammetry. USA. 95.
- Shariat M., Azizi A., Saadatseresht M., 2008. Analysis and the solutions for generating a true digital ortho photo in close range photogrammetry. *The International Archives of the Photogrammetry, Remote Sensing and Spatial Information Sciences*. Vol XXXVII, Part B4, Beijing, 439-442.
- Sigle M.; Heuchel T. 2001. *MATCH-AT: Recent Developments and Performance*. *Photogrammetric week 01*. 189-194.
- Sužiedelytė-Visockienė, J.; Bručas, D. 2009. Digital photogrammetry for building measurements and reverse-engineering. *Geodesy and Cartography*, 35(2), 61–65.
- Sužiedelytė-Visockienė, J.; Bručas, D. 2009. Influence of digital camera errors on the photogrammetric image processing. *Geodesy and Cartography*, t.35, No. 1, 29-33.
- Sužiedelytė-Visockienė, J.; Kumetaitienė A.; Bagdžiūnaitė R. 2011. Accuracy analysis of different surface reconstruction modelling methods of heritage objects, digitalized according to photogrammetric data. *Environmental Engineering, Volume 3*. The 8th International Conference, 1493.
- Wiedemann A. 2005. Digital Architectural Photogrammetry for Building Registration. Berlin, Germany.
- Wiedemann A.; Moré J.; Suthau T.; Theodoropoulou I.; Weferling U.; Ergün B. 2001. Comparison of bundle block adjustments for close range applications. *Fourth Turkish-German Joint Geodetic Days*. Paper presented to the conference organized at Berlin, Germany, April 2-6, Vol I, 211-218.

Wojtas A. M. 2010. Off-the-shelf close-range photogrammetric software for cultural heritage documentation at Stonehenge. *International Archives of Photogrammetry, Remote Sensing and Spatial Information Sciences*, Vol. XXXVIII, Part 5. Commission V Symposium, Newcastle upon Tyne, UK. 603-607.

Web pages:

Analyzing photogrammetric software *AICON 3D Studio* [Accessed 2011-04-28]. Available from internet:

<http://www.aicon3d.de/start.html>

3D measurement system *DPA* [Accessed 2011-05-09]. Available from internet:

http://www.qfp-service.it/pdf/AICON_DPA_english_05-2010%5B1%5D.pdf

Digital photogrammetric system *Inpho* [Accessed 2011-04-28]. Available from internet:

http://www.inpho.de/index.php?seite=photogrammetric_systems

Digital photogrammetric system *PhotoMod* [Accessed 2011-01-24]. Available from internet:

<http://www.infomap-rs.net/index.php?lang=en&tabid=51>

Digital photogrammetric workstations [Accessed 2011-04-24]. Available from internet:

[http://www.gim-international.com/issues/articles/id530-](http://www.gim-international.com/issues/articles/id530-Digital_Photogrammetric_Workstations.html)

[Digital_Photogrammetric_Workstations.html](http://www.gim-international.com/issues/articles/id530-Digital_Photogrammetric_Workstations.html)

Ground control points and aerial triangulation [Accessed 2011-04-28]. Available from internet:

http://www.pvts.net/pdfs/ortho/ortho_scp4.pdf

Program *PATB*. [Accessed 2011-04-26]. Available from internet:

<http://www.k2-photogrammetry.de/products/patb.html>

The accuracy of photogrammetric surveys [Accessed 2011-05-09]. Available from internet:

<http://www.blm.gov/cadastral/Manual/73man/id33.htm>

Triangulated irregular network (TIN) [Accessed 2011-02-03]. Available from internet:

http://en.wikipedia.org/wiki/Triangulated_irregular_network

APPENDIXES

Appendix 1. PhotoMod aerial triangulation report

== 2011 m. geguļus 17 d. == 08:58:11 ==

Отчет по уравниванию блока

 Блок: VU_S3

Количество маршрутов: 1

Количество стереопар: 2

 Параметры уравнивания:

метод независимых маршрутов

полиномиальные поправки: 2-го порядка, XYZ

система координат: Cartesian Left

вес уравнений на опорные точки: 1

вес уравнений на связующие точки: 1

используются поправки дрейфа центров GPS по маршрутам

Единицы измерения: m

 Элементы внешнего ориентирования

 Снимок: P912

центр проекции

1.037072 -62.712047 81.077643

матрица поворота

0.9801212734 0.0702928984 0.1855295066

-0.0267664474 0.9734315563 -0.2274083608

-0.1965854691 0.2179218064 0.9559624677

альфа, омега, каппа (град.)

-10.9832059902 13.1445389733 -1.5750651602

 Снимок: P915

центр проекции

1.249430 -68.732966 81.757177

матрица поворота

0.9857994289 0.0739597295 0.1507628744

-0.0429762619 0.9790039823 -0.1992592369

-0.1623346137 0.1899504172 0.9682800794

альфа, омега, каппа (град.)

-8.8499911615 11.4936445739 -2.5135531811

 Снимок: P918

центр проекции

0.964182 -56.166147 79.841174

матрица поворота

0.9735332144 0.0584419427 0.2209470972

-0.0041481032 0.9711119898 -0.2385881314

-0.2285079291 0.2313569592 0.9456522002

альфа, омега, каппа (град.)

-13.1509671481 13.8032257161 -0.2447373327

 Каталог точек

(m)	N	X	Y	Z	E _{xy}	E _z
опорные						
	102	9.824	-74.167	50.354	0.003	-0.004
	105	6.496	-70.721	49.527	0.001	0.007
	106	4.776	-68.223	48.909	0.002	0.004
	107	12.166	-62.236	48.021	0.001	-0.007
	109	13.703	-69.257	48.819	0.007	0.007
	110	15.988	-72.718	50.119	0.003	-0.005
	111	16.056	-65.708	48.418	0.002	0.004
	600	0.483	-75.332	50.715	0.002	0.004
	602	0.963	-67.368	48.887	0.005	-0.019
	603	0.212	-63.192	47.789	0.003	0.010
	итого 10 точек					
контрольные						
	итого 0 точек					
сгушения						
	итого 0 точек					
связующие						
	*1	20.020	-70.451	47.898		
	*2	12.200	-75.850	51.283		
	*5	6.738	-67.674	49.077		
	*6	9.369	-68.980	49.053		
	*7	0.529	-68.199	48.990		
	*8	2.149	-62.758	47.714		
	*9	10.226	-62.823	47.667		
	*621	15.024	-68.415	31.516		
	итого 8 точек					

 Оценка точности уравнивания блока
 Превышения допусков отмечены знаком "*".

 Сводная информация об ошибках по блоку

 Ошибки по опорным точкам

N	X _{ср} -X _г	Y _{ср} -Y _г	Z _{ср} -Z _г	E _{xy} (m)
допуск:	0.020	0.020	0.020	0.020
102	-0.003	-0.002	-0.004	0.003
105	0.001	-0.000	0.007	0.001
106	0.001	-0.001	0.004	0.002
107	0.001	-0.001	-0.007	0.001
109	0.001	0.007	0.007	0.007
110	0.002	-0.002	-0.005	0.003
111	-0.002	-0.002	0.004	0.002
600	0.001	0.002	0.004	0.002
602	-0.002	-0.004	-0.019	0.005
603	0.000	0.003	0.010	0.003
средний модуль:	0.001	0.002	0.007	0.003
СКО:	0.002	0.003	0.008	0.003
максимум:	0.003	0.007	0.019	0.007
всего точек (разностей):				
10 (10	10	10	10)

центры проекции

N	X _{ср} -X _г	Y _{ср} -Y _г	Z _{ср} -Z _г	E _{xy} (m)
допуск:	0.020	0.020	0.020	0.020
средний модуль:	0.000	0.000	0.000	0.000
СКО:	0.000	0.000	0.000	0.000
максимум:	0.000	0.000	0.000	0.000
всего точек (разностей):				
0 (0	0	0	0)

Ошибки по контрольным точкам

N	X _{ср} -X _г	Y _{ср} -Y _г	Z _{ср} -Z _г	E _{xy} (m)
допуск:	0.020	0.020	0.020	0.020
средний модуль:	0.000	0.000	0.000	0.000
СКО:	0.000	0.000	0.000	0.000
максимум:	0.000	0.000	0.000	0.000
всего точек (разностей):				
0 (0	0	0	0)

центры проекции

N	X _{ср} -X _г	Y _{ср} -Y _г	Z _{ср} -Z _г	E _{xy} (m)
допуск:	0.020	0.020	0.020	0.020
средний модуль:	0.000	0.000	0.000	0.000
СКО:	0.000	0.000	0.000	0.000
максимум:	0.000	0.000	0.000	0.000
всего точек (разностей):				
0 (0	0	0	0)

Ошибки по связующим точкам (от среднего)

N	X-X _{ср}	Y-Y _{ср}	Z-Z _{ср}	E _{xy} (m)
допуск:	0.020	0.020	0.020	0.020
средний модуль:	0.003	0.003	0.014	0.004
СКО:	0.003	0.003	0.016	0.004
максимум:	0.005	0.005	0.032*	0.007
всего точек (разностей):				
7 (14	14	14	14)
внутри маршрутов				
N	X-X _{ср}	Y-Y _{ср}	Z-Z _{ср}	E _{xy} (m)
допуск:	0.020	0.020	0.020	0.020
средний модуль:	0.003	0.003	0.014	0.004
СКО:	0.003	0.003	0.016	0.004
максимум:	0.005	0.005	0.032*	0.007
всего точек (разностей):				
7 (14	14	14	14)
между маршрутами				
N	X-X _{ср}	Y-Y _{ср}	Z-Z _{ср}	E _{xy} (m)
допуск:	0.020	0.020	0.020	0.020
средний модуль:	0.000	0.000	0.000	0.000
СКО:	0.000	0.000	0.000	0.000
максимум:	0.000	0.000	0.000	0.000
всего точек (разностей):				
0 (0	0	0	0)

Ошибки по точкам сгущения (от среднего)				
N	X-X _{ср}	Y-Y _{ср}	Z-Z _{ср}	E _{xy} (m)
допуск:	0.020	0.020	0.020	0.020
средний модуль:	0.000	0.000	0.000	0.000
СКО:	0.000	0.000	0.000	0.000
максимум:	0.000	0.000	0.000	0.000
всего точек (разностей):				
0 (0	0	0	0)

Ошибки по связи - центры проекции (от среднего)				
N	X-X _{ср}	Y-Y _{ср}	Z-Z _{ср}	E _{xy} (m)
допуск:	0.020	0.020	0.020	0.020
средний модуль:	0.000	0.000	0.000	0.000
СКО:	0.000	0.000	0.000	0.000
максимум:	0.000	0.000	0.000	0.000

всего точек (разностей) :				
	1 (2	2	2)

Ошибки по связующим точкам (на снимках)				
N	x_пр-х_изм	y_пр-у_изм	E _{xy} (мм)	
допуск:	4.699	4.699	4.699	
средний модуль:	0.256	0.510	0.638	
СКО:	0.404	0.728	0.832	
максимум:	1.453	2.518	2.519	
всего точек (разностей) :				
	18 (43	43	43)

Ошибки по точкам сгущения (на снимках)				
N	x_пр-х_изм	y_пр-у_изм	E _{xy} (мм)	
допуск:	4.699	4.699	4.699	
средний модуль:	0.000	0.000	0.000	
СКО:	0.000	0.000	0.000	
максимум:	0.000	0.000	0.000	
всего точек (разностей) :				
	0 (0	0	0)

Детализированная информация об ошибках

Ошибки по опорным точкам					
	N	X-Xг	Y-Yг	Z-Zг	E _{xy} (m)
	допуск:	0.020	0.020	0.020	0.020
102	P915-P912	-0.003	-0.002	-0.004	0.003
105	P912-P918	0.006	-0.003	-0.006	0.007
	P915-P912	-0.004	0.003	0.019	0.005
106	P912-P918	0.002	0.000	0.008	0.002
	P915-P912	0.001	-0.002	-0.001	0.002
107	P912-P918	0.001	-0.001	-0.007	0.001
109	P912-P918	0.002	0.004	-0.007	0.005
	P915-P912	-0.001	0.011	0.020*	0.011
110	P915-P912	0.002	-0.002	-0.005	0.003
111	P912-P918	0.000	-0.003	-0.003	0.003
	P915-P912	-0.004	-0.000	0.012	0.004

600	P415-P412	0.001	0.002	0.004	0.002
602	P912-P918	-0.007	0.001	0.014	0.007
	P915-P912	0.003	-0.009	-0.051*	0.010
603	P412-P418	0.000	0.003	0.010	0.003
центры проекции					
	N	X-Xr	Y-Yr	Z-Zr	Еху (м)
	допуск:	0.020	0.020	0.020	0.020

Ошибки по контрольным точкам					
	N	X-Xr	Y-Yr	Z-Zr	Еху (м)
	допуск:	0.020	0.020	0.020	0.020

центры проекции					
	N	X Xr	Y Yr	Z Zr	Еху (м)
	допуск:	0.020	0.020	0.020	0.020

Ошибки по связующим точкам (от среднего)					
	N	X Xcp	Y Ycp	Z Zcp	Еху (м)
	допуск:	0.020	0.020	0.020	0.020
*5	P912-P918	0.002	0.002	0.013	0.003
	P415-P412	-0.002	-0.002	-0.013	0.003
*6	P912-P918	0.005	-0.002	-0.011	0.005
	P915-P912	-0.005	0.002	0.011	0.005
105	P912-P918	0.005	-0.003	-0.012	0.006
	P915 P912	0.005	0.003	0.012	0.006
106	P912-P918	0.001	0.001	0.004	0.001
	P915-P912	-0.001	-0.001	-0.004	0.001
109	P912-P918	0.002	-0.003	-0.014	0.004
	P915-P912	-0.002	0.003	0.014	0.004
111	P412-P418	0.002	-0.001	-0.008	0.003
	P915-P912	-0.002	0.001	0.008	0.003
602	P912-P918	-0.005	0.005	0.032*	0.007
	P915-P912	0.005	-0.005	-0.032*	0.007

Ошибки по точкам сгущения (от среднего)

N	X-Хер	Y-Уер	Z-Зер	Эку (m)
допуск:	0.020	0.020	0.020	0.020

 Ошибки по связи - центры проекции (от среднего)

N	X-Хер	Y-Уер	Z-Зер	Эку (m)
допуск:	0.020	0.020	0.020	0.020
P912				
P912-P918	0.000	0.000	0.000	0.000
P915-P912	0.000	0.000	0.000	0.000

 Ошибки по связующим точкам (на снимках)

N	x пр-х изм	y пр-у изм	Эку (мм)
допуск:	4.099	4.099	4.099
*1			
P912	0.201	0.140	0.245
P918	-0.483	-0.492	0.689
*2			
P912	-0.034	0.974	0.974
P915	-0.230	-0.198	0.303
*5			
P912	-0.011	1.019	1.019
P915	0.571	0.751	0.944
P918	-0.575	0.318	0.657
*6			
P912	0.006	0.555	0.555
P915	0.439	-0.310	0.538
P910	0.402	0.251	0.500
*7			
P912	-0.159	0.090	0.183
P918	0.264	0.185	0.323
*8			
P912	0.124	0.029	0.127
P918	0.187	0.445	0.483
*9			
P912	0.044	-0.019	0.048
P918	-0.143	-0.375	0.401
-G21			
P912	-0.023	1.090	1.091
P915	-0.145	0.153	0.211
102			
P912	-0.010	1.033	1.033
P915	0.120	0.100	0.161
105			
P912	-0.008	0.768	0.768
P915	0.614	-0.561	0.832
P918	0.681	0.074	0.685
106			
P912	-0.014	0.390	0.391
P915	-0.145	-0.120	0.189
P918	-0.073	0.670	0.674
107			
P912	0.005	0.027	0.009
P918	-0.229	0.328	0.400

109	P912	0.035	-0.651	0.652
	P915	0.347	0.903	0.967
	P918	0.240	-0.023	0.241
110	P912	-0.055	-2.518	2.519
	P915	-0.388	-0.058	0.392
111	P912	0.044	-0.237	0.241
	P915	0.026	0.556	0.556
	P918	-0.144	-0.057	0.155
600	P912	0.101	-1.164	1.168
	P915	0.323	-0.154	0.358
602	P912	-0.018	-1.166	1.166
	P915	-1.453	1.460	2.060
	P918	-1.359	-1.489	2.016
603	P912	-0.167	-0.019	0.168
	P918	0.277	0.015	0.277

 Ошибки по точкам сгущения (на снимках)

N	x_пр-x_изм	y_пр-y_изм	Еху (мм)
допуск:	4.699	4.699	4.699

Appendix 2. *Inpho* aerial triangulation statistics file of the images which are corrected from the digital camera *Canon EOS 1D Mark III* objective distortions

Statistic file-pries kalibravima

MATCH-AT statistic file

Project : V:\dar vienas\Kopie von Kopie von Kopie von 22.prj

Date of creation : Sun May 22 15:47:21 2011

1. Summary:

```

-----
sigma 0 in micron                0.5
number block points              18
number of images                 3
number of iteration              5
redundandancy                   50

mean std dev ground   x          0.004 [units of terrain system]
                      y          0.004 [units of terrain system]
                      z          0.008 [units of terrain system]

mean std dev ori     omega      62.5 [mgrd]
                      phi        79.2 [mgrd]
                      kapp       24.0 [mgrd]

mean std dev ori     x          0.040 [units of terrain system]
                      y          0.032 [units of terrain system]
                      z          0.018 [units of terrain system]

rms image points      x          0.000 [micron]
                      y          0.000 [micron]

rms control in image x          1.257 [micron]
                      y          1.089 [micron]

rms control in terr  x          0.006 [units of terrain system]
                      y          0.008 [units of terrain system]
                      z          0.008 [units of terrain system]

max res. control     x          0.016 [units of terrain system]
                      y         -0.021 [units of terrain system]
                      z         -0.017 [units of terrain system]

rms check points     x          0.000 [units of terrain system]
                      y          0.000 [units of terrain system]
                      z          0.000 [units of terrain system]

max res. check       x          0.000 [units of terrain system]
                      y          0.000 [units of terrain system]
                      z          0.000 [units of terrain system]

```

2. Estimated orientation parameters and standard deviations:

```

-----
photo ID      omega[grd]  phi[grd]  kappa[grd]  X      Y
Z      std.ome[mgrd]  std.phi[mgrd]  std.kappa[mgrd]  std.X  std.Y
std.Z
81.877      P915  12.235810  10.082963  -4.751286  -68.499  1.594
0.015      61.526      77.707      22.714      0.040      0.031
81.006      P912  14.822668  12.709091  -4.704093  -62.274  1.072
0.017      60.255      77.442      23.275      0.039      0.031
79.849      P918  15.686157  14.885071  -3.950543  -55.754  0.983
0.022      65.804      82.394      26.146      0.041      0.034

```

3. GNSS observations and residuals:

Statistic file-pries kalibravima
 photo ID X Y Z res x res y res z
 P915 no GNSS observation given
 P912 no GNSS observation given
 P918 no GNSS observation given

4. Adjusted coordinates including control/check points and standard deviations:

fold	point check	ID blund	x	y	z	sx	sy	sz	code
			given	given	given	given	res	res	res
			102	-74.161	9.829	50.356	0.004	0.004	0.007
6	2	0	0	-74.165	9.827	50.358	-0.004	-0.002	0.002
			105	-70.719	6.497	49.520	0.003	0.003	0.005
6	3	0	0	-70.721	6.495	49.520	-0.002	-0.002	-0.000
			106	-68.223	4.776	48.903	0.003	0.003	0.005
6	3	0	0	-68.222	4.775	48.905	0.001	-0.001	0.002
			107	-62.237	12.155	48.038	0.004	0.004	0.007
6	2	0	0	-62.235	12.165	48.028	0.002	0.010	-0.010
			109	-69.280	13.723	48.829	0.003	0.004	0.006
6	3	0	0	-69.264	13.702	48.812	0.016	-0.021	-0.017
			110	-72.712	15.979	50.118	0.004	0.005	0.007
6	2	0	0	-72.716	15.986	50.124	-0.004	0.007	0.006
			111	-65.704	16.051	48.400	0.004	0.004	0.006
6	3	0	0	-65.706	16.058	48.414	-0.002	0.007	0.014
			600	-75.337	0.482	50.713	0.005	0.004	0.007
6	2	0	0	-75.334	0.482	50.711	0.003	-0.000	-0.002
			602	-67.360	0.962	48.906	0.004	0.004	0.006
6	3	0	0	-67.364	0.965	48.906	-0.004	0.003	0.000
			603	-63.190	0.211	47.774	0.005	0.004	0.007
6	2	0	0	-63.195	0.212	47.779	-0.005	0.001	0.005
			901	-75.658	1.059	50.785	0.006	0.004	0.014
5	2	0	0						
-999999986991104.000				-999999986991104.000				-999999986991104.000	
			902	-70.828	1.181	49.534	0.004	0.004	0.008
5	3	0	0						
-999999986991104.000				-999999986991104.000				-999999986991104.000	
			903	-67.548	1.062	48.891	0.004	0.004	0.008
5	3	0	0						
-999999986991104.000				-999999986991104.000				-999999986991104.000	
			904	-62.782	1.041	47.647	0.005	0.004	0.014
5	2	0	0						
-999999986991104.000				-999999986991104.000				-999999986991104.000	
			905	-67.802	6.652	48.843	0.003	0.003	0.007
5	3	0	0						
-999999986991104.000				-999999986991104.000				-999999986991104.000	
			906	-68.984	9.367	49.047	0.003	0.003	0.007
5	3	0	0						
-999999986991104.000				-999999986991104.000				-999999986991104.000	
			908	-75.607	12.126	50.916	0.006	0.006	0.014
5	2	0	0						
-999999986991104.000				-999999986991104.000				-999999986991104.000	
			909	-70.370	20.005	47.926	0.006	0.009	0.011
5	3	0	0						
-999999986991104.000				-999999986991104.000				-999999986991104.000	

3. Photo observations and residuals:

vy	photo	point	status	fold	automa	x	vx	y
1.7	P918	107	1	2	0	1897.1	3.9	4694.4
-1.3	P912	107	1	2	0	9951.1	-3.7	5502.6
-1.8	P918	111	1	3	0	-3122.1	-2.9	9738.7
0.8	P912	109	1	3	0	-642.2	3.2	7069.3
1.8	P912	905	1	3	0	1826.8	-2.3	-2935.1

	Statistic file-pries kalibravima								
-2.1	P915	109	1	3	0	6309.8	-1.8	8738.5	
-2.2	P918	905	1	3	0	-6532.1	1.1	-3549.4	
1.5	P912	906	1	3	0	-125.8	1.7	1043.5	
0.9	P912	111	1	3	0	4449.5	2.1	10535.8	
-2.0	P912	600	1	2	0	-10375.5	0.2	-13045.6	
2.0	P915	600	1	2	0	-2335.7	-0.1	-11714.6	
-1.9	P918	602	1	3	0	-6147.8	0.1	-12454.4	
1.7	P915	110	1	2	0	870.8	0.3	12063.1	
-1.5	P915	906	1	3	0	7186.1	-0.9	2611.7	
1.5	P912	602	1	3	0	2820.1	-0.5	-11895.0	
1.4	P915	111	1	3	0	11358.6	0.5	12272.1	
-1.3	P912	110	1	2	0	-5996.8	-0.6	10318.0	
0.4	P918	603	1	2	0	738.9	-1.3	-13664.5	
1.4	P918	902	1	3	0	-11653.6	-0.1	-12122.9	
0.4	P915	905	1	3	0	9326.0	1.1	-1386.8	
-0.9	P912	105	1	3	0	-2777.2	-0.8	-3274.3	
-0.3	P912	603	1	2	0	9753.7	1.0	-12942.1	
-1.0	P915	902	1	3	0	5099.9	-0.1	-10209.6	
0.8	P918	105	1	3	0	-11083.4	0.4	-3812.5	
-0.0	P918	906	1	3	0	-8187.4	-0.8	412.3	
0.8	P912	901	1	2	0	-10890.2	0.0	-12103.0	
-0.8	P915	901	1	2	0	-2905.7	-0.0	-10774.1	
0.7	P918	106	1	3	0	-7251.9	-0.2	-6417.6	
-0.5	P915	106	1	3	0	8888.7	0.4	-4304.7	
-0.5	P915	909	1	3	0	4274.1	0.0	16400.8	
0.5	P915	602	1	3	0	10755.9	0.1	-10319.5	
-0.2	P912	102	1	2	0	-8207.5	-0.5	1589.5	
-0.5	P912	903	1	3	0	2519.4	0.1	-11736.8	
-0.4	P912	902	1	3	0	-2833.9	0.3	-11685.1	
0.4	P918	904	1	2	0	1403.5	0.0	-12298.4	
-0.4	P912	904	1	2	0	10326.8	0.0	-11560.2	
0.4	P912	909	1	3	0	-2007.8	-0.0	14521.2	
-0.0	P915	105	1	3	0	4756.0	0.3	-1778.1	
0.2	P915	903	1	3	0	10436.0	-0.0	-10168.8	
0.2	P918	903	1	3	0	-6416.8	-0.0	-12294.7	
-0.2	P912	106	1	3	0	1263.1	-0.1	-5836.8	
0.0	P915	102	1	2	0	-946.3	0.2	3109.8	
0.2	P918	909	1	3	0	-8838.9	0.0	13712.8	
	P918	109	1	3	0	-8245.7	-0.1	6363.4	

```
Statistic file-pries kalibravima
-0.1          P912      908      1      2      0    -10529.1    -0.0    4955.7
-0.0          P915      908      1      2      0     -3422.6      0.0    6543.0
0.0
```

End of MATCH-AT statistic file

Appendix 3. *Inpho* aerial triangulation report of the images which are corrected from the digital camera *Canon EOS 1D Mark III* objective distortions

aat-pries kalibravima

Start Post Processing: Sun May 22 15:47:21 2011

```
=====
Active Block                : complete Block
Number of photos            : 3
Number of strips            : 1

Photo scale                 : 1:635
Mean terrain height [m]    : 50

Automatic blunder detection : OFF

Use all adjusted points in project file
as control (absolute mode) : OFF
```

Control parameter for block adjustment :

```
-----
Selfcalibration            : OFF
GNSS-Mode                  : OFF
Drift-Mode                  : OFF
IMU-Mode                    : OFF
Earth's curvature correction : OFF
Atmospheric correction      : ON
Do not eliminate manual points : OFF
```

Standard deviations (a-priori) :

```
-----
Ground control (planimetry) [m]
  Set
  0 (=default)              : 0.020

Ground control (height) [m]
  Set
  0 (=default)              : 0.020

Automatic image points [mm]
  Set
  0 (=default)              : 0.001

Image points of ground control and manual measurements [mm] : 0.006
```

Used Cameras in block:

```
-----
  1 CanonEOS1DMarkIII
    Distortion                : Coefficients
```

Tie Point Generator

```
-----
created 15 observations for photo P915
created 18 observations for photo P912
created 13 observations for photo P918
```

total of 46 measurements in 3 photos are used for adjustment (total 3 photos)

```

                                aat-pries kalibravima
sigma naught      336.2 micron (15:47:55)
sigma naught      106.8 micron (15:48:00)
sigma naught      1.0 micron (15:48:06)
sigma naught      0.5 micron (15:48:10)

found      8 points connecting  2 photos
found      10 points connecting 3 photos

number of observations      122
number of unknowns         72
redundancy                  50

RMS automatic points in photo (number: 0)
  x      0.0 micron
  y      0.0 micron

RMS control and manual points in photo (number: 46)
  x      1.3 micron
  y      1.1 micron

RMS control points with default standard deviation set (number: 10)
  x      0.006 [meter]
  y      0.008 [meter]

RMS control points with default standard deviation set (number: 10)
  z      0.008 [meter]

sigma naught      0.5 micron (15:48:16)
standard deviations of exterior orientation parameters (px, py, pz in [meter]
omega,phi,kappa in [deg/1000] )

      photo ID      px      py      pz      omega      phi      kappa
      P912      0.039      0.031      0.017      54.2298      69.6976      20.9474
      P915      0.040      0.031      0.015      55.3733      69.9365      20.4430
      P918      0.041      0.034      0.022      59.2233      74.1548      23.5311

mean standard deviations of rotations
omega      56.3 [deg/1000]
phi        71.3 [deg/1000]
kappa      21.6 [deg/1000]

max standard deviations of rotations
omega      59.2 [deg/1000] at photo      P918
phi        74.2 [deg/1000] at photo      P918
kappa      23.5 [deg/1000] at photo      P918

mean standard deviations of translations
x      0.040 [meter]
y      0.032 [meter]
z      0.018 [meter]

max standard deviations of translations
x      0.041 [meter] at photo      P918
y      0.034 [meter] at photo      P918
z      0.022 [meter] at photo      P918

residuals horizontal control points in [meter]

      control point ID      rx      ry
      102      -0.004      -0.002
      105      -0.002      -0.002
      106      0.001      -0.001
      107      0.002      0.010
      109      0.016      -0.021
      110      -0.004      0.007
      111      -0.002      0.007
      600      0.003      -0.000
      602      -0.004      0.003

```

603 aat-pries kalibravima 0.001
 -0.005

residuals vertical control points in [meter]

control point ID	rz
102	0.002
105	-0.000
106	0.002
107	-0.010
109	-0.017
110	0.006
111	0.014
600	-0.002
602	0.000
603	0.005

max standard deviations of terrain points

x	0.006 [meter] at point	901
y	0.009 [meter] at point	909
z	0.014 [meter] at point	904

mean standard deviations of terrain points

x	0.004
y	0.004
z	0.008

exterior orientation parameters (px, py, pz in [meter] omega,phi,kappa in [deg])
 rotations from terrain to photo (rotated axes)

photo ID	px	py	pz	omega	phi	kappa
P912	-62.274	1.072	81.006	13.3404	11.4382	-4.2337
P915	-68.499	1.594	81.877	11.0122	9.0747	-4.2762
P918	-55.754	0.983	79.849	14.1175	13.3966	-3.5555

=====

WARNING: Suspect orientation angle(s) (> 4.50000 [deg]) in following photo(s):

photo	omega	phi	kappa
P912	13.34040	11.43818	-4.23368
P915	11.01223	9.07467	-4.27616
P918	14.11754	13.39656	-3.55549

WARNING: Suspect standard deviation for orientation angle(s) (> 27.00000 [deg/1000]) in following photo(s):

photo	omega	phi	kappa
P912	54.22984	69.69759	20.94739
P915	55.37330	69.93648	20.44304
P918	59.22329	74.15477	23.53113

Sigma naught : 0.5 [micron] = 0.1 [pixel in level 0]

Elapsed time = 0 hour 1 min. 7 sec.

End of Post Processing: Sun May 22 15:48:26 2011

Appendix 4. Inpho aerial triangulation statistics file of the original images

Statistic file-po kalibravimo

MATCH-AT statistic file

Project : V:\GERULIS PRJ po kalibravimo\Kopie von Kopie von Kopie von Kopie von Kopie von 22.prj

Date of creation : Sun May 22 16:39:17 2011

1. Summary:

```

-----
sigma 0 in micron                0.5
number block points              18
number of images                 3
number of iteration              3
redundancy                      50

mean std dev ground  x          0.004 [units of terrain system]
                      y          0.004 [units of terrain system]
                      z          0.007 [units of terrain system]

mean std dev ori   omega        55.5 [mgrd]
                   phi          70.1 [mgrd]
                   kapp         21.4 [mgrd]

mean std dev ori   x            0.035 [units of terrain system]
                   y            0.028 [units of terrain system]
                   z            0.016 [units of terrain system]

rms image points   x            0.000 [micron]
                   y            0.000 [micron]

rms control in image x          0.838 [micron]
                    y          1.201 [micron]

rms control in terr x          0.006 [units of terrain system]
                    y          0.009 [units of terrain system]
                    z          0.004 [units of terrain system]

max res. control  x            0.016 [units of terrain system]
                    y           -0.025 [units of terrain system]
                    z           -0.011 [units of terrain system]

rms check points  x            0.000 [units of terrain system]
                   y            0.000 [units of terrain system]
                   z            0.000 [units of terrain system]

max res. check    x            0.000 [units of terrain system]
                   y            0.000 [units of terrain system]
                   z            0.000 [units of terrain system]

```

2. Estimated orientation parameters and standard deviations:

```

-----
photo ID      omega[grd]  phi[grd]   kappa[grd]  X      Y
Z      std.ome[mgrd]  std.phi[mgrd]  std.kappa[mgrd]  std.X  std.Y
std.Z
81.496      P915  12.431744  10.399697   -4.774838  -68.493  1.502
0.014      54.600      68.866      20.251      0.035    0.028
80.637      P912  14.969854  12.806504   -4.712475  -62.398  1.015
0.015      53.532      68.532      20.736      0.034    0.027
79.479      P918  15.882515  14.875309   -3.981950  -55.951  0.905
0.019      58.385      72.877      23.269      0.036    0.030

```

3. GNSS observations and residuals:

Statistic file-po kalibravimo

photo ID	X	Y	Z	res x	res y	res z
P915	no GNSS observation given					
P912	no GNSS observation given					
P918	no GNSS observation given					

4. Adjusted coordinates including control/check points and standard deviations:

fold	point check	ID blund	x	y	z	sx	sy	sz	code
			given	given	given	given	res	res	res
		102	-74.158		9.826	50.358	0.003	0.003	0.006
6	2	0	-74.165		9.827	50.358	-0.007	0.001	0.000
		105	-70.717		6.493	49.518	0.003	0.003	0.005
6	3	0	-70.721		6.495	49.520	-0.004	0.002	0.002
		106	-68.224		4.773	48.904	0.003	0.003	0.005
6	3	0	-68.222		4.775	48.905	0.002	0.002	0.001
		107	-62.240		12.154	48.028	0.003	0.004	0.006
6	2	0	-62.235		12.165	48.028	0.005	0.011	0.000
		109	-69.280		13.727	48.823	0.003	0.003	0.005
6	3	0	-69.264		13.702	48.812	0.016	-0.025	-0.011
		110	-72.712		15.985	50.119	0.004	0.004	0.006
6	2	0	-72.716		15.986	50.124	-0.004	0.001	0.005
		111	-65.702		16.056	48.411	0.004	0.004	0.006
6	3	0	-65.706		16.058	48.414	-0.004	0.002	0.003
		600	-75.331		0.478	50.710	0.004	0.004	0.006
6	2	0	-75.334		0.482	50.711	-0.003	0.004	0.001
		602	-67.363		0.963	48.905	0.003	0.003	0.005
6	3	0	-67.364		0.965	48.906	-0.001	0.002	0.001
		603	-63.196		0.213	47.782	0.004	0.004	0.006
6	2	0	-63.195		0.212	47.779	0.001	-0.001	-0.003
		901	-75.646		1.051	50.812	0.006	0.004	0.012
5	2	0					-999999986991104.000		
-999999986991104.000			-999999986991104.000						
		902	-70.825		1.179	49.532	0.004	0.003	0.007
5	3	0					-999999986991104.000		
-999999986991104.000			-999999986991104.000						
		903	-67.549		1.061	48.889	0.003	0.003	0.007
5	3	0					-999999986991104.000		
-999999986991104.000			-999999986991104.000						
		904	-62.788		1.042	47.662	0.004	0.004	0.012
5	2	0					-999999986991104.000		
-999999986991104.000			-999999986991104.000						
		905	-67.804		6.649	48.849	0.003	0.003	0.006
5	3	0					-999999986991104.000		
-999999986991104.000			-999999986991104.000						
		906	-68.985		9.365	49.049	0.003	0.003	0.006
5	3	0					-999999986991104.000		
-999999986991104.000			-999999986991104.000						
		908	-75.604		12.118	50.931	0.005	0.005	0.012
5	2	0					-999999986991104.000		
-999999986991104.000			-999999986991104.000						
		909	-70.373		20.036	47.931	0.005	0.008	0.010
5	3	0					-999999986991104.000		
-999999986991104.000			-999999986991104.000						

3. Photo observations and residuals:

vy	photo	point	status	fold	automa	x	vx	y
-3.0	P918	903	1	3	0	-6272.5	-1.1	-12193.8
1.9	P912	903	1	3	0	2673.7	2.0	-11663.9
-2.2	P912	603	1	2	0	9878.4	-0.7	-12801.1
2.1	P918	603	1	2	0	885.8	0.8	-13569.8
	P918	109	1	3	0	-8131.0	-0.7	6498.2

Statistic file-po kalibravimo								
-2.1	P912	902	1	3	0	-2691.2	-1.7	-11609.4
-1.3	P912	110	1	2	0	-5862.0	-1.2	10455.6
-1.7	P915	110	1	2	0	1021.9	0.8	12197.2
1.8	P912	909	1	3	0	-1864.2	-1.8	14621.0
0.7	P915	102	1	2	0	-803.2	-0.8	3252.1
-1.8	P912	109	1	3	0	-493.9	1.8	7229.7
-0.5	P915	909	1	3	0	4400.7	0.9	16450.1
-1.6	P912	102	1	2	0	-8114.9	0.4	1708.6
1.8	P918	106	1	3	0	-7146.4	0.2	-6350.0
1.6	P915	903	1	3	0	10583.8	-1.0	-10060.2
1.1	P918	111	1	3	0	-2989.1	-1.1	9892.8
-1.0	P918	909	1	3	0	-8672.8	0.9	13782.1
1.0	P915	106	1	3	0	9086.6	0.5	-4221.7
-1.2	P918	902	1	3	0	-11478.0	0.9	-11982.7
1.0	P918	904	1	2	0	1554.0	-0.0	-12220.3
-1.3	P912	904	1	2	0	10457.1	-0.0	-11437.2
1.3	P912	111	1	3	0	4613.4	1.2	10678.6
0.3	P918	107	1	2	0	2073.7	1.1	4841.5
0.4	P918	905	1	3	0	-6437.7	-0.2	-3470.3
-1.2	P912	906	1	3	0	22.6	1.2	1163.9
-0.2	P918	906	1	3	0	-8099.9	-0.6	521.6
1.0	P918	105	1	3	0	-10970.9	-0.5	-3719.6
0.9	P915	906	1	3	0	7389.1	-0.6	2736.9
-0.8	P915	109	1	3	0	6484.3	-0.1	8872.5
1.0	P915	111	1	3	0	11475.4	-0.5	12343.1
0.8	P912	905	1	3	0	1991.1	0.3	-2856.7
0.9	P912	602	1	3	0	2973.8	-0.5	-11812.3
-0.8	P915	902	1	3	0	5266.0	0.9	-10139.7
0.3	P912	107	1	2	0	10127.9	-0.9	5618.2
0.3	P912	908	1	2	0	-10419.4	-0.0	5080.9
-0.8	P915	908	1	2	0	-3300.1	0.0	6697.1
0.7	P912	106	1	3	0	1425.0	-0.6	-5783.2
-0.2	P912	901	1	2	0	-10728.9	0.0	-11970.9
0.7	P915	901	1	2	0	-2771.5	-0.0	-10712.2
-0.7	P915	602	1	3	0	10895.7	0.4	-10203.4
0.5	P912	105	1	3	0	-2652.9	0.5	-3201.3
-0.3	P915	105	1	3	0	4955.2	-0.2	-1688.6
-0.5	P918	602	1	3	0	-6006.5	0.1	-12356.1
0.4								

```
Statistic file-po kalibravimo
0.3      P915      905      1      3      0      9530.7      -0.2      -1287.1
0.1      P915      600      1      2      0      -2198.2      -0.1      -11638.3
0.1      P912      600      1      2      0      -10201.7      -0.0      -12903.2
```

End of MATCH-AT statistic file

Appendix 5. Inpho aerial triangulation report of the original images

aat-po kalibravimo

Start Post Processing: Sun May 22 16:39:18 2011

=====

Active Block	: complete Block
Number of photos	: 3
Number of strips	: 1

Photo scale	: 1:609
Mean terrain height [m]	: 50

Automatic blunder detection	: OFF
-----------------------------	-------

Use all adjusted points in project file as control (absolute mode)	: OFF
--	-------

Control parameter for block adjustment :

Selfcalibration	: OFF
GNSS-Mode	: OFF
Drift-Mode	: OFF
IMU-Mode	: OFF
Earth's curvature correction	: OFF
Atmospheric correction	: ON
Do not eliminate manual points	: OFF

Standard deviations (a-priori) :

Ground control (planimetry) [m]

Set	
0 (=default)	: 0.020

Ground control (height) [m]

Set	
0 (=default)	: 0.020

Automatic image points [mm]

Set	
0 (=default)	: 0.001

Image points of ground control and manual measurements [mm]	: 0.006
---	---------

Used Cameras in block:

1 CanonEOS1DMarkIII	
Distortion	: Coefficients

Tie Point Generator

created	15 observations for photo	P915
created	18 observations for photo	P912
created	13 observations for photo	P918

total of 46 measurements in 3 photos are used for adjustment (total 3 photos)

```

                                aat-po kalibravimo
sigma naught      0.5 micron (16:39:39)
sigma naught      0.5 micron (16:39:42)

found      8 points connecting  2 photos
found      10 points connecting  3 photos

number of observations      122
number of unknowns         72
redundancy                  50

RMS automatic points in photo (number: 0)
  x      0.0 micron
  y      0.0 micron

RMS control and manual points in photo (number: 46)
  x      0.8 micron
  y      1.2 micron

RMS control points with default standard deviation set (number: 10)
  x      0.006 [meter]
  y      0.009 [meter]

RMS control points with default standard deviation set (number: 10)
  z      0.004 [meter]

sigma naught      0.5 micron (16:39:46)
standard deviations of exterior orientation parameters (px, py, pz in [meter]
omega,phi,kappa in [deg/1000] )

```

photo ID	px	py	pz	omega	phi	kappa
P912	0.034	0.027	0.015	48.1791	61.6792	18.6625
P915	0.035	0.028	0.014	49.1402	61.9796	18.2262
P918	0.036	0.030	0.019	52.5466	65.5897	20.9421

```

mean standard deviations of rotations
omega  50.0 [deg/1000]
phi    63.1 [deg/1000]
kappa  19.3 [deg/1000]

max standard deviations of rotations
omega  52.5 [deg/1000] at photo P918
phi    65.6 [deg/1000] at photo P918
kappa  20.9 [deg/1000] at photo P918

mean standard deviations of translations
x      0.035 [meter]
y      0.028 [meter]
z      0.016 [meter]

max standard deviations of translations
x      0.036 [meter] at photo P918
y      0.030 [meter] at photo P918
z      0.019 [meter] at photo P918

residuals horizontal control points in [meter]

```

control point ID	rx	ry
102	-0.007	0.001
105	-0.004	0.002
106	0.002	0.002
107	0.005	0.011
109	0.016	-0.025
110	-0.004	0.001
111	-0.004	0.002
600	-0.003	0.004
602	-0.001	0.002
603	0.001	-0.001

```

                                aat-po kalibravimo
residuals vertical control points in [meter]
                                control point ID      rz
                                102      0.000
                                105      0.002
                                106      0.001
                                107      0.000
                                109     -0.011
                                110      0.005
                                111      0.003
                                600      0.001
                                602      0.001
                                603     -0.003

max standard deviations of terrain points
  x      0.006 [meter] at point      901
  y      0.008 [meter] at point      909
  z      0.012 [meter] at point      901

mean standard deviations of terrain points
  x      0.004
  y      0.004
  z      0.007

exterior orientation parameters (px, py, pz in [meter] omega,phi,kappa in [deg] )
rotations from terrain to photo (rotated axes)
                                photo ID      px      py      pz      omega      phi      kappa
                                P912     -62.398      1.015      80.637      13.4729      11.5259      -4.2412
                                P915     -68.493      1.502      81.496      11.1886      9.3597      -4.2974
                                P918     -55.951      0.905      79.479      14.2943      13.3878      -3.5838

=====

WARNING: Suspect orientation angle(s) (> 4.50000 [deg]) in following photo(s):
                                photo      omega      phi      kappa
                                P912     13.47287      11.52585      -4.24123
                                P915     11.18857      9.35973      -4.29735
                                P918     14.29426      13.38778      -3.58375

WARNING: Suspect standard deviation for orientation angle(s) (> 27.00000 [deg/1000]) in
following photo(s):
                                photo      omega      phi      kappa
                                P912     48.17914      61.67922      18.66254
                                P915     49.14019      61.97964      18.22622
                                P918     52.54662      65.58971      20.94213

Sigma naught :      0.5 [micron] =      0.1 [pixel in level 0]
Elapsed time = 0 hour 0 min. 39 sec.
End of Post Processing: Sun May 22 16:39:54 2011

```

Appendix 6. *BLUH* bundle triangulation report of the images which are corrected from the digital camera *Canon EOS 1D Mark III* objective distortions

bluh-pries kalibravima.lst

```

=====
PROGRAM  BLUH      LEIBNIZ UNIVERSITY HANNOVER      JUL 2010
        -----  BUNDLE BLOCK ADJUSTMENT  -----
                INSTITUTE OF PHOTOGRAMMETRY AND GEOINFORMATION
DATE: 22.05.2011   19:33:07
=====

VERSION FUER HS NEUBRANDENBURG FROM L.UNI.HANNOVER

TEXT

default
=====

DAXYZ
daxyz.dat

DAPOR
dapor.dat

BLUINF
bluinf.dat

DABLUH
dabluh.dat

NUMBER OF PHOTOS      GPS      GPSWXY      GPSWZ      GPS ANTENNA OFFSET
                      3        0          .300       .300       .000       .000       .000       3.

CALIBRATED FOCAL LENGTH 660
50.758

MAXI  IW      GW(1)    GW(2)    GW(3)  IB      FEG REC.SCALE ABIT IOUT APPR IFR
  10   1      1.000    1.000    1.0  0      20.0         0.  .81   0   0   0

          FROM PT      TO POINT    WEIGHT    AD PAR    WARNING          OUTSIDE
          0              0          1.000     0         50. 999999999999999

. SYSIM LIST
0      0      Y

      REA      REB      REC      REC2    IMAR    IMA2
      .050     5.00    4.40    3.00     0       0
                                                    N

APRIORI STANDARD DEVIATIONS: CONTROL POINTS SX = SY = 1.000
                                           SZ = 1.000
          PHOTO COORDINATES Sy = SX = 1.0

      IPPP      IPU      IFILT    NGPSIT    NGPSHI    IEROUT    ISTAR
      3         18       7         0         0         1         3

PHOTO NUMBER LIST
  915  1      912  1      918  1

          0      0

CONTROL POINTS

      POINT      X          Y          Z      FSP      FSZ
      102      -74.165    9.827    50.358  .02     .02
      105      -70.721    6.495    49.520  .02     .02
    
```

```

bluh-pries kalibravima.lst
106      -68.222      4.775      48.905      .02      .02
107      -62.235      12.165      48.028      .02      .02
109      -69.264      13.702      48.812      .02      .02
110      -72.716      15.986      50.124      .02      .02
111      -65.706      16.058      48.414      .02      .02
600      -75.334      .482      50.711      .02      .02
602      -67.364      .965      48.906      .02      .02
603      -63.195      .212      47.779      .02      .02
    
```

RANGE OF PHOTO COORDINATES
X MINIMUM = -11.654 X MAXIMUM = 11.359
Y MINIMUM = -13.665 Y MAXIMUM = 16.401
R MAXIMUM = 20.119 FACTOR = 8.08172

UP TO 18 POINTS / PHOTO

10 X,Y-CONTROL: .137 .057 10 Z-CONTROL: 1.291

NO.ITER	MS CORR X	MS CORR Y [ground unit]	MS CORR Z	SIGMA 0 (ITER) [microns]	TIME
0	.885213E-01	.114311E+00	.775095E+00	48.9	19:33:07
10 X,Y-CONTROL:	.171	.118	10 Z-CONTROL:	.354	
1	.110633E+00	.480971E-01	.409258E+00	24.3	19:33:07

CAMERA PROJECTION CENTER	MEAN HEIGHT TERRAIN	PHOTO SCALE FOR [ft]:	192.	16. inch/ft
1	81.	49.	630.	

MAIN KAPPA FOR DATA SET 1 : -1.602 3 3

10 X,Y-CONTROL:	.007	.011	10 Z-CONTROL:	.022	
2	.117667E+00	.730071E-01	.216426E+00	1.6	19:33:07
10 X,Y-CONTROL:	.006	.010	10 Z-CONTROL:	.020	
3	.361015E-02	.276170E-02	.484955E-02	1.4	19:33:07
10 X,Y-CONTROL:	.006	.010	10 Z-CONTROL:	.020	
4	.145749E-04	.176711E-04	.396784E-04	1.4	19:33:07

STANDARD DEVIATIONS OF PHOTO ORIENTATIONS

PHOTO	SPHI	SOMEGA	SKAPPA	SX	SY	SZ
918	.00280	.00252	.01331	.023	.021	.015
912	.00115	.00060	.00450	.010	.006	.004
915	.00101	.00052	.00399	.012	.003	.004

PHOTO ORIENTATION	[GRADS]	SEQUENCE OF ROTATION: PHI, OMEGA, KAPPA				
PHOTO	PHI	OMEGA	KAPPA	EASTING	NORTHING	HEIGHT
915	10.2262	12.1016	-2.7999	-68.522	1.584	81.870
912	12.9964	14.5412	-1.7172	-62.303	1.063	81.006
918	15.2827	15.2650	-.2458	-55.780	.976	79.854

PHOTO ORIENTATIONS IN ROTATION SEQUENCE OMEGA, PHI, KAPPA [GRADS]
STORED IN DAPORO.DAT

PHOTO ORIENTATIONS IN PAT-B-FORMAT STORED IN DAPORP.DAT

BLUH ORIENTATIONS WITH ROTATION SEQUENCE PHI OMEGA KAPPA [GRADS]
STORED IN dapor.dat

default

ADJUSTED COORDINATES ERROR LIMIT FOR LISTING RESIDUALS 20.00 MICRONS

bluh-pries kalibravima.1st										
POINT NAME	EASTING	NORTHING	HEIGHT	PHOTOS/POINT	DATASNO		MAX			
D.I.:	IMAGE	Dx [microns]	Dy	P ROB.E.	Dx EAST	Dy NORTH				
DCP: DIFFERENCE AT OBJECT COORDS. OF CONTROL POINTS SWEIGHT										
102		-74.161	9.829	50.349	2	BASE	6.30			
	DCPXY	-.004	-.002		CP	102	50.000			
	DCPZ			.009	CZ	102				
105		-70.720	6.497	49.519	3					
	DCPXY	-.001	-.002		CP	105	50.000			
	DCPZ			.001	CZ	105				
106		-68.224	4.776	48.902	3					
	DCPXY	.002	-.001		CP	106	50.000			
	DCPZ			.003	CZ	106				
109		-69.279	13.721	48.833	3					
	DCPXY	.015	-.019		CP	109	50.000			
	DCPZ			-.021	CZ	109				
110		-72.712	15.980	50.112	2	BASE	6.30			
	DCPXY	-.004	.006		CP	110	50.000			
	DCPZ			.012	CZ	110				
111		-65.704	16.053	48.398	3					
	DCPXY	-.002	.005		CP	111	50.000			
	DCPZ			.016	CZ	111				
600		-75.337	.483	50.709	2	BASE	6.30			
	DCPXY	.003	-.001		CP	600	50.000			
	DCPZ			.002	CZ	600				
602		-67.361	.962	48.905	3					
	DCPXY	-.003	.003		CP	602	50.000			
	DCPZ			.001	CZ	602				
901		-75.659	1.060	50.779	2	BASE	6.30			
902		-70.828	1.181	49.531	3					
903		-67.549	1.062	48.890	3					
905		-67.802	6.652	48.843	3					
906		-68.984	9.367	49.047	3					
908		-75.608	12.126	50.911	2	BASE	6.30			
909		-70.368	20.004	47.928	3					
107		-62.234	12.145	48.071	2	BASE	6.62			
	DCPXY	-.001	.020		CP	107	50.000			
	DCPZ			-.043	CZ	107				
603		-63.191	.211	47.768	2	BASE	6.62			
	DCPXY	-.004	.001		CP	603	50.000			
	DCPZ			.011	CZ	603				
904		-62.782	1.041	47.649	2	BASE	6.62			

=====

ROOT MEAN SQUARE OF DIFFERENCES AT CONTROL POINTS FOR UNIT WEIGHT

10 HORIZONTAL CONTROL POINTS RMSE X = +/- .006 +/- .303

RMSE Y = +/- .010 +/- .524

10 VERTICAL CONTROL POINTS RMSE Z = +/- .020 +/- 1.017

[ground units]

MEAN DIFFERENCE AT CONTROL POINTS:

X: .000 Y: .000 Z: .000 [ground units]

AVERAGE BASE FOR 2-RAY-POINTS: 6.43

bluh-pries kalibravima.1st

MEAN SQUARE ERRORS			[microns]		
POINT CODE	NO IN GROUP	NO PHOT PTS	INT MSE X	INT MSE Y	
CPZ	1	10	25	1.31	.51
CPXY	2	10	25	1.09	.54
ADJUS	4	18	46	.76	1.09
MEAN				1.01	.84

MEAN SQUARE CORRECTIONS OF LAST ITERATION
 X: .0030 Y: .0057 Z: .0151 [ground units]

OBSERVATIONS	UNKNOWN	REDUNDANCE	SIGMA 0	
122	72	50	1.36	19:33:07
			[microns]	

+++++ APRIORI STANDARD DEVIATIONS SHOULD BE CHANGED IN BLIM TO: +++++
 SIGMA APRIORI : 1.
 CONTROL POINTS X,Y: .43 Z: 1.02
 ++++++

MEAN VALUES OF RESIDUALS AND MSE IN RADIAL COMPONENTS

1ST LINE	RADIUS	[CM]
2ND LINE	MEAN RADIAL	[MICRONS]
3RD LINE	MSE RADIAL	[MICRONS]
4TH LINE	MSE TANGENTIAL	[MICRONS]
5TH LINE	NUMBER OF POINTS IN GROUP	

DATA SET 1

.0	.1	.2	.4	.5	.6	.7	.9	1.0	1.1	1.2	1.4	1.5	1.6	1.7
.0	.2	.0	.0	.0	.0	.0	.1	.0	.0	-.1	.1	.0	.0	.0
.0	.2	.0	.2	.0	.0	.1	.1	.1	.2	.1	.1	.1	.0	.1
.0	.2	.0	.1	.0	.0	.2	.0	.1	.2	.0	.1	.0	.1	.1
0	1	0	4	3	3	5	1	13	10	5	4	5	1	5

MSE (RADIAL) = +/- .1 MSE (TANGENTIAL) = +/- .1 60 PHOTO POINTS

MEAN SQUARE NADIR ANGLE : 19.0

MEAN PHOTO SCALE = 1: 656.1 3 PHOTOS
 FOR [ft]: 1: 200. = 17. in/ft

ADJUSTED COORDINATES COMPUTED : DATE: 22.05.2011 19:33:07
 =====

default

POINT NAME	EASTING	NORTHING	HEIGHT	RAYS	Type	Class
102	-74.161	9.829	50.349	2	Control	XYZ
105	-70.720	6.497	49.519	3	Control	XYZ
106	-68.224	4.776	48.902	3	Control	XYZ
107	-62.234	12.145	48.071	2	Control	XYZ
109	-69.279	13.721	48.833	3	Control	XYZ
110	-72.712	15.980	50.112	2	Control	XYZ
111	-65.704	16.053	48.398	3	Control	XYZ
600	-75.337	.483	50.709	2	Control	XYZ
602	-67.361	.962	48.905	3	Control	XYZ
603	-63.191	.211	47.768	2	Control	XYZ
901	-75.659	1.060	50.779	2		
902	-70.828	1.181	49.531	3		
903	-67.549	1.062	48.890	3		
904	-62.782	1.041	47.649	2		
905	-67.802	6.652	48.843	3		
906	-68.984	9.367	49.047	3		
908	-75.608	12.126	50.911	2		

```
bluh-pries kalibravima.lst
909      -70.368      20.004      47.928      3
```

POINT COORDINATES STORED IN daxyz.dat

DATA FOR TRANSFER TO BLAN STORED IN bluinf.dat

OUTPUT FILES

```
-----
OBJECT COORDINATES      : daxyz.dat
ORIENTATIONS PHI OMEGA KAPPA: dapor.dat
ORIENTATIONS OMEGA PHI KAPPA: daporo.dat
ORIENTATIONS PAT-B-FORMAT  : daporp.dat
RESIDUALS AT IMAGE POSITIONS: resi.dat
DATA FOR TRANSFER TO BLAN  : bluinf.dat
```

END OF BLUH DATE: 22.05.2011 19:33:07

Appendix 7. BLUH bundle triangulation report of the original images

```

bluh-po kalibravimo.1st

=====
PROGRAM  BLUH      LEIBNIZ UNIVERSITY HANNOVER      JUL 2010
      -----  BUNDLE BLOCK ADJUSTMENT  -----
      INSTITUTE OF PHOTOGRAMMETRY AND GEOINFORMATION
DATE: 23.05.2011  17:48:57
=====

VERSION FUER HS NEUBRANDENBURG FROM L.UNI.HANNOVER

TEXT
default
=====

DAXYZ
daxyz.dat

DAPOR
dapor.dat

BLUINF
bluinf.dat

DABLUH
dabluh.dat

NUMBER OF PHOTOS      GPS      GPSWXY      GPSWZ      GPS ANTENNA OFFSET
                   3         0         .300         .300         .000         .000         .000      3.

CALIBRATED FOCAL LENGTH 660
50.793

MAXI  IW      GW(1)      GW(2)      GW(3) IB      FEG REC.SCALE ABIT IOUT APPR IFR
 10   1       1.000      1.000      1.0  0      20.0         0.  .81      0   0   0

      FROM PT      TO POINT      WEIGHT      AD PAR      WARNING      OUTSIDE
                   0             0             1.000      0  0      50. 999999999999999

. SYSIM LIST
0     0     Y

      REA      REB      REC      REC2      IMAR      IMA2
      .050      5.00      4.40      3.00      0         0

APRIORI STANDARD DEVIATIONS: CONTROL POINTS SX = SY = 1.000
                                  SZ = 1.000
      PHOTO COORDINATES Sy = Sx = 1.0

      IPPP      IPU      IFILT      NGPSIT      NGPSHI      IEROUT      ISTAR
      3         18         7         0         0         1         3

PHOTO NUMBER LIST
915  1         912  1         918  1

      0         0

CONTROL POINTS

      POINT      X         Y         Z      FSP      FSZ
      102      -74.165      9.827      50.358      .02      .02
      105      -70.721      6.495      49.520      .02      .02
    
```

```

bluh-po kalibravimo.1st
106      -68.222      4.775      48.905      .02      .02
107      -62.235      12.165      48.028      .02      .02
109      -69.264      13.702      48.812      .02      .02
110      -72.716      15.986      50.124      .02      .02
111      -65.706      16.058      48.414      .02      .02
600      -75.334      .482      50.711      .02      .02
602      -67.364      .965      48.906      .02      .02
603      -63.195      .212      47.779      .02      .02
    
```

```

RANGE OF PHOTO COORDINATES
X MINIMUM = -11.478 X MAXIMUM = 11.675
Y MINIMUM = -13.570 Y MAXIMUM = 16.450
R MAXIMUM = 20.059 FACTOR = 8.10622
    
```

UP TO 18 POINTS / PHOTO

```

10 X,Y-CONTROL: .159 .061 10 Z-CONTROL: 1.014
    
```

NO.ITER	MS CORR X	MS CORR Y [ground unit]	MS CORR Z	SIGMA 0 (ITER) [microns]	TIME
0	.971177E-01	.954997E-01	.598418E+00	46.6	17:48:57
10 X,Y-CONTROL:	.118	.064	10 Z-CONTROL:	.169	
1	.488001E-01	.116911E-01	.381980E+00	17.2	17:48:57

```

CAMERA PROJECTION MEAN HEIGHT TERRAIN PHOTO SCALE
1 81. 49. 633. FOR [ft]: 193. 16. inch/ft
    
```

```

MAIN KAPPA FOR DATA SET 1 : -1.584 3 3
10 X,Y-CONTROL: .044 .030 10 Z-CONTROL: .119
2 .739378E-01 .372847E-01 .114805E+00 1.4 17:48:57
10 X,Y-CONTROL: .044 .030 10 Z-CONTROL: .119
3 .171855E-02 .524448E-03 .246304E-02 1.4 17:48:57
    
```

STANDARD DEVIATIONS OF PHOTO ORIENTATIONS

PHOTO	SPHI	SOMEGA	SKAPPA	SX	SY	SZ
918	.00276	.00222	.01670	.029	.028	.019
912	.00186	.00064	.00485	.013	.003	.009
915	.00108	.00065	.00318	.012	.008	.007

PHOTO ORIENTATION [GRADS]	SEQUENCE OF ROTATION: PHI, OMEGA, KAPPA			EASTING	NORTHING	HEIGHT
PHOTO	PHI	OMEGA	KAPPA			
915	10.0067	12.4416	-3.0728	-69.753	2.395	82.060
912	12.5729	14.2980	-1.7183	-62.561	2.161	81.319
918	16.9407	15.9781	.0621	-54.964	2.118	79.850

PHOTO ORIENTATIONS IN ROTATION SEQUENCE OMEGA, PHI, KAPPA [GRADS]
STORED IN DAPORO.DAT

PHOTO ORIENTATIONS IN PAT-B-FORMAT STORED IN DAPORP.DAT

BLUH ORIENTATIONS WITH ROTATION SEQUENCE PHI OMEGA KAPPA [GRADS]
STORED IN dapor.dat

default

ADJUSTED COORDINATES ERROR LIMIT FOR LISTING RESIDUALS 20.00 MICRONS

POINT NAME	EASTING	NORTHING	HEIGHT	PHOTOS/POINT	DATASNO	MAX
D.I.:	IMAGE	Dx [microns]	Dy	P ROB.E.	Dx EAST	Dy NORTH
DCP: DIFFERENCE AT OBJECT COORDS. OF CONTROL POINTS SWEIGHT						

bluh-po kalibravimo.1st

102	-74.175	9.841	50.364	2	BASE	7.23
DCPXY	.010	-.014	CP	102	50.000	
DCPZ			-.006	CZ	102	
105	-70.715	6.493	49.540	3		
DCPXY	-.007	.002	CP	105	50.000	
DCPZ			-.020	CZ	105	
106	-68.200	4.764	48.914	3		
DCPXY	-.022	.011	CP	106	50.000	
DCPZ			-.009	CZ	106	
109	-69.259	13.691	48.822	3		
DCPXY	-.005	.011	CP	109	50.000	
DCPZ			-.010	CZ	109	
110	-72.721	15.974	50.106	2	BASE	7.23
DCPXY	.005	.012	CP	110	50.000	
DCPZ			.018	CZ	110	
111	-65.711	16.035	48.401	3		
DCPXY	.005	.023	CP	111	50.000	
DCPZ			.013	CZ	111	
600	-75.337	.499	50.690	2	BASE	7.23
DCPXY	.003	-.017	CP	600	50.000	
DCPZ			.021	CZ	600	
602	-67.358	.959	48.900	3		
DCPXY	-.006	.006	CP	602	50.000	
DCPZ			.006	CZ	602	
901	-75.645	1.051	50.811	2	BASE	7.23
902	-70.825	1.174	49.532	3		
903	-67.544	1.061	48.889	3		
905	-67.802	6.644	48.850	3		
906	-68.987	9.364	49.050	3		
908	-75.603	12.115	50.930	2	BASE	7.23
909	-70.372	20.039	47.935	3		
107	-62.228	12.180	48.019	2	BASE	7.74
DCPXY	-.007	-.015	CP	107	50.000	
DCPZ			.009	CZ	107	
603	-63.180	.218	47.760	2	BASE	7.74
DCPXY	-.015	-.006	CP	603	50.000	
DCPZ			.019	CZ	603	
904	-62.788	1.042	47.661	2	BASE	7.74

=====

ROOT MEAN SQUARE OF DIFFERENCES AT CONTROL POINTS FOR UNIT WEIGHT

10 HORIZONTAL CONTROL POINTS	RMSE X = +/- .008	+/- .215
	RMSE Y = +/- .020	+/- .490
10 VERTICAL CONTROL POINTS	RMSE Z = +/- .002	+/- 1.926

[ground units]

MEAN DIFFERENCE AT CONTROL POINTS:

X: .000 Y: .000 Z: .000 [ground units]

AVERAGE BASE FOR 2-RAY-POINTS: 7.43

MEAN SQUARE ERRORS [microns]

```

bluh-po kalibravimo.1st
POINT CODE      NO IN GROUP    NO PHOT PTS    INT MSE X      INT MSE Y
CPZ             1              10             25             2.01          .73
CPXY            2              10             25             1.67          .20
ADJUS           4              18             46             .85           1.20
MEAN
                10              46             1.58          .72
    
```

MEAN SQUARE CORRECTIONS OF LAST ITERATION
X: .0030 Y: .0068 Z: .0164 [ground units]

```

OBSERVATIONS    UNKNOWNNS      REDUNDANCE      SIGMA O
                122              72              50              =====
                1.36              17:48:57
                [microns]
    
```

++++++ APRIORI STANDARD DEVIATIONS SHOULD BE CHANGED IN BLIM TO: ++++++
SIGMAO APRIORI : 7.
CONTROL POINTS X,Y: .49 Z: 1.03
+++++

MEAN VALUES OF RESIDUALS AND MSE IN RADIAL COMPONENTS
1ST LINE RADIUS [CM]
2ND LINE MEAN RADIAL [MICRONS]
3RD LINE MSE RADIAL [MICRONS]
4TH LINE MSE TANGENTIAL [MICRONS]
5TH LINE NUMBER OF POINTS IN GROUP

```

DATA SET 1
.0 .1 .2 .4 .5 .6 .7 .9 1.0 1.1 1.2 1.4 1.5 1.6 1.7
.0 .4 .0 .0 .0 -.0 .3 .1 .0 .1 -.6 .3 .4 .3 .1
.0 .4 .0 .4 .0 .0 .1 .1 .6 .5 .6 .4 .6 .4 .7
.0 .1 .0 .3 .0 .2 .2 .0 .7 .5 .1 .5 .4 .4 .6
0 1 0 4 3 3 5 1 13 10 5 4 5 2 4
    
```

MSE (RADIAL) = +/- .1 MSE (TANGENTIAL) = +/- .1 60 PHOTO POINTS

MEAN SQUARE NADIR ANGLE : 17.6

MEAN PHOTO SCALE = 1: 655.1 3 PHOTOS
FOR [ft]: 1: 200. = 17. in/ft

ADJUSTED COORDINATES COMPUTED : DATE: 23.05.2011 17:48:57
=====

default

POINT NAME	EASTING	NORTHING	HEIGHT	RAYS	Type	Class
102	-74.175	9.841	50.364	2	Control	XYZ
105	-70.714	6.493	49.540	3	Control	XYZ
106	-68.200	4.764	48.914	3	Control	XYZ
107	-62.228	12.180	48.019	2	Control	XYZ
109	-69.259	13.691	48.822	3	Control	XYZ
110	-72.721	15.974	50.106	2	Control	XYZ
111	-65.711	16.035	48.401	3	Control	XYZ
600	-75.337	.499	50.690	2	Control	XYZ
602	-67.358	.959	48.900	3	Control	XYZ
603	-63.180	.218	47.760	2	Control	XYZ
901	-75.645	1.051	50.811	2		
902	-70.825	1.174	49.532	3		
903	-67.544	1.061	48.889	3		
904	-62.788	1.042	47.661	2		
905	-67.802	6.644	48.850	3		
906	-68.987	9.364	49.050	3		
908	-75.603	12.115	50.930	2		
909	-70.372	20.039	47.935	3		

bluh-po kalibravimo.1st
POINT COORDINATES STORED IN daxyz.dat

DATA FOR TRANSFER TO BLAN STORED IN bluinf.dat

OUTPUT FILES

OBJECT COORDINATES : daxyz.dat
ORIENTATIONS PHI OMEGA KAPPA: dapor.dat
ORIENTATIONS OMEGA PHI KAPPA: daporo.dat
ORIENTATIONS PAT-B-FORMAT : daporp.dat
RESIDUALS AT IMAGE POSITIONS: resi.dat
DATA FOR TRANSFER TO BLAN : bluinf.dat

END OF BLUH DATE: 23.05.2011 17:48:57

Appendix 8. The programme of Republican scientific conference “*Civil Engineering and Geodesy*”**RESPUBLIKINĖS MOKSLO KONFERENCIJOS
“CIVILINĖ INŽINERIJA IR GEODEZIJA”
2010 spalio 22 d.****DIENOTVARKĖ**

Mokslo komiteto pirmininkas

doc. dr. V. Č. Aksamitauskas

Mokslo komiteto sekretorius prof. dr. M. Burinskienė

Organizacinio komiteto pirmininkas – doc., dr. G. Paliulis

Sekretorius – doc., dr. A. Gasilionis

GEODEZIJOS SEKCIJA**1 posėdis 10.00 – 11.30 2709 a.**

1. Č. Aksamitauskas. Stasiui Vytautui Kazakevičiui 80 m.
2. J. Vaitkevičienė, A. Kumetaitienė. Žemės sklypų kadastrinių matavimų tikrinimo ir derinimo kokybės įvertinimas.
3. L. Papšienė, G. Beconytė. Lietuvos erdvinės informacijos infrastruktūros vystymo prielaidos.
4. D. Levinskaitė, A. Stanionis, A. Zakarevičius. Žemės plutos įtempimų pokyčių kaita Lietuvos teritorijoje.
5. I. Jonauskienė. Žemės sklypų kokybės tyrimas.
6. R. Birvydienė. Sunkio anomalijos ir jų nustatymo Lietuvos teritorijoje galimybės.
7. J. Sužiedelytė-Visockienė, R. Bagdžiūnaitė. VGTU personalo Erasmus programos įgyvendinimas ir mobilumo rezultatai.
8. J. Pavliukovič, B. Ruzgienė. Skaitmeninės programinės sistemos geoduomenims gauti.
9. J. Sužiedelytė-Visockienė, A. Pranskevičiūtė. Pastatų matavimai skaitmeninės fotogrametrijos metodu.
10. D. Sabaitis. Apskritiminių skalių tipai ir jų matavimo būdai.
11. D. Popovas. Sunkio lauko kitimo poveikis geodeziniams matavimams.

2 posėdis. 11.45 – 13.15

12. J. Tropikaitė. Nekilnojamųjų turto daiktų kadastrinių matavimų kokybės kontrolė.
13. B. Gaidamovič. Refrakcijos įtakos tyrimas pagal Lietuvos geodezinio vertikaliojo tinklo niveliavimo duomenis.
14. G. Kostygova. Žemės sklypo plano sudarymas CAD programine įranga.
15. A. Zubanov. Šilo tilto deformacijų analizė.
16. G. Dmitrijev. Automatizuoto komparatoriaus valdymo principai ir algoritmai.
17. G. Sriubė. Melioracijos projektų susiejimas su LKS–94 koordinatų sistema.
18. R. Uleckaitė. Išmatuotų Žemės plutos deformacijų rodiklių tikslumo tyrimas modeliavimo būdu.
19. E. Penšina. Laiko sistemų taikomų geodezinėje astronomijoje analizė.
20. A. Šilkaitė. Žemės poliaus judėjimo poveikis astronominėms koordinatėms.
21. R. Gaidytė. 2D ir 3D statinių modeliavimo ypatumai.
22. A. Savickis. Virtualiųjų GPS referencinių stočių tinklo taikant koordinatų korektūrą sudarymas.
23. S. Norkutė, R. Putrimas. Vertikaliojo tinklo linijos Jonava-Zarasai niveliavimo rezultatų analizė.
24. E. Dagilytė, V. Budrytė. Žemės dangos skaitmeninių vaizdų koreliacinė analizė.

3 posėdis. 13.45 – 15.15

25. E. Videiko. Senųjų žemėlapių susiejimas ir transformavimas į bendrąją sistemą.
26. M. Mankauskas. Sunkio vertikaliojo gradiento tyrimas.
27. E. Zalanskaitė. Jonosferos įtakos GPS matavimams analizė.
28. E. Žilius. Vertikaliųjų Žemės plutos judesių įtaka horizontaliesiems judesiams.
29. V. Stukaitė. Melioracijos rekonstrukcijos projekto geodezinių darbų analizė.

30. V. Nareiko. ArcGIS programinės įrangos uždavinių automatizavimo analizė.
31. O. Čepaitė. Gravimetrinių matavimų duomenų apdorojimo analizė.
32. A. Gelžinytė. Vertikaliųjų Žemės plutos judesių linijoje Jonava-Kybartai prognozavimo modeliai.
33. A. Lingytė. Namų ūkio ūkininko sodybos plėtros projekto geodezinių darbų aspektai.
34. T. Gintvainytė. Telšių rajono žemės sklypų registravimo nekilnojamojo turto registre analizė.
35. I. Šapola. Vilniaus miesto nekilnojamojo turto objektų verčių analizė taikant „ArcGIS“.
36. P. Timinskas. Vilniaus urėdijos geoinformacinės sistemos projektavimas.
37. V. Bondzinskas. Skaitmeninės topografinės nuotraukos sudarymas atliekant statybos projektavimo darbus.
38. A. Žutautas. Palydovinių sistemų apžvalga.
39. D. Volungevičiūtė. Pataisos, redukuojant atstumus į LKS-94 kartografinę projekciją.
40. E. Butkutė. Skirtingose koordinatų sistemose sudarytų žemėlapių palyginimas.

Diskusijos

**VILNIAUS GEDIMINO TECHNIKOS
UNIVERSITETAS
APLINKOS INŽINERIJOS FAKULTETAS**



CIVILINĖ INŽINERIJA IR GEODEZIJA

RESPUBLIKINĖS MOKSLO KONFERENCIJOS

PROGRAMA

2010 M. SPALIO 22 D.